

Article

From Sphingosine Kinase to Dihydroceramide Desaturase: A Structure-Activity Relationship (SAR) Study of the Enzyme Inhibitory and Anticancer Activity of 4-((4-(4-chlorophenyl)thiazol-2-ylamino)phenol (SKI-II)

Luigi Aurelio, Carmen Scullino, Melissa Pitman, Anna Sexton, Vitoria Oliver, Lorena Davies, Richard Rebello, Luc Furic, Darren John Creek, Stuart Pitson, and Bernard L. Flynn

J. Med. Chem., **Just Accepted Manuscript** • DOI: 10.1021/acs.jmedchem.5b01439 • Publication Date (Web): 18 Jan 2016

Downloaded from <http://pubs.acs.org> on January 20, 2016

Just Accepted

“Just Accepted” manuscripts have been peer-reviewed and accepted for publication. They are posted online prior to technical editing, formatting for publication and author proofing. The American Chemical Society provides “Just Accepted” as a free service to the research community to expedite the dissemination of scientific material as soon as possible after acceptance. “Just Accepted” manuscripts appear in full in PDF format accompanied by an HTML abstract. “Just Accepted” manuscripts have been fully peer reviewed, but should not be considered the official version of record. They are accessible to all readers and citable by the Digital Object Identifier (DOI®). “Just Accepted” is an optional service offered to authors. Therefore, the “Just Accepted” Web site may not include all articles that will be published in the journal. After a manuscript is technically edited and formatted, it will be removed from the “Just Accepted” Web site and published as an ASAP article. Note that technical editing may introduce minor changes to the manuscript text and/or graphics which could affect content, and all legal disclaimers and ethical guidelines that apply to the journal pertain. ACS cannot be held responsible for errors or consequences arising from the use of information contained in these “Just Accepted” manuscripts.

1
2
3 **Title**
4
5

6 From Sphingosine Kinase to Dihydroceramide Desaturase: A Structure-Activity Relationship

7
8 (SAR) Study of the Enzyme Inhibitory and Anticancer Activity of 4-((4-(4-chlorophenyl)thiazol-2-
9
10
11 yl)amino)phenol (SKI-II).
12

13 **Authors**
14

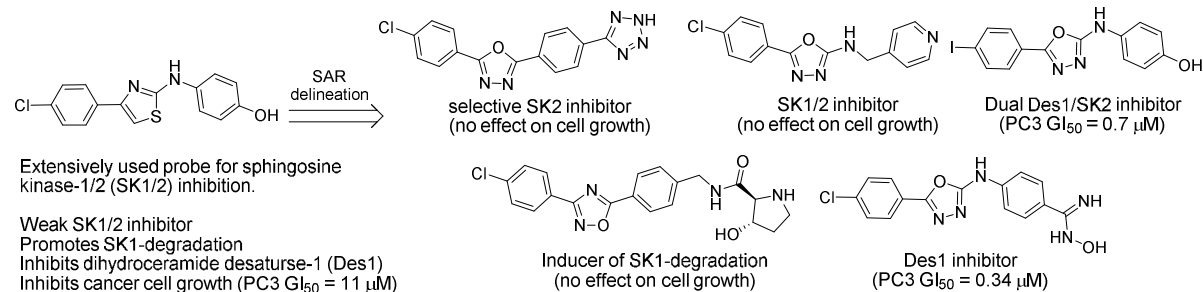
15
16 Luigi Aurelio,^a Carmen V. Scullino,^a Melissa R. Pitman,^b Anna Sexton,^a Victoria Oliver,^a Lorena
17
18 Davies,^b Richard J. Rebello,^c Luc Furic,^c Darren J. Creek,^a Stuart M. Pitson,^{b*} Bernard L. Flynn.^{a*}
19

20
21 ^a Monash Institute of Pharmaceutical Science, Monash University, 381 Royal Pde, Parkville, VIC,
22
23 3052, Australia
24

25
26 ^b Centre for Cancer Biology, University of South Australia and SA Pathology, Frome Road,
27
28 Adelaide SA, 5000, Australia
29

30
31 ^c Cancer Program, Monash Biomedicine Discovery Institute and Department of Anatomy and
32
33 Developmental Biology, Clayton, VIC, 3800, Australia
34
35

36
37
38
39
40 **Abstract**
41



55 The sphingosine kinase (SK) inhibitor, SKI-II, has been employed extensively in biological
56
57 investigations of the role of SK1 and SK2 in disease and has demonstrated impressive anticancer
58
59

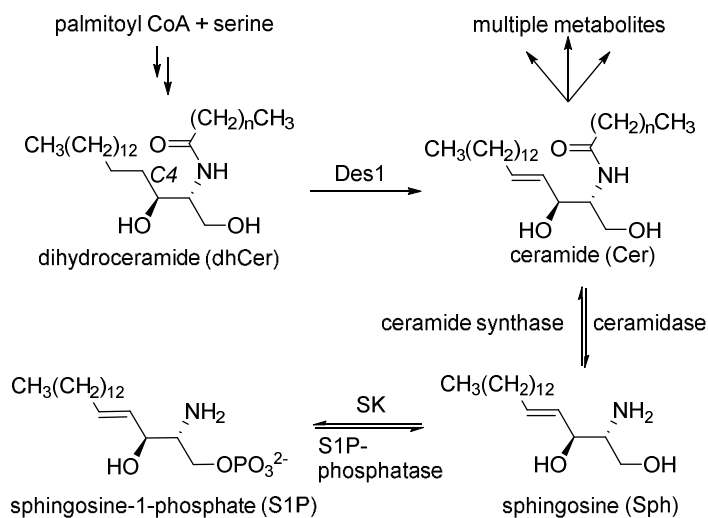
1
2
3 activity in vitro and in vivo. However, interpretations of results using this pharmacological agent
4
5 are complicated by several factors: poor SK1/2 selectivity; additional activity as an inducer of
6
7 SK1-degradation; and off-target effects, including its recently identified capacity to inhibit
8
9 dihydroceramide desaturase-1 (Des1). In this study we have delineated the structure-activity
10
11 relationship (SAR) for these different targets and correlated them to that required for anticancer
12
13 activity and determined that Des1 inhibition is primarily responsible for the antiproliferative
14
15 effects of SKI-II and its analogues. In the course of these efforts a series of novel SK1, SK2 and
16
17 Des1 inhibitors have been generated, including compounds with significantly greater anticancer
18
19 activity.
20
21
22

23 24 **Introduction**

25
26
27 Over the last fifteen years there has been considerable interest in identifying the biological
28
29 functions of sphingolipid metabolites and the role they play in diseases such cancer, autoimmune
30
31 disease, inflammation, pain, macular degeneration, asthma and fibrosis.¹ The *de novo* synthesis of
32
33 sphingolipids commences with palmitoyl CoA, which is converted into the central lipid ceramide
34
35 (Cer) in four steps, the last step being the introduction of the double bond at C4 by
36
37 dihydroceramide desaturase-1 (Des1) (Scheme 1). Ceramide is regarded as the central lipid in this
38
39 biosynthetic pathway from which many other bioactive metabolites are generated, usually in
40
41 reversible steps from which ceramide can be regenerated by salvage pathways. Of significant
42
43 interest has been the reversible conversion of Cer into sphingosine (Sph) and sphingosine-1-
44
45 phosphate (S1P) (Fig 1). Cer and Sph are pro-apoptotic signaling lipids whereas S1P promotes cell
46
47 growth and survival (anti-apoptotic and pro-mitogenic).^{1a,g,k} Consequently, sphingosine kinases
48
49 (SKs), which produce S1P, can play an important role in determining cell fate, providing a
50
51 “rheostat” for cancer cell survival and death.² There are two isoforms of SK, SK1 and SK2. SK1
52
53 exists in the cytosol and SK2 predominantly in the nucleosome and other organelles.^{1a,c,g,k} SK1 is
54
55 subject to tight regulation and is upregulated in many cancers where it is thought to play a key role
56
57
58
59
60

1
2
3 in disease progression through increases in S1P and decreases in Cer and Sph levels, promoting
4
5 tumour growth and survival.^{1a,e,j,o,2} Thus a number of groups have pursued SK1 inhibitors in order
6
7 to reverse this prosurvival effect of the Cer/Sph/S1P rheostat.^{3,4} SK2 inhibitors are also being
8
9 sought and may induce different mechanisms of cancer cell death to those mediated by SK1
10
11 inhibitors.³ Notwithstanding the compelling rationale for targeting sphingosine kinases, the
12
13 emergence of different SK1/2 inhibitors has met with conflicting results regarding their anticancer
14
15 potential.³ Early inhibitors included a series of Sph analogues (not shown) with mixed SK1/2
16
17 selectivity and IC₅₀ values in range of 5-30 μM and the non-lipid-like inhibitors, SKI-II **1** and
18
19 ABC294640 **2** (Fig 1). Compound **1** was identified by Smith and coworkers from a high
20
21 throughput screen in 2003,^{4a} it exhibits some selectivity towards SK2 as a kinase inhibitor (Ki:
22
23 SK2 = 7.9 μM, SK1 = 16 μM) but is a more powerful promoter of SK1-degradation (100% SK1
24
25 ablation at 10 μM)⁵ and has recently been identified as an inhibitor of Des1 activity (Ki = 0.3
26
27 μM).⁶ The SK1-degradation induced by **1** is proposed to arise from its binding to an allosteric site,
28
29 distinct from the enzymatic site, which promotes polyubiquination and proteasomal degradation of
30
31 SK1.⁵ Compound **2**, was also discovered by Smith and co-workers and is a selective inhibitor of
32
33 SK2 (Ki = 10 μM).⁷ Both **1** and **2** have been used in a large number of studies directed at
34
35 evaluating the therapeutic potential of targeting SKs in cancer and other indications, both have
36
37 exhibited favorable efficacy in cancer models and **2** has been progressed to clinical trials.^{7,8} Despite
38
39 exhibiting a variety of potentially valuable anticancer properties, **1** and **2** are only moderately
40
41 potent and in recent years a number of more potent (IC₅₀ < 1 μM) and more selective SK1/2
42
43 inhibitors have emerged. These include the SK1 selective inhibitors **3**,^{4b} **4**,^{4c,d} and PF-543 **5**^{4e} and a
44
45 dual SK1/2 inhibitor **6**,^{4h,i} (Fig 1). Like **1**, **5** is also a promoter of proteasomal degradation of SK1
46
47 and presumably also has some affinity for the allosteric site on SK1.^{4g} However, in contrast to **1**, **4**-
48
49 **6** do not show any antiproliferative effects at concentrations that fully suppress S1P production
50
51 in cells, casting doubt on the use of SK1 inhibitors as proapoptotic agents in cancer therapy.^{3,4d,e,i,l}
52
53
54
55
56
57
58
59
60

Similar conflicts arise in the case of SK2, where the moderately potent SK2 inhibitors **6**^{4h,i} and SLR080811 **7**^{4f} do not exhibit antiproliferative effects, whereas the less potent SK2 inhibitors K145 **8**^{4j} and MP-A08 **9**^{4k} do show increases in Cer concentrations and cancer cell apoptosis (GI_{50} = 5-30 μ M). Herein, we report our SAR studies on **1** and attempts to correlate the SAR for SK1/2 inhibition to the SAR for the antiproliferative effects in androgen-independent PC3 prostate cancer cells (SK1 expression is raised in PC3 cells relative to androgen-dependent LNCap prostate cancer cells).⁹ We have found that these two SARs diverge and that inhibition of these kinases cannot account the anticancer activity of **1** and our broader compound series. We have also studied the SAR of **1** in relation to SK1-degradation and inhibition of Des1 activity. The SAR of Des1 inhibition correlates to that required for inhibition of PC3 cell growth, indicating that Des1 inhibition is a key driver of the anticancer effects of **1** and its analogues, which is also supported by lipidomic studies in PC3 cells. In the course of this effort a number of substantially more potent inhibitors of some of these enzymes and of PC3 cell growth have been identified.



Des1 = dihydroceramide desaturase-1
 SK = sphingosine kinase

Scheme 1: Spingolipid Biosynthesis

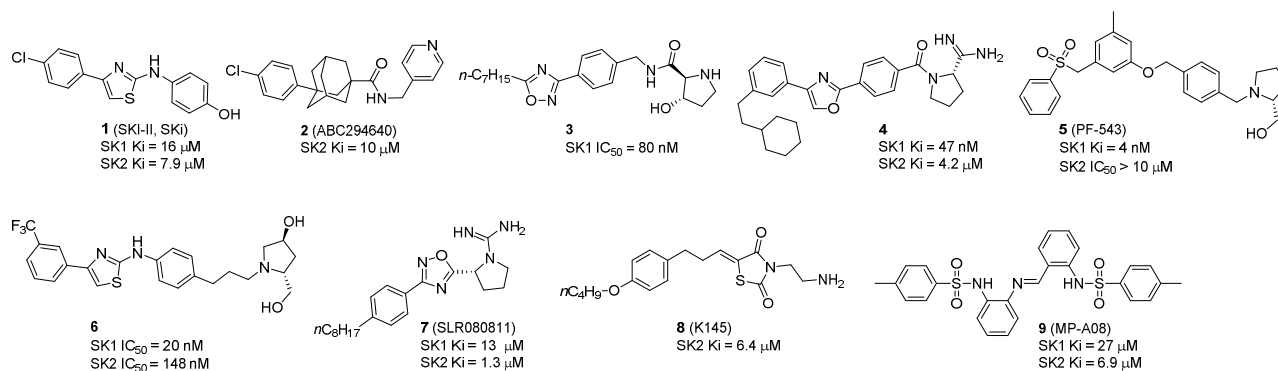
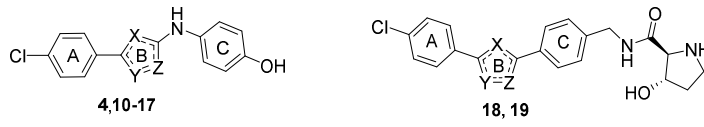


Figure 1: Structures of SK1/2 targeting agents.

SAR Studies: Our SAR studies of **1** have been directed to modifications of the B-ring (Table 1) and of groups R^a, R^b, L and the C-ring (Table 2). As part of our SAR-guided exploration of **1**, we sought to identify useful replacements of the 2-aminothiazole and 4-aminophenol moieties as they are likely to be subject to rapid metabolism to form reactive metabolites (bioactivation), potentially compromising *in vivo* drug exposure and safety.¹⁰ We have also avoided generating lipid-like, amphiphilic structures that are apparent in a number of the more potent SK1 inhibitors **3-6** and which are known to complicate cellular readouts, including through surfactant associated cytotoxicity.⁴ⁱ SK1/2 inhibition was measured at a single concentration (10 μ M) and recorded as %SK1/2 activity relative to vehicle (DMSO) control.¹¹ PC3 cell growth was measured using an MTS colorimetric assay and is given as the concentration required to inhibit 50% of cell growth (GI₅₀). Selected compounds were also evaluated for SK1-degradation, Des1 inhibition, lipidomics analysis and clonogenic potential in PC3 cells (see below). SK1 inhibitors **1**, **3** and **5** were used as comparators in these studies. As expected, **1** gave only a modest level of inhibition of SK1 (%SK1 = 78) and SK2 (%SK2 = 90) and inhibited PC3 cell growth (GI₅₀ = 11 μ M) with a potency that is broadly similar to that seen with other cell lines (Table 1, entry 3).^{4a,5a} Consistent with their reported high potency towards SK1, **3** (IC₅₀ = 80 nM)^{4b} and **5** (IC₅₀ = 3 nM)^{4c} gave low %SK1 values, 6% and 1%, respectively, and were much less potent towards SK2 (Table 1, entries 1 and

2). Compound **5** inhibited PC3 cell growth at a relatively high concentration ($GI_{50} = 19 \mu M$) compared to its SK1 inhibition and **3** was inactive ($GI_{50} > 100 \mu M$). The cytotoxicity observed with **5** (PC3 $GI_{50} = 19 \mu M$) may arise from its amphiphilic nature as has been reported for the similarly amphiphilic compound **6**.⁴ⁱ Interestingly, all of our novel bioisosteric B-ring analogues of **1**, **10-17** (Table 1, entry 4-11) gave higher levels of SK1/2 inhibition, with oxazole **17** giving the best SK1 potency and selectivity (Table 1, entry 11, %SK1 = 17, %SK2 = 53). The most potent PC3 cell growth inhibitor, 1,3,4-oxadiazole **10** ($GI_{50} = 1.63 \mu M$), is almost ten times more potent than **1** (Table 1, cf entries 3 and 4). Given the frequent use of the pyrrolidine ring as a polar head group in **3-7** we also prepared two hybrid structures of **1** and **3**, compounds **18** and **19** (Table 1, entries 12 and 13) but both of these were much less active than **3** towards SK1 and effectively devoid of any PC3 cell growth inhibition.

Table 1: B-ring Modifications.



Entry	B-ring	ID	%SK1 10 μM^a	%SK2 10 μM^a	GI_{50} PC3 ^b
1.		3	6 ± 2	112 ± 6	>100
2.		5	1 ± 2	45 ± 9	19
3.		1	78 ± 2	90 ± 7	11 ± 2
4.		10	43 ± 4	44 ± 8	1.6 ± 0.4
5.		11	55 ± 4	70 ± 3	2.4

6.		12	50 ± 5	55 ± 4	40
7.		13	50 ± 4	77 ± 15	44
8.		14	34 ± 4	64 ± 8	2.6
9.		15	75 ± 4	78 ± 8	ND
10.		16	55 ± 2	68 ± 1	ND
11.		17	17 ± 5	56 ± 4	3.0
12.		18	62 ± 10	106 ± 24	77
13.		19	41 ± 4	118 ± 18	>100

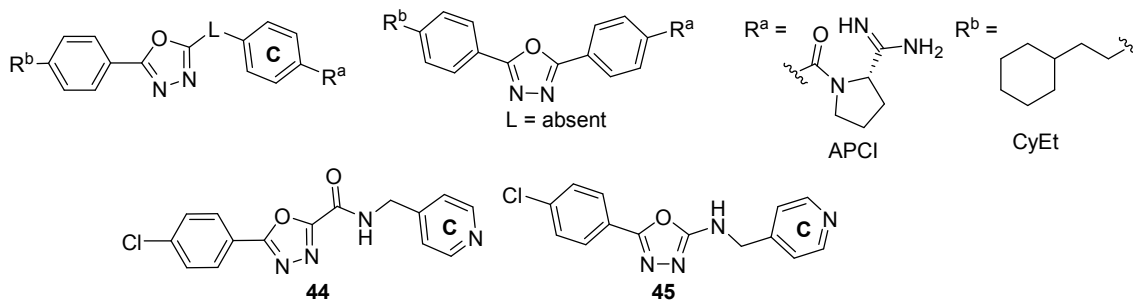
^a The activity of purified recombinant SK1 and SK2 were determined in the presence of 10 μM compound using an *in vitro* SK enzyme assay with 10 μM Sph and 100 μM ATP (n = 3).¹²

^b PC3 cell growth was measured using an MTS colorimetric assay at eight concentrations (10⁻⁸ - 10⁻⁴ M, n = 3 per concentration) and is given as the concentration required to inhibit 50% of cell growth (GI₅₀). Where given, the standard deviations (±) is based on 3 independent GI₅₀ determinations.

The 1,3,4-oxadiazole **10** was selected for further SAR studies exploring the effects of modifying the linker (L), polar head group R^a and hydrophobic tail R^b on SK1/2 activity and PC3 cell growth (Table 2). Removal of the amino (NH) L-group in **10** to give **20**, had no effect on the SK1/2 inhibition but completely removed its cell growth inhibitory activity (Table 2, cf entries 1 and 2).

1
2
3 Several alternative L-groups were also evaluated: L = S, C(O)NH, and CH₂NH (Table 2, entries 3-
4
5 5). Of these, L = CH₂NH (**23**), gave the greatest improvement in SK1/2 inhibitory activity (Table
6
7 2, entry 5) and only **22** and **23** inhibited PC3 cell growth. A key observation in the SAR of
8
9 compounds **10** and **20-23** (Table 2, entries 1-5) is the apparent requirement of a 4-aminophenol for
10
11 antiproliferative activity, which is not required for SK1/2 inhibition. The 4-aminophenol is
12
13 commonly linked to redox activity,⁹ indicating that the antiproliferative activity of **1**, **10**, **22** and **23**
14
15 may arise from a redox-active target (see below).
16
17

18
19 We also evaluated a series of polar head groups R^a to replace OH in **10** in the presence and absence
20
21 of L = NH (Table 2, entries 6-18). MacDonald, Webster and Lynch have shown that the amidine
22
23 (C(NH)NH₂) is a useful polar head group in promoting SK1/2 inhibition, in particular the
24
25 acylpyrrolidine-2-carboximidamide (APCI) group, as in **4** (Fig 1).^{4c-f} We evaluated the simple
26
27 amidine (C(NH)NH₂) head-group and APCI as well as a number of other neutral, basic and acidic
28
29 isosteres of the amidine and OH groups: R^a = NH₂, CH₂NH₂, CO₂H, C(O)NH₂, C(NH)NHOH and
30
31 tetrazole (Table 2, entries 6-17). Considering first the effect these variations in R^a on SK1/2
32
33 inhibition for where L is absent (entries 6-13), the carboxamide **27** (%SK1 = 22) and tetrazole **31**
34
35 (%SK2 = 14) gave the best SK1/2 inhibitory activity and were selective for SK1 and SK2,
36
37 respectively (Table 2, entries 9 and 13). The amidine **28**, amidine oxime **29** and APCI **30** head
38
39 groups (R^a) were least effective in SK1/2 inhibition (Table 2, entries 10 - 12). The introduction of
40
41 L = NH for these different R^a groups saw little effect on carboxamide **33** SK1/2 inhibitory activity
42
43 (%SK1 = 20), whereas the tetrazole **35** showed reduced activity. By contrast, the introduction of L
44
45 = NH conferred a marked increase in potency of amidine **33** (%SK2 = 14) over **28** towards SK2
46
47 (Table 2, cf entries 11 and 15). With respect to PC3 cell growth of the compounds **24-36** (Table 2,
48
49 entries 6-18), only four compounds showed any activity: **28** (GI₅₀ = 45 μM), **34** (GI₅₀ = 0.34 μM)
50
51 and **35** (GI₅₀ = 15 μM). Again there is no correlation between SK1/2 inhibition and PC3 cell
52
53 growth inhibition in this series.
54
55
56
57
58
59
60

Table 2: Modifications of R^{a/b}, L and C-Ring.

Entry	R ^a	-L-	R ^b	ID	%SK1 ^a 10 μM	%SK2 ^a 10 μM	GI ₅₀ PC3 ^a (μM)
1.	OH	NH	Cl	10	43 ± 4	44 ± 8	1.6 ± 0.4
2.	OH	absent	Cl	20	42 ± 8	40 ± 3	>100
3.	OH	-S-	Cl	21	107 ± 27	79 ± 22	>100
4.	OH	-C(O)-NH-	Cl	22	78 ± 8	139 ± 18	22
5.	OH	-CH ₂ -NH-	Cl	23	22 ± 3	39 ± 3	51
6.	NH ₂	absent	Cl	24	53 ± 10	50 ± 11	>100
7.	CH ₂ NH ₂	absent	Cl	25	51 ± 8	57 ± 4	>100
8.	CO ₂ H	absent	Cl	26	57 ± 10	40 ± 8	>100
9.	C(O)NH ₂	absent	Cl	27	22 ± 5	104 ± 12	>100
10.	C(NH)NH ₂	absent	Cl	28	73 ± 5	89 ± 11	45 ± 21
11.	C(NH)NHOH	absent	Cl	29	105 ± 13	102 ± 5	70
12.	APCI	absent	Cl	30	69 ± 6	135 ± 16	>100
13.	tetrazole	absent	Cl	31	133 ± 7	14 ± 10	>100
14.	C(O)NH ₂	-NH-	Cl	32	20 ± 2	43 ± 12	>100

15.	C(NH)NH ₂	-NH-	Cl	33	46 ± 17	14 ± 7	>100
16.	C(NH)NHOH	-NH-	Cl	34	93 ± 23	121 ± 8	0.34 ± 0.05
17.	tetrazole	-NH-	Cl	35	44 ± 8	70 ± 6	15
18.	C=N-OH	-NH-	Cl	36	41 ± 15	71 ± 9	>100
19.	OH	-NH-	H	37	53 ± 27	23 ± 2	8.1 ± 2.1
20.	OH	-NH-	CF ₃	38	35 ± 14	17 ± 2	1.0 ± 0.8
21.	OH	-NH-	I	39	53 ± 1	3 ± 0.1	0.7 ± 0.14
22.	OH	-NH-	CyEt	40	56 ± 14	144 ± 51	50
23.	C-ring = pyr	-C(O)NHCH ₂ -	Cl	41	133 ± 21	73 ± 8	>100
24.	C-ring = pyr	-NHCH ₂ -	Cl	42	3 ± 1	39 ± 12	>100

^a See Table 1.

We also undertook a preliminary examination of the SAR associated with hydrophobic group R^b (Table 2 entries, 19-22). Replacement of Cl with hydrophobic groups of increasing size H, CF₃, I, (**37-39**) led to successively increased inhibition of SK2, with **39** (R^b = I) proving quite potent and selective towards SK2 (%SK2 = 3) (Table 2, entries 19-21). On the other hand, the much larger (cyclohexyl)ethyl (CyEt) group, that proved effective in promoting the SK1 inhibitory activity of **4**^{4c,d} and analogues of **3**^{4b} (not shown) diminished its activity towards SK2 (Table 2, entry 22). Like other 4-aminophenols, **40-43** all inhibited PC3 cell growth, with **39** showing the greatest activity, GI₅₀ = 0.7 μM (Table 2, entry 21). In this series (**37-40**), the SAR for SK2 inhibition does appear to coincide with inhibition of PC3 cell growth (Table 2, entries 19-22).

We next explored the use of the 4-pyridyl ring present in the SK2 inhibitor **2** (Fig 1), as an alternative C-ring. We employed two linker groups for this: L = -C(O)NHCH₂- and -NHCH₂-, **41** and **42**, respectively (Table 2, entries 23 and 24). Only **42** showed any appreciable SK1/2

inhibitory activity, but in contrast to **2**, proved to be a moderately selective SK1 inhibitor (%SK1 = 3, %SK2 = 39).

We determined the IC₅₀ values of our most potent SK1/2 inhibitors **42** and **39** (Table 3) and compared these to the most potent SK1 inhibitor yet to be identified **5** (Fig 1). The previously reported IC₅₀ (SK1) values for **5** of 3 and 28 nM were obtained at 3 and 5 μM of Sph, respectively,^{4e,g} our value of 387 nM was obtained at 10 μM of Sph. These variations are consistent with the substrate (Sph) competitive binding kinetics of **5**.^{4e} While the dual SK inhibitor **42** is not as potent as **5**, it is a more drug-like species (lower MW and cLogP) that exhibits a superior lipophilicity-corrected ligand efficiency (LELP): **5** LELP = 16 cf **42** LELP = 10 (Table 3).¹³ Compounds with LELP values of > 10 are considered unlikely to achieve suitable concentrations in vivo to modulate their target.¹²

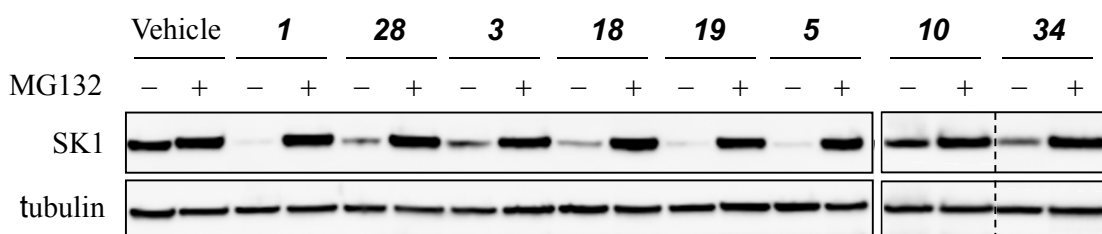
Table 3: IC₅₀ values of selected compounds

Entry	Cmpnd	SK1 IC ₅₀ ^a (μM)	SK2 IC ₅₀ ^a (μM)	LELP ^a
1	5	0.387	17.0	16.2
3	39	>20	1.9	9.8
4	42	3.1	5.5	10.0

^a Inhibitory constants for purified recombinant enzymes were obtained by an in vitro SK enzyme assay with 1mM ATP, 10μM Sph, and the compounds at concentrations of 0.005 - 10 μM. Data represent mean two independent experiments.

We further evaluated a selected series of our compounds for their capacity to induce SK1-degradation (Fig 2). SK1-degradation was measured using our previously described assay where expression of FLAGTM epitope-tagged SK1 is induced in HEK293 cells and the effect of the compounds on degradation of this existing protein is selectively assessed by Western blot after 16 h.^{5a} The proteasome inhibitor MG132 was also included in these assays to demonstrate the

1
2
3 involvement of the proteasome in the SK1-degradation induced by these compounds. As
4
5 previously demonstrated, **1** completely ablates SK1 levels at 10 μ M in a MG132-dependent
6
7 manner.^{5a} In fact, SK1-degradation is likely to be the primary source of SK inhibition by **1** in cells
8
9 as it is only a weak inhibitor of SK1/2 kinase activity. All other compounds used in this study that
10
11 induced SK1-degradation also did so in an MG132-dependent manner (Fig 2). Comparison of **1**
12
13 with the close structural analog **10**, shows **1** to be a much more effective promoter SK1-
14
15 degradation than **10** despite the fact that **10** is a more potent SK1 kinase inhibitor (Table 1, entries
16
17 3 and 4). This comparison indicates that, consistent with the allosteric model,⁵ SK1-degradation is
18
19 independent SK1 kinase inhibition. Presumably, the exchange of the thiazole ring in **1** for the
20
21 oxadiazole ring in **10** has decreased affinity for the allosteric site and increased affinity for either
22
23 the ATP or Sph binding sites on SK1 and SK2. A comparison of the close structural analogues **3**,
24
25 **18** and **19** further supports the finding that SK1-kinase inhibition and SK1-degradation are
26
27 independent effects. **3** is a potent inhibitor of SK1 kinase activity and modest inducer of SK1-
28
29 degradation, whereas **18** and **19** are much less potent SK1 kinase inhibitors but very effective in
30
31 SK1-degradation. None of these compounds, **3**, **18**, **19** exhibited significant PC3 cell growth
32
33 inhibition (Table 1 entries 1, 12 and 13). The Pfizer compound **5** is both a potent inducer of SK1-
34
35 degradation and inhibitor of SK1 kinase activity. Also, our most potent inhibitor of PC3 cell
36
37 growth, amidine oxime **34**, is a moderate promoter of SK1-degradation and has no SK1/2 kinase
38
39 inhibitory activity (Table 2, entry 15). These comparisons indicate the promotion of SK1-
40
41 degradation, SK1-kinase inhibition and cell growth inhibition are all independent effects though
42
43 some compounds may exhibit more than one of these effects.
44
45
46
47
48
49
50
51
52



1
2
3 **Figure 2:** Effect of the compounds on SK1 protein degradation. Expression of FLAG epitope-
4 tagged SK1 was induced HEK293 cells and the effect of applying the compounds to cells for 16 h
5 at 10 μ M on degradation of this existing protein selectively quantified by Western blot.
6
7
8

9
10 The close correlation of PC3 cell growth inhibition with the presence of redox active groups
11 indicates that inhibition of a redox-active enzyme may be responsible for this effect. This overlaps
12 with the recent finding that Des1 activity is potently inhibited by **1** ($K_i = 0.3 \mu$ M).⁶ To investigate
13 this further we examined several of our antiproliferative compounds as well as several close
14 structural analogues that do not exhibit antiproliferative effects for inhibition of Des1 activity (Fig
15 3). Des1 activity was obtained by measurement of the fluorescently labeled ceramide analogue,
16 C6-NBD-dhCer, in Jurkat cells as described previously.¹⁴ The conversion of C6-NBD-dhCer to
17 C6-NBD-Cer is attributed to Des1 since the alternative Des-subtype, Des2, gives rise to significant
18 C4-hydroxylation, which was not observed with this study (no detectable C4-hydroxylation of C6-
19 NBD-dhCer) and because C4-hydroxysphingolipids are hardly present in Jurkat cells.¹³ Since the
20 assay is performed in whole cells, the direct target leading to the Des1 inhibition cannot be easily
21 discerned and may include other elements in the electron transport pathway associated with Des1
22 activity. Indeed, Cingolani *et. al.*⁶ propose **1** to be an indirect inhibitor of Des1, possibly targeting
23 the upstream enzyme, NADH-cytochrome b5 reductase (CBR5), due to it being a non-competitive
24 inhibitor of Des1 and it being structurally dissimilar to the endogenous substrate, dhCer. Our
25 evaluation of **1** and the structurally related phenols **10**, **20** and **39** revealed all the 4-aminophenols
26 **1**, **10** and **39** to be quite potent inhibitors of Des1, whereas the simpler phenol **20** was inactive (Fig
27 3). This correlates with the PC3 cell growth inhibition where **1**, **10** and **39** inhibit cell growth but
28 **20** is inactive (Tables 1 and 2). It also overlaps with the SAR of the known inhibitor of Des1,
29 fenretinide **43** (Fig 4),¹⁵ which also contains a 4-aminophenol and is an inhibitor PC3 cell growth
30 ($GI_{50} \sim 2 \mu$ M).¹⁶ **43** is believed to be a direct inhibitor of Des1 that initially shows competitive
31 inhibition but becomes an irreversible inhibitor over longer incubation times.¹⁴ The 4-aminophenol
32
33
34
35
36
37
38
39
40
41
42
43
44
45
46
47
48
49
50
51
52
53
54
55
56
57
58
59
60

1
2
3 in **43** group may play an important role in mediating its irreversible inhibition of Des1, where Des1
4
5 oxidation of this group generates a reactive iminoquinone intermediate **44** that reacts with
6
7 nucleophilic sites on the protein, leading to time dependent irreversible inhibition of Des1 (Fig 4).
8
9 A similar mechanism may be operating in the case of **1** and the related 4-aminophenols prepared in
10
11 this study, in which case they may also operate as direct inhibitors of Des1. The amidine oxime **34**
12
13 completely inhibited Des1 activity at 10 μM but showed little activity at 1 μM . Alkyloximes have
14
15 been previously shown to undergo oxidation to nitroso groups that form high affinity complexes
16
17 with the iron in the redox enzyme prostaglandin synthase.¹⁷ Amidine oxime **34** may also undergo
18
19 oxidative activation to form a nitroso intermediate **45** that forms a high affinity complex with the
20
21 Fe_2O_2 in Des1. Consistent with the redox activation of **34**, is the much reduced activity of the
22
23 structurally similar amidine **33** and aldimine oxime **36**, which are more resistant to oxidation. If
24
25 redox activation is involved in the inhibition of Des1 activity by **34**, then it is likely to be a highly
26
27 targeted effect requiring quite specific structural interactions as the structurally related amidine
28
29 oxime **29** showed no Des1 inhibitory activity at 10 μM . Of these related structures, **29**, **33**, **34** and
30
31 **36** only the active Des1 inhibitor **34**, showed any significant activity against PC3 cell growth,
32
33 which is constant with what was seen for the phenolic compounds (**1**, **10**, **20** and **39**).
34
35 Notwithstanding the suggested possibilities for the direct inhibition of Des1 by these redox
36
37 sensitive compounds, it remains a significant possibility that other enzymes in the redox cycling
38
39 pathway are the target of these inhibitors.
40
41
42
43
44

45 Inhibition of Des1 activity and associated increases in dhCer are known to give rise to both
46
47 apoptotic and autophagic cell death.¹⁸ Lipidomic analysis of **1** and **34** in PC3 cells (10 μM)
48
49 indicates that Des1 inhibition dominates their effects on sphingolipid synthesis, with significant
50
51 increases in total dhCer levels but little effect on total Cer, Sph and S1P levels (Fig 5). Since **34**
52
53 inhibited PC3 cell growth at a concentration of $< 1 \mu\text{M}$ we also undertook lipidomic analysis of
54
55 this compound in PC3 cells at 1.0 μM , but it showed no effect on dhCer levels (data not shown).
56
57
58
59
60

This indicates that while Des1 inhibition alone may explain the anticancer effects of **1** (PC3 GI₅₀ = 11 μM) and many of its other 4-aminophenols analogues (Table 1 and 2), it is likely that the cell growth inhibitory effects of **34** (PC3 GI₅₀ = 0.34 μM) involves another target(s) in addition to Des1. Alternatively, these different irreversible inhibitors may have different rates of oxidative activation and inhibition of Des1. The time period of drug exposure in the PC3 cell growth inhibition assay (72 h) is much longer than that in the Des1 assay (3 h) and in the lipidomics study (5 h). Further evaluation of the inhibition kinetics of **1** and **34** are required in order to verify that they are irreversible inhibitors of Des1 and if the time course of Des1 inhibition can explain current apparent differences in the level of Des1 inhibition and PC3 cell growth inhibition for **34**.

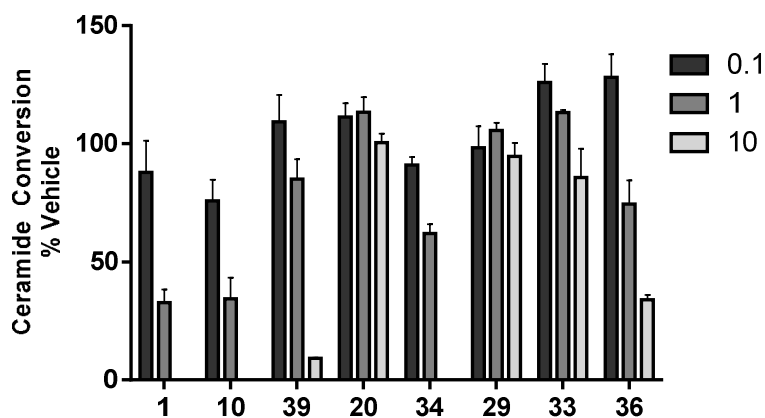


Figure 3, Inhibition of Des1: Des1 activity was obtained by measurement of C6-NBD-Cer conversion in Jurkat cells pre-labeled with C6-NBD-Cer (10 μM). Cells were treated with vehicle or inhibitor (0.1, 1, 10 μM) for 3 h. Data represent mean ± SD of three independent experiments.

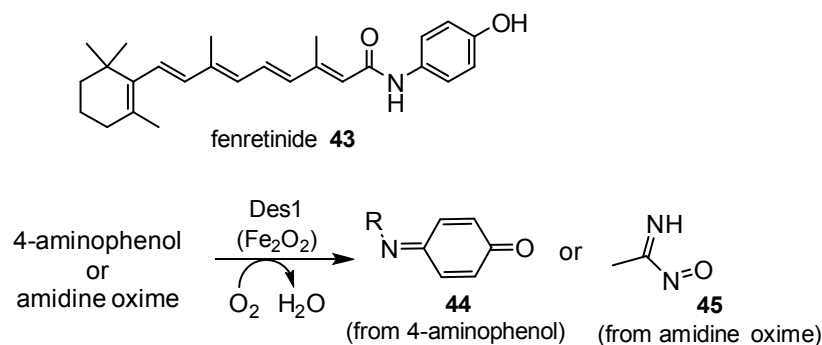


Figure 4: Fenretinide and irreversible inhibition of Des1.

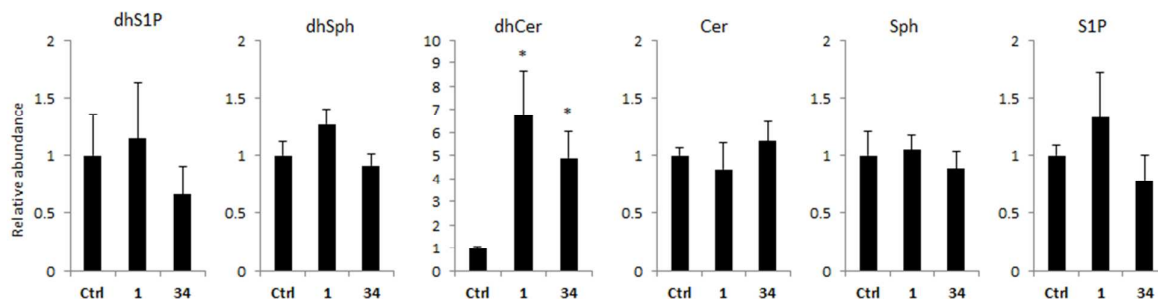


Figure 5, Lipidomic analysis: Effects on sphingolipid levels of **1** and **34** at 10 μ M in PC3 prostate cancer cells.

The correlation between redox-activity and antiproliferative effects seen with **1** and its analogues does not easily extend to the SK2 inhibitor **2**, which does not contain such a moiety. Nonetheless, consistent with the Amgen group's studies,⁴ⁱ our results indicate that the antiproliferative effects seen with **2** are unlikely to arise from inhibition of SK2 kinase activity alone as the potent SK2 inhibitors **31** and **33** (%SK2 = 14 for both) had no effect on PC3 cell growth even at high concentrations (100 μ M). The estrogen receptor has been identified as a potential off target for **2**, which it antagonizes in similar manner to tamoxifen.¹⁹ However, this may not explain all the anticancer effects seen with **2**, which may still involve contributions from SK2 inhibition. Very recently, **2** has been reported to be a weak inhibitor of Des1.²⁰ SK2 inhibition may act

cooperatively with Des1 inhibition in the antiproliferative effects seen with **39** (PC3 GI_{50} = 0.7 μ M) and **2** (GI_{50} = 28-30 μ M in several prostate cancer cells line).²⁰

To test if the antiproliferative compounds **1**, **10** and **34** inhibit the clonogenic potential of PC3 cells, we performed soft agar colony formation assays (Fig 6).²¹ All compounds showed qualitatively similar potency to inhibit anchorage-independent growth in soft agar compared to that obtained in the plated assays. For example, the most potent compound, **34**, has an IC_{50} of 0.5 μ M and 0.34 μ M in the soft agar and plated assays, respectively.

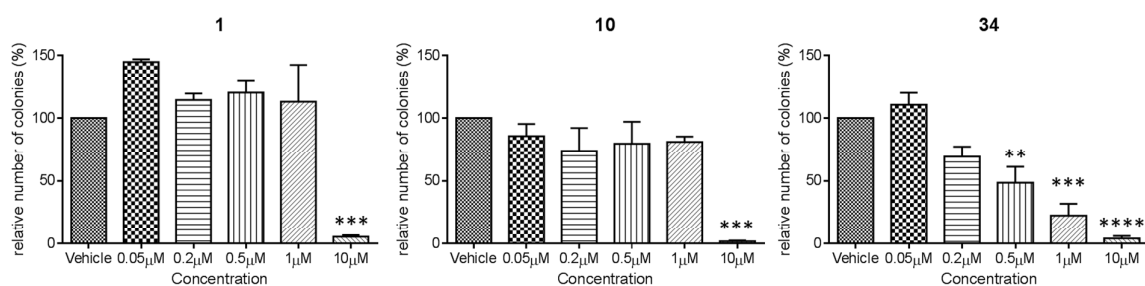
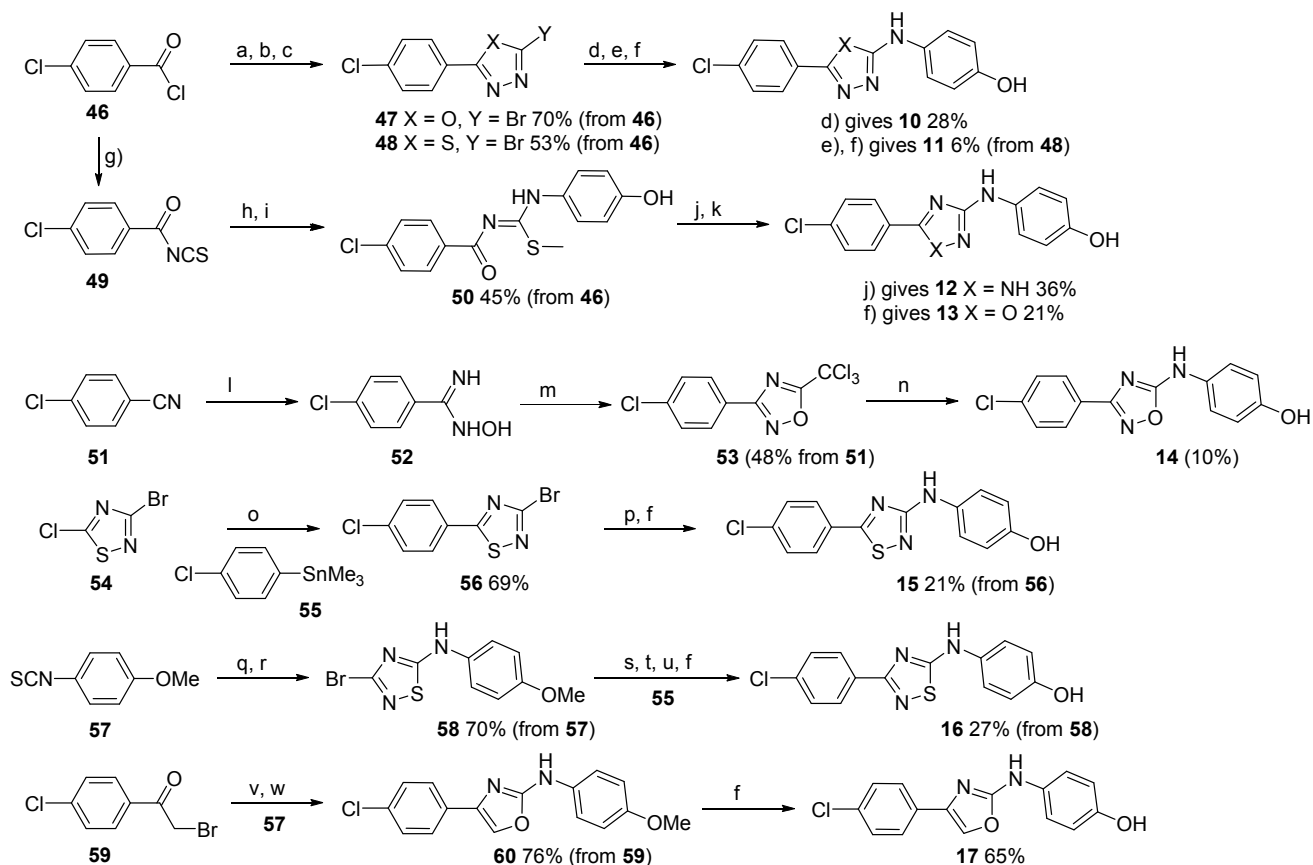


Figure 6: Inhibition of colony formation in soft agar. PC3 cells were seeded in soft agar and treated with increasing concentrations of each compound. Data represent mean \pm SEM of three independent experiments performed in duplicate. ** P <0.01. *** P <0.001 **** P <0.0001.

Synthetic Chemistry: The synthesis of bioisosteric replacements of the thiazole ring (Table 1) involved the preparation of a series of oxadiazoles, thiadiazoles, triazoles and oxazoles (Scheme 2). The 1,3,4-oxadiazole **10** and 1,3,4-thiadiazole **11**, were both prepared through nucleophilic substitution of the corresponding heteroaryl bromides **47** and **48**. Heteroaryl bromides **47** and **48** were prepared by known methods, involving cyclocondensation of 4-chlorobenzoyl chloride (**46**) with hydrazine carboxamide (or thiocarboxamide), followed by Sandmeyer reaction to convert the initially formed heteroaryl amines (not shown) into bromides.²² Bromide **47** underwent direct substitution by 4-aminophenol to give **10** in a low yield (28%). This direct substitution failed altogether in the case of the corresponding thiadiazol, necessitating the use of 4-methoxyaniline in

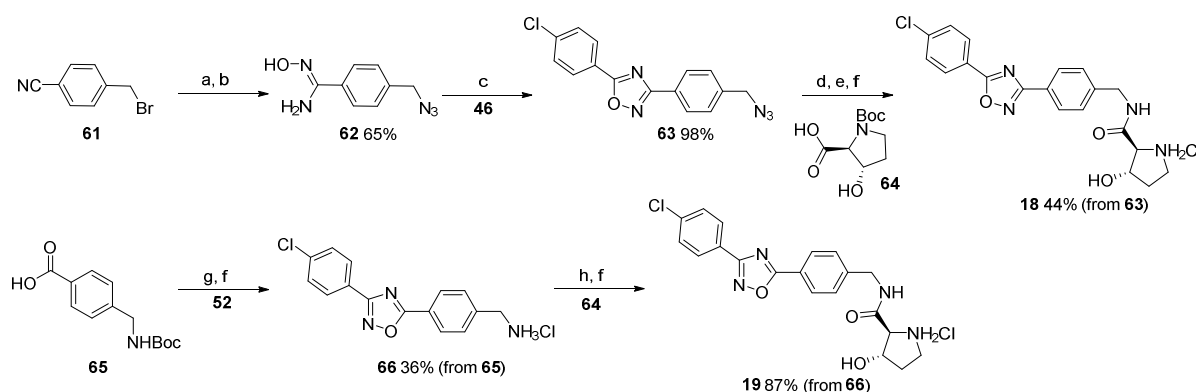
1
2
3 the nucleophilic aromatic substitution followed by demethylation to give **11** (6% from **48**). The
4
5 triazole **12** and 1,2,4-oxadiazole **13** were also obtained from benzoyl chloride **46**, involving initial
6
7 conversion to the benzoyl isothiocyanate **49** followed by reaction with 4-aminophenol and MeI to
8
9 give a S-methylthiourea **50**²³ and cyclocondensation with hydrazine and hydroxylamine to give
10
11 that gives **12** (36%) and **13** (21%), respectively. Preparation of the alternative 1,2,4-oxadiazole **14**
12
13 involved conversion of 4-chlorobenzonitrile (**51**) into the amidine oxime **52**, followed by
14
15 cyclocondensation with trichloroacetic anhydride to give **53** (71%),²⁴ which undergoes
16
17 nucleophilic aromatic substitution with 4-aminophenol, displacing the trichloromethyl moiety to
18
19 give **14** (10%). Thiadiazole **15** was obtained from selective substitution of the
20
21 bromochlorothiadiazole **54** (Scheme 2). Chemoselective Pd-mediated Stille coupling of **54** with the
22
23 aryl stannane **55** selectively substitutes the activated chloro group to give the bromothiadiazole
24
25 **56**,²⁵ this is subject to nucleophilic aromatic substitution with 4-methoxyaniline and demethylation
26
27 to yield **15** (21%). The isomeric thiadiazole **16** was obtained by sequential treatment of the 1-
28
29 isothiocyanato-4-methoxybenzene (**57**) with sodium cyanogen and bromine, to yield the 3-bromo-
30
31 1-2,4-thiadiazole **58** (70%).²⁶ This material was Boc-protected, coupled to stannane **55** and then
32
33 deprotected and demethylated to give **16** (27%). Oxazole **17** was prepared from α -bromoketone **59**,
34
35 initial displacement of the bromo group with NaN₃ and reaction with PPh₃ gives an aza-Wittig
36
37 reagent (not shown) that reacts with the isothiocyanate **57** to give oxazole **60** (76%), which is
38
39 demethylated to give **17** (65%).
40
41
42
43
44
45
46
47
48
49
50
51
52
53
54
55
56
57
58
59
60



Scheme 2: a) $\text{H}_2\text{NC(X)NHNH}_3\text{Cl}$ (X = O or S), NaHCO_3 , AcONa , H_2O . b) H_2SO_4 , rt (X = S); POCl_3 , toluene, 140°C (X = O). c) isopentyl nitrite, CuBr_2 , MeCN , rt. d) 4-Aminophenol, DIPEA, DMF , 70°C . e) 4-Methoxyaniline, DIPEA, DMF , 105°C . f) BBr_3 , CH_2Cl_2 . g) NH_4SCN , acetone, rt. h) 4-Aminophenol, acetone, reflux. i) MeI , K_2CO_3 , THF , 0°C . j) $\text{N}_2\text{H}_4\cdot\text{H}_2\text{O}$, EtOH , reflux. k) $\text{NH}_2\text{OH}\cdot\text{HCl}$, DBU , EtOH , reflux. l) $\text{NH}_2\text{OH}\cdot\text{HCl}$, Et_3N , EtOH , reflux. m) trichloroacetic anhydride, 110°C . n) 4-Aminophenol, DBU , DMSO , rt. o) $\text{Pd}(\text{PPh}_3)_4$ 5 mol%, CuTC 10 mol%, **55**, 1,4-dioxane, reflux. p) 4-methoxyphenol, DIPEA, NMP , microwave: 160°C . q) NaNHCN , acetone, rt. r) Br_2 , EtAc , rt. s) Boc_2O , DMAP , 1,4-dioxane, rt. t) $\text{Pd}(\text{PPh}_3)_4$ 5 mol%, **55**, 1,4-dioxane, reflux. u) TFA , CH_2Cl_2 , rt. v) NaN_3 , acetone, rt. w) **57**, PPh_3 , dioxane, 100°C .

The two hybrid structures of **1** and the Genzyme SK1 inhibitor **3**, compounds **18** and **19**, were prepared as described in Scheme 3. Preparation of **18** commenced with the 4-(bromomethyl)-

benzonitrile, the bromo group was substituted for an azide (NaN_3) and the nitrile converted into an amidine oxime **62** (65%) which was cyclocondensed with 4-chlorobenzoyl chloride (**46**) to give the 1,2,4-oxadiazole **63** (98%).²⁷ Reduction of azide **63** into an amine and coupling with the Boc-protected hydroxyproline **64** and deprotection gave **18** (44%). Its oxadiazole isomer **19** was prepared by cyclocondensation of the acid **65** (activated as a mixed anhydride) with the amidine oxime **52** followed by deprotection to give **66** (36%), which is then coupled to the Boc-protected hydroxyproline **64** and deprotected to give **19** (87%).



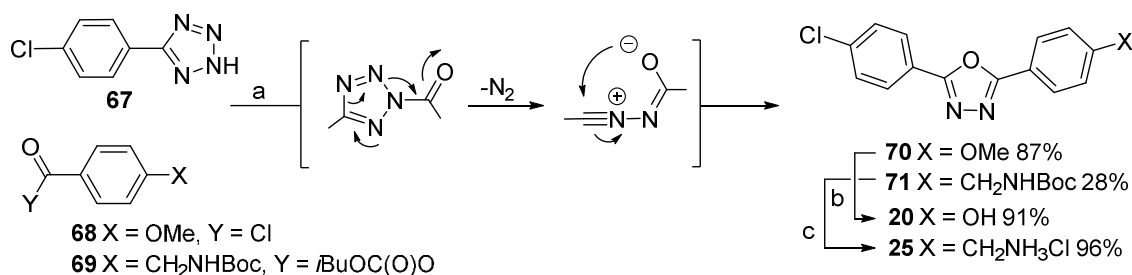
Scheme 3: a) NaN_3 , DMF, rt. b) $\text{NH}_2\text{OH}\cdot\text{HCl}$, Et_3N , EtOH, reflux. c) **46**, pyridine, xylene, reflux. d) $\text{NH}_4\cdot\text{HCO}_2$, Zn, MeOH, rt. e) DIPEA, HATU, DMF, rt. f) EtOAc, HCl in dioxane. g) *N*-methymorpholine, isobutylchloroformate, dioxane, rt, then **52** and reflux. h) HATU, DIPEA, EtOAc.

SAR studies directed to finding alternatives to the 4-aminophenol group were all based on analogues of 1,3,4-oxadiazole ring system **10**. Direct access to systems in which the amino linker unit (L) was absent (diaryl-1,3,4-oxadiazoles) could be attained through cyclocondensation of the tetrazole **67** with benzoyl chlorides **68** and **69** to give **70** (87%) and **71** (28%) followed by demethylation and deprotection to provide test compounds **20** (91%) and **25** (96%), respectively (Scheme 4). The bromo-oxadiazole **47** also served as useful substrate for Suzuki coupling to give

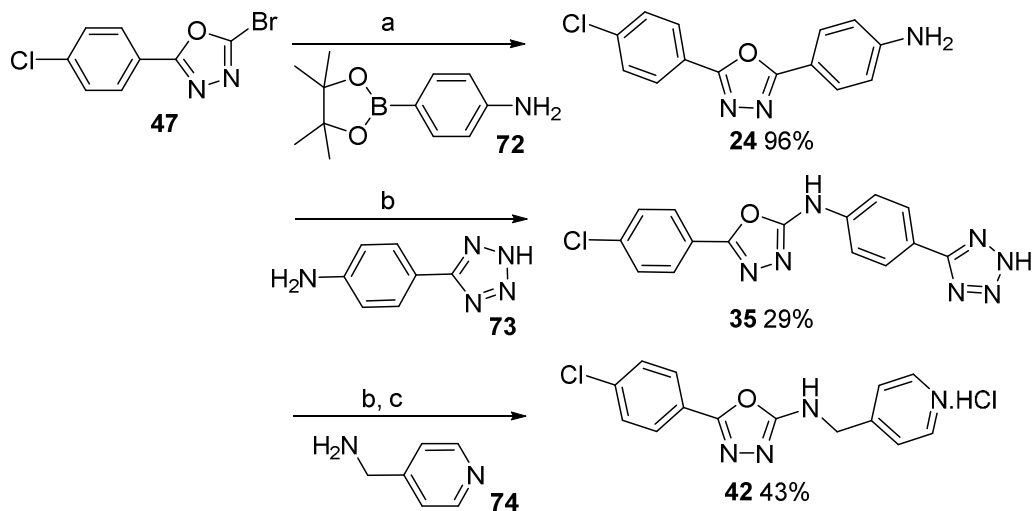
24 (96%) and through nucleophilic substitution with amines to give **35** (29%) and **42** (43%) (Scheme 5).

Many of the test compounds were achieved through cyclocondensation of the hydrazine amide **75** with different electrophiles (Scheme 6). Cyclocondensation of **75** with chloroacetic acid or ethyl oxalyl chloride in POCl₃ delivered the functionalised oxadiazoles **76**²⁸ and **77**²⁹, respectively, which could be converted into test compounds **22**, **23** and **41** by nucleophilic substitution (Scheme 6). Hydrolysis and decarboxylation of the ester in **77** afforded the C5-unsustituted oxadiazole **82**, which was coupled to 4-iodobenzonitrile to give **83** (75%) using a previously described Cu-mediated C-H activation process.³⁰ Cyclocondensation of the hydrazine amide **75** with CS₂ gave thiol **78**,³¹ which was used in a Cu-mediated coupling with 4-iodoanisole to give sulfide **21** (60%). **75** was also cyclocondensed with benzoyl chloride **79** and 4-isothiocyanatobenzonitrile (**80**) to give the carboxylic acid **26** (83%) (after ester hydrolysis) and nitrile **81** (67%), respectively.

The carboxylic acid **26** and the two nitriles **81** and **83** were used in the synthesis of other test compounds (Schemes 7 and 8). The carboxylic acid **26** was converted to the simple amide **27** (43%) and the proline derivative, amidine **30** (10% over 3 steps) (Scheme 7). Nitrile **83** was converted to the tetrazole **31** (71%), by cycloaddition of NaN₃ (Scheme 8). Both nitriles **83** and **81** were converted into amidine oximes **29** (52%) and **34** (66%) and amidines **28** (66%) and **33** (27%) upon addition of LiHMDS and NH₂OH, respectively (Scheme 8). Hydration of **81** gave the simple amide **32** (94%) and DIBAL reduction afforded an aldehyde (not shown) that gave the aldimine oxime **36** (20%) upon Schiff's condensation with NH₂OH.

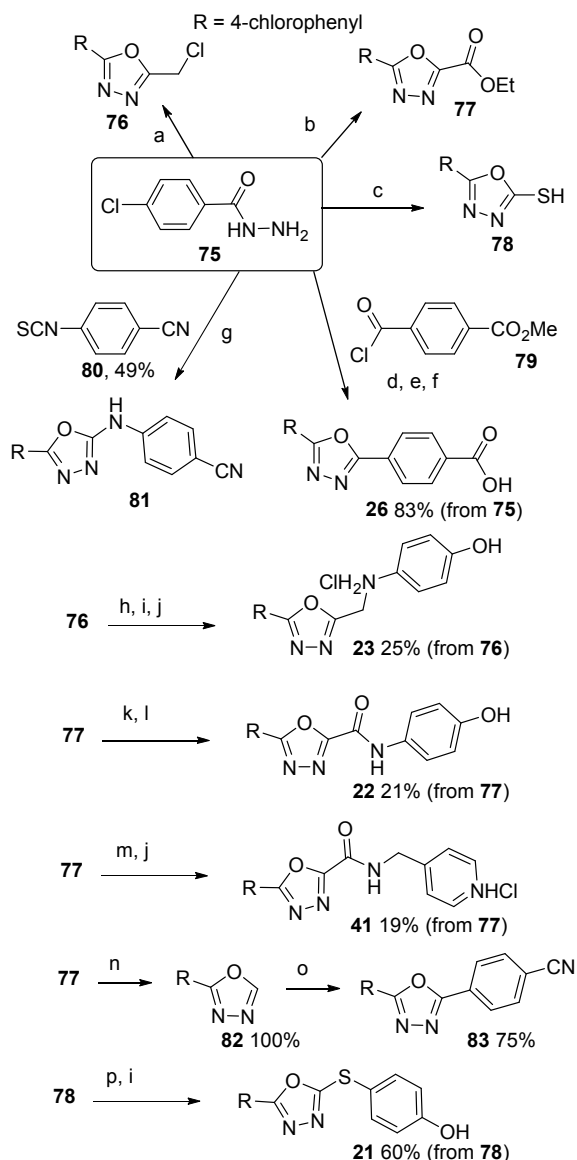


1
2
3 **Scheme 4:** a) Pyridine, toluene, reflux. b) BBr₃, CH₂Cl₂. c) HCl in dioxane, EtOAc

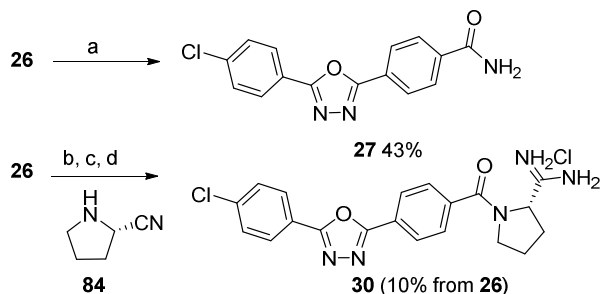


31
32
33
34
35
36
37
38
39
40
41
42
43
44
45
46
47
48
49
50
51
52
53
54
55
56
57
58
59
60

Scheme 5: a) Pd(PPh₃)₄ 10 mol%, Na₂CO₃, DMF, 80 °C. b) DIPEA, DMF, heat. c) HCl in dioxane, EtOAc

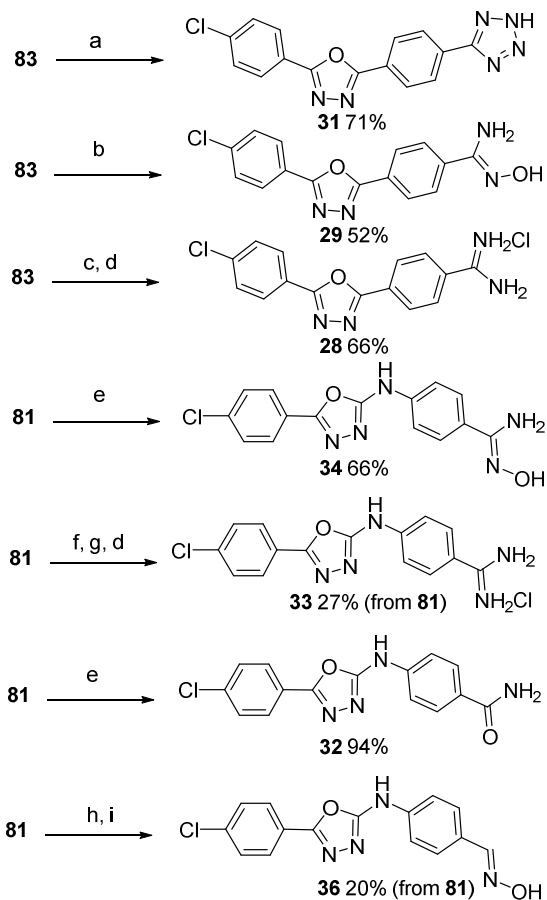


Scheme 6: a) Chloroacetic acid POCl_3 , reflux. b) Ethyl oxalyl chloride, then POCl_3 , 100 °C. c) CS_2 , KOH, MeOH, reflux. d) **79**, pyridine, rt. e) POCl_3 , reflux. f) LiOH, THF/ H_2O , then HCl(aq). g) THF, rt, then tosyl chloride, pyridine, reflux. h) 4-Methoxyaniline, DMSO, K_2CO_3 , rt. i) BBr_3 , CH_2Cl_2 . j) EtOAc, HCl dioxane. k) LiOH, THF/ H_2O , rt. l) 4-Aminophenol, HATU, Et_3N , DMF, rt. m) **74**, EtOH, reflux. n) LiOH, THF/ H_2O , rt, then HCl(aq) pH = 1-2, rt. o) 4-Iodobenzonitrile, CuI 20 mol%, 1,10-phenanthroline 40 mol%, Cs_2CO_3 , DMSO, 100 °C. p) CuI 5 mol%, 1,10-phenanthroline 10 mol%, K_2CO_3 , DMF, 120 °C.



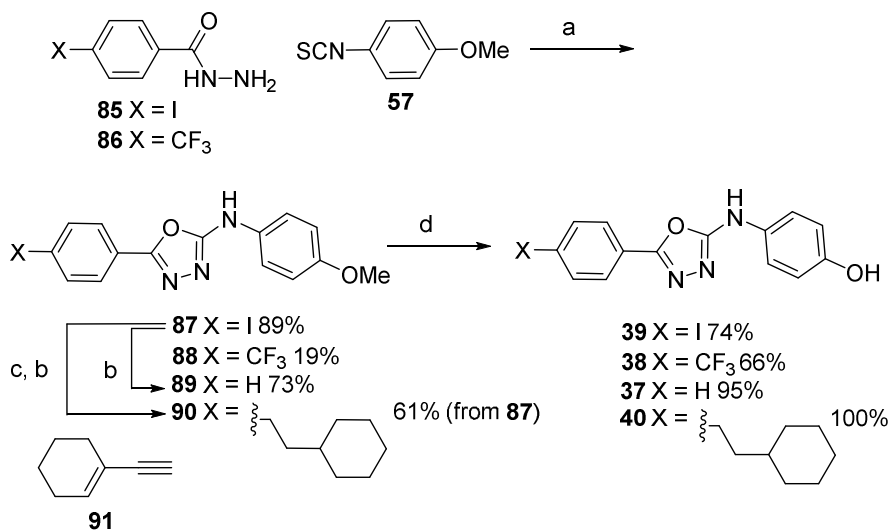
20
21
22
23
24
25
26
27
28
29

Scheme 7: a) Oxalyl chloride, CH_2Cl_2 , DMF cat., NH_4OH , rt. b) **84**, HATU, Et_3N , DMF, rt. c) LiHMDS, THF, rt. d) EtOAc, HCl dioxane.



Scheme 8: a) NH_4Cl , NaN_3 , DMF, 100 °C. b) $\text{NH}_2\text{OH}\cdot\text{HCl}$, Et_3N , EtOH, reflux. c) NaOMe, NH_4Cl , MeOH, 50 °C. d) EtOAc, HCl dioxane. e) H_2SO_4 , H_2O , rt. f) Boc_2O , DMAP 2 mol%, dioxane. g) LiHMDS, THF, HCl (aq). h) DIBAL, toluene, then HCl (aq). i) $\text{NH}_3\text{OH}\cdot\text{Cl}$, Et_3N , MeOH, rt.

A small number of analogues of **1** wherein the chloro substituent was removed or replaced was also generated for this study (Scheme 9). These were prepared by reaction of the benzoyl hydrazine amides **85** and **86** with the isothiocyanate **57** to give **87** (89%) and **88** (19%), respectively. The iodo group in **87** was removed by hydrogenation to give **89** (73%) and coupled to ethynylcyclohexene **91** followed by hydrogenation to give **90** (61%). Demethylation of **87-90** yielded the test compounds **37**, **38**, **39** and **40**.



Scheme 9: a) THF, rt, then TosCl, pyridine, reflux. b) Pd/C, H_2 (g), 1 atm, MeOH / EtOAc, rt. c) **91**, $\text{Pd}(\text{PPh}_3)_2\text{Cl}_2$ 5 mol%, CuI 3 mol%, DMF, Et_3N , rt. d) BBr_3 , CH_2Cl_2

Conclusion: This study delineates the SAR of the extensively utilized SK1/2 inhibitor **1** (SKI-II)⁸ that is also known to induce SK1-degradation⁵ and inhibit Des1.⁶ SK1-kinase inhibition and induction of SK1-degradation appear to be independent effects, where different compounds give rise to either of these effects though some compounds do both. This is consistent with the previous

1
2
3 proposal that compounds may either bind to the substrate (Sph) domain to inhibit SK1-kinase
4
5 activity or to an allosteric site to promote proteasomal degradation of SK1 and that some
6
7 compounds, such as **1** and **5**, do both.^{5c} However, while our data are consistent with this allosteric
8
9 model, other explanations for small molecule promoted SK1-proteasomal degradation, including
10
11 off-target effects, remain a possibility. Importantly, our data do show that PC3 cell growth is not
12
13 inhibited by inhibition of SK1-kinase activity or by SK1-degradation and that inhibition of Des1 is
14
15 the most likely source of the anticancer activity of **1** and its congeners. While SK2 inhibition in
16
17 isolation does not appear to exert a cell growth inhibitory effects (e.g. **31**), the combination of Des1
18
19 and SK2 inhibition may have cooperative effects (e.g. **39**), which also may be of relevance to
20
21 clinical candidate **2**,²⁰ but this cooperativity needs to be further verified. These findings should be
22
23 borne in mind when interpreting findings made using **1** and **2** as probes for SK1/2 activity.^{7,8}
24
25
26
27

28 In the course of this study new lead compounds have been identified exhibiting different activities:
29
30 selective SK2-inhibition by **31** (Table 2, entry 13), dual SK2/Des1 inhibition by **39** (Table 2, entry
31
32 21 and Fig 3); SK1/2 kinase inhibition by **42** (Table 2, entry 24); SK1-degradation by **19** (Fig 2);
33
34 and Des1 and PC3 cell growth inhibition by **34** (Table 2, entry 16 and Fig 3). These new leads
35
36 provide a basis for future studies which will focus on better understanding the source of each of
37
38 these activities and further optimizing them to create valuable probes and potential therapeutics.
39
40
41

42 **Experimental**

43 **PC3 cell viability assays**

44
45 Routine cell culture: PC3 prostate cancer cell lines were cultured in DMEM (containing 10% fetal
46
47 calf serum and penicillin-streptomycin). Cells were grown at 37 °C with 5 % CO₂ and passaged
48
49 when 80-90% confluent 4 times before use. Cells were harvested by trypsin treatment (5 min) then
50
51 quenched with an equal volume of serum containing media and the cell suspension then
52
53 centrifuged at 200 xg for 5 min and the pellet resuspended in 5 mL of media. Cells were exposed
54
55
56
57
58
59
60

1
2
3 to Trypan blue (excludes dead cells) and counted with a haemocytometer. Before treatment with
4
5 drug compounds, cells were plated at 2,500 cells/well in 96 well plates and incubated at 37 °C with
6
7 5 % CO₂ in a humidified incubator for 24 h. Drug stock solutions (50 or 10 mM) were diluted x
8
9 1000 in media to a final concentration of either 50 μM or 10 μM with a DMSO vehicle
10
11 concentration of 0.1%. Compounds were then serially diluted in media (containing 0.1% DMSO)
12
13 to give 8 final concentrations, all at 0.1% DMSO. Cell culture supernatants were aspirated and
14
15 replaced with drug containing media. Drug treatments were performed in duplicate wells, while
16
17 potential plate layout-specific variation in cell growth was accounted for by addition of a vehicle
18
19 control (0.1% DMSO). An untreated control (media only) and active compound control (50 μM **1**)
20
21 was included in each assay. Cells were then incubated with drug compounds at 37 °C with 5 %
22
23 CO₂ in a humidified incubator for 72 h prior to assay. Cell media were diluted with CellTitre
24
25 AQueous One Solution to produce a final concentration of 317 μg/mL. Cell culture supernatants
26
27 were then aspirated from wells and replaced with 100 μL of CellTitre solution. Triplicate cell-free
28
29 control wells containing only CellTitre solution were also included in each assay. Cells were then
30
31 incubated at 37 °C with 5 % CO₂ in a humidified incubator for 1 h at which time absorbance was
32
33 read at 490 nm with a microplate reader. When analysing data, background absorbance (taken from
34
35 cell-free control wells) was subtracted from each reading. To determine percentage inhibition of
36
37 cell viability, absorbance readings for each drug treatment were expressed as a fraction of the
38
39 vehicle control (0.1% DMSO) readings. For each drug concentration the mean (± SEM) is
40
41 calculated and a sigmoidal curve is fitted to the data and used to calculate the IC₅₀ of each
42
43 compound.
44
45
46
47
48
49

50 **Sphingosine kinase-1/2 Activity Assay**

51
52
53 The SphK assays employed, measures SK activity through the production of ³²P-labelled S1P
54
55 following the addition of exogenous Sph and [³²P] ATP as described previously.¹¹
56
57
58
59
60

1
2
3 Activities of SK1 and SK2 were determined using identical assay conditions with the exception
4 that SK1 assays used 3ng/assay recombinant His-tagged human SK1, while SK2 assays used
5 30ng/assay recombinant human SK2.¹²
6
7
8

9
10 Compounds were dissolved in DMSO at 10 mM, the mixture was vortexed (and sonicated if
11 necessary). Stock solutions were kept at 4 °C until used. Aliquots were made containing 100 µM
12 drug compound. These aliquots were then diluted in assay buffer: 100mM Tris/HCl buffer (pH 7.4)
13 containing, 100 mM NaCl, 1 mM sodium orthovanadate, 10 mM NaF to make up a 10 µM
14 solution.
15
16
17
18
19
20

21 **Measurement of dihydrosphingosine desaturase-1 (Des1) activity:**

22
23 Measurement of Des1 activity was performed by HPLC using intact Jurkat cells labeled with
24 DhCer-C6-NBD as described previously¹⁴ with modifications to enhance sensitivity and
25 reproducibility. These modifications included the use of parental Jurkat cells, 0.5% serum in the
26 culture media, and cell harvesting via centrifugation at 500 xg to maximise ceramide extraction.
27
28 Extracted samples (50 µl) were analysed on a Waters HPLC coupled to a fluorescence detector
29 using a 30cm C18 reverse-phase column eluted with 1 ml/min 20% H₂O and 80% acetonitrile with
30 0.1% trifluoroacetic acid. NBD-labelled substrate and product were quantitated with excitation and
31 emission wavelengths of 465 nm and 530 nm, respectively.
32
33
34
35
36
37
38
39
40
41
42

43 **Lipidomics method**

44
45 In vitro cultured PC3 cells were exposed to test compounds (10 µM) or vehicle control (0.1%
46 DMSO) for five hours. Cells were lifted with trypsin, quenched and washed with cold saline (4
47 °C), counted and adjusted to 10⁶ cells per sample. Lipids were extracted from cell pellets by
48 addition of 200 µL chloroform/methanol/water (1:3:1) and three freeze-thaw cycles. Protein and
49 cellular debris was removed by centrifugation and samples stored at -20 °C for <1 week until LC-
50 MS analysis.
51
52
53
54
55
56
57
58
59
60

1
2
3 Lipid analysis utilized LC-MS with reversed phase chromatography (Dionex Ultimate RSLC3000;
4 Thermo) and high resolution mass spectrometry (Q-Exactive; Thermo). 10 μ L sample was injected
5 onto an Ascentis Express C8 column (5cm x2.1mm, 2.7 μ m; Supelco Analytical), with 30 minute
6 gradient elution. Mobile phase A consisted of 40% Isopropanol, 60% H₂O, 2 mM formic acid, 8
7 mM ammonium formate. Mobile phase B: 2% H₂O in isopropanol, 2 mM formic acid, 8 mM
8 ammonium formate. The gradient ran from 0% B to 20% B in 1.5min, to 28% B (7 min) to 35% B
9 (8 min) to 65% B (24 min) at a flow rate of 200 μ L/min, and increased to 100% B at 500 μ L/min
10 (25-27 min), and returned to 100% A (29 min). The mass spectrometer was operated in positive
11 and negative mode (rapid switching) electrospray ionization with a mass resolution of 140,000 and
12 mass accuracy < 2ppm. Data-dependent high resolution (17,500) MSMS was performed on pooled
13 extracts to confirm lipid identifications.

14
15
16 Lipidomics data was analysed using the IDEOM software³² to provide relative quantification of all
17 detected features. Lipids and other metabolites were identified according to accurate mass, with
18 additional manual curation of significant lipids based on retention time and MSMS fragmentation
19 spectra. Ceramides and other sphingolipids were quantified by targeted extraction of peak areas for
20 extracted ion chromatograms using the Tracefinder software (Thermo).

21 22 23 **Soft agar assay:**

24
25
26 To test clonogenic potential and anchorage independent growth of PC3 cells, we performed colony
27 formation assay as previously described.²¹ Briefly, in a 6-well plate, 5,000 filtered PC3 cells were
28 added in the presence of 0.35% low melting point agarose onto a bed of 0.7% low melting point
29 agarose with RPMI media containing 10% Fetal Bovine Serum (FBS) final concentration and
30 allowed to solidify as a single cell suspension at 4 °C for 4 min before incubation at 37 °C in a
31 high CO₂ cell culture incubator. Compounds were diluted in RPMI media and added to cells 24 h
32 after incubation. Plates were incubated at 37 °C for 21 days. Subsequently, media were removed

1
2
3 and colonies visualized after incubation with 0.005% crystal violet (Sigma, USA) solution for 1
4
5 hour at 37 °C. Colonies were scanned and whole wells were counted for positively stained
6
7 colonies.
8
9

10 **Synthesis of test compounds:**

11
12
13 **General:** All reactions were performed under an inert atmosphere of anhydrous N₂ (g) using dry
14 glassware. Tetrahydrofuran (THF), dimethylformamide (DMF) and dichloromethane (DCM) were
15 dried using a commercial solvent purification system. 1,2-Dichloroethane (DCE) and
16 diisopropylethylamine (DIPEA) were purchased in an anhydrous form and stored under nitrogen.
17
18 Other solvents and reagents were used as supplied by commercial vendors without further
19 purifications. Petroleum spirits with a boiling point range of 40-60 °C was used in
20 chromatography. Column (flash) chromatography was performed on either 40-60 μm silica gel or
21 neutral alumina (activation grade III), as indicated. ¹H NMR spectra were recorded at 400 MHz
22 and are reported as follows: chemical shift (δ_H) (integration, multiplicity and coupling constant
23 (Hz)). The following abbreviations were used to explain multiplicities: s = singlet, d = doublet, t =
24 triplet, q = quartet, m = multiplet, br = broad, dd = doublet of doublets, dt = doublet of triplets. ¹³C
25 NMR spectra were recorded at 100 MHz reported in terms of chemical shift (δ_C). All chemical
26 shifts were calibrated using residual nondeuterated solvent as an internal reference and are reported
27 in parts per million relative to trimethylsilane. LCMS was performed using a photodiode array
28 detector (214/254 nm) coupled directly to an electrospray ionization source and a single
29 quadrupole mass analyser (Agilent 6120 Quadrupole MS). The associated LC component
30 employed RP-HPLC carried out at 30 °C on a 5 μm C₈ column, 50 x 4.60 mm (ID). The following
31 buffers were used; buffer A 99.9% H₂O, 0.1% formic acid and buffer B 99.9% CH₃CN, 0.1%
32 formic acid. The following gradient was used with a flow rate of 0.5 mL/min and total run time of
33 12 min; 0–4 mins 95% buffer A and 5% buffer B, 4–7 mins 0% buffer A and 100% buffer B, 7–12
34 mins 95% buffer A and 5% buffer B. High-resolution mass spectra (HRMS) were recorded on a
35
36
37
38
39
40
41
42
43
44
45
46
47
48
49
50
51
52
53
54
55
56
57
58
59
60

1
2
3 time of flight mass spectrometer fitted with either an electrospray (ESI) or atmospheric pressure
4 ionization (APCI) ion source. Compound purity was determined using HPLC and is > 95% for all
5 test compounds, except **15** (93.2%) and **42** (93.8%).
6
7
8

9
10 **5-(4-Chlorophenyl)-N-(4-hydroxyphenyl)-1,3,4-oxadiazol-2-amine 10.**

11
12 2-Bromo-5-(4-chlorophenyl)-1,3,4-oxadiazole (**47**)²² (0.1 g, 0.385 mmol), 4-aminophenol (0.105 g,
13 0.963 mmol) and DIPEA (164 μ L, 0.963 mmol) in DMF (1.5 mL) were heated at 70 °C for 3 h.
14 The cooled solution was partitioned between EtOAc (150 mL) and water (100 mL). The aqueous
15 layer was removed and the organic layer was washed with water (3 \times 100 mL), then brine (20 mL).
16 The organic layer was dried over MgSO₄, concentrated and chromatographed on silica gel eluting
17 with 50% EtOAc in petroleum spirit providing **10** as a beige solid (0.031 g, 28% yield). Mp 252 °C
18 dec. ¹H NMR (400 MHz, DMSO) δ 10.31 (s, 1H), 9.16 (s, 1H), 7.87 (d, J = 8.6 Hz, 2H), 7.63 (d, J
19 = 8.6 Hz, 2H), 7.39 (d, J = 8.9 Hz, 2H), 6.77 (d, J = 8.9 Hz, 2H). ¹³C NMR (101 MHz, DMSO) δ
20 160.4, 156.7, 152.6, 135.3, 130.3, 129.5, 127.1, 122.9, 119.0, 115.5. LCMS R_f (min) = 5.44. MS
21 m/z 288.0 (M + H). HR-ESI calcd for C₁₄H₁₁ClN₃O₂⁺ (M + H) 288.0534, found 288.0534.
22
23
24
25
26
27
28
29
30
31
32
33
34
35
36

37 **4-((5-(4-Chlorophenyl)-1,3,4-thiadiazol-2-yl)amino)phenol 11.**

38
39 2-Bromo-5-(4-chlorophenyl)-1,3,4-thiadiazole (**48**)²² (0.53 g, 1.925 mmol), 4-methoxyaniline
40 (0.595 g, 4.815 mmol) and DIPEA (820 μ L, 4.815 mmol) in DMF (1 mL) were heated at 100–105
41 °C for 2 days. The cooled solution was partitioned between EtOAc (150 mL) and HCl (aq) (0.5 M,
42 100 mL). The aqueous layer was removed and the organic layer was washed with water (3 \times 100
43 mL), then brine (20 mL). The organic layer was dried over MgSO₄ then concentrated to a semi-
44 solid that was triturated with DCM providing the intermediate methyl ether as a golden coloured
45 solid that was filtered and washed with DCM (0.132 g, 22% yield). ¹H NMR (400 MHz, DMSO) δ
46 10.36 (s, 1H), 7.90 – 7.81 (m, 2H), 7.61 – 7.51 (m, 4H), 7.00 – 6.91 (m, 2H), 3.74 (s, 3H).
47
48
49
50
51
52
53
54
55
56
57
58
59
60

1
2
3 BBr₃ (19 μL, 0.2 mmol) was added at to a solution of the methyl ether (above) (0.05 g, 0.157
4 mmol) in dry DCM (5 mL) at 0 °C and stirred at this temperature for 3h. The reaction was quench
5 by dropwise addition of NaHCO₃ (aq) (sat., 1 mL), followed by EtOAc (20 mL) and vigorously
6 stirred for 2 min. H₂O (5 mL) was added to the stirred solution followed by 6 M HCl (aq) until pH
7 = 2. The aqueous layer was removed and the organic layer was washed with water (3 × 30 mL),
8 then brine (20 mL). The organic layer was dried over MgSO₄ and concentrated to a solid that was
9 triturated with EtOAc that was filtered and washed with EtOAc and finally CHCl₃ providing **11** as
10 a light brown powder (0.013 g, 27% yield). Mp = 252 °C. ¹H NMR (400 MHz, DMSO) δ 10.22 (s,
11 1H), 9.23 (s, 1H), 7.84 (d, *J* = 8.7 Hz, 2H), 7.55 (d, *J* = 8.7 Hz, 2H), 7.41 (d, *J* = 8.9 Hz, 2H), 6.77
12 (d, *J* = 8.9 Hz, 2H). ¹³C NMR (101 MHz, DMSO) δ 165.5, 155.2, 153.1, 134.4, 132.5, 129.4,
13 129.2, 128.2, 120.0, 115.6. LCMS *R*_f (min) = 5.66. MS *m/z* 304.0 (M + H). HR-ESI calcd for
14 C₁₄H₁₁ClN₃OS⁺ (M + H) 303.0233, found 303.0230.
15
16
17
18
19
20
21
22
23
24
25
26
27
28
29

30 **4-((5-(4-Chlorophenyl)-4H-1,2,4-triazol-3-yl)amino)phenol 12.**

31
32 Methyl (Z)-*N'*-(4-chlorobenzoyl)-*N*-(4-hydroxyphenyl)carbamimidothioate (**50**)²³ (0.5 g, 1.559
33 mmol) in EtOH (20 mL) was added N₂H₄·H₂O (380 μL, 7.793 mmol) and the mixture was refluxed
34 for 5 h. The cooled solution was concentrated to a solid that was taken up in water (30 mL) and
35 neutralised with AcOH. The resultant solid was filtered and washed with water providing a white
36 solid (0.290 g). The solid was chromatographed on silica gel eluting with 50% EtOAc in petroleum
37 spirit providing **12** as a white solid (0.161 g, 36% yield). Mp = 281 °C. ¹H NMR (400 MHz,
38 DMSO) δ 12.50 (bs, 1H), 9.27 – 8.56 (m, 2H), 7.96 (d, *J* = 8.5 Hz, 2H), 7.70 – 7.43 (m, 2H), 7.35
39 (d, *J* = 8.4 Hz, 2H), 6.69 (d, *J* = 7.9 Hz, 2H). LCMS *R*_f (min) = 5.23. MS *m/z* 287.0 (M + H). HR-
40 ESI calcd for C₁₄H₁₂ClN₄O⁺ (M + H) 287.0694, found 287.0693.
41
42
43
44
45
46
47
48
49
50
51
52
53
54

55 **4-((5-(4-Chlorophenyl)-1,2,4-oxadiazol-3-yl)amino)phenol 13.**

1
2
3 Methyl (Z)-*N*'-(4-chlorobenzoyl)-*N*-(4-hydroxyphenyl)carbamimidothioate (**50**)²³ (0.5 g, 1.559
4 mmol) was added to a mixture of NH₂-OH.HCl (0.542 g, 7.795 mmol) and DBU (1.63 mL, 10.913
5 mmol) in EtOH (20 mL) in which the mixture was refluxed for 4 h. The cooled solution was
6 concentrated to a residue that was taken up in water (30 mL) and neutralised with 6M HCl (aq).
7 The resultant solid was filtered and washed with water providing a white solid (0.308 g). The solid
8 was dissolved in DCM (300 mL) and filtered through a short silica column eluting with 50%
9 EtOAc in petroleum spirit and recrystallised from EtOH providing **15** as a white solid (0.092 g,
10 21% yield). Mp 119–122 °C. ¹H NMR (400 MHz, DMSO) δ 9.65 (s, 1H), 9.05 (s, 1H), 8.06 (d, *J* =
11 8.8 Hz, 2H), 7.71 (d, *J* = 8.8 Hz, 2H), 7.30 (d, *J* = 9.0 Hz, 2H), 6.74 (d, *J* = 8.9 Hz, 2H). ¹³C NMR
12 (101 MHz, DMSO) δ 171.6, 165.7, 151.9, 137.8, 131.8, 129.7, 129.4, 122.6, 118.7, 115.4. LCMS
13 *R*_f (min) = 5.80. MS *m/z* 288.0 (M + H). HR-ESI calcd for C₁₄H₁₁ClN₃O₂⁺ (M + H) 288.0534,
14 found 288.0532.
15
16
17
18
19
20
21
22
23
24
25
26
27
28
29
30
31

32 4-((3-(4-Chlorophenyl)-1,2,4-oxadiazol-5-yl)amino)phenol **14**.

33
34 3-(4-Chlorophenyl)-5-(trichloromethyl)-1,2,4-oxadiazole (**53**)²⁴ (0.613 g, 2.057 mmol) was
35 dissolved in DMSO (9.2 mL) followed by 4-aminophenol (0.748 g, 6.859 mmol) and DBU (1.04
36 mL, 6.909 mmol) at rt. The mixture was stirred at for 3 h then diluted with EtOAc (50 mL) and
37 washed with 1M HCl (aq) (20 mL), then water (4 × 20 mL) and finally brine (20 mL). The organic
38 layer was dried over MgSO₄ and concentrated to a black/brown semi-solid. The crude was
39 triturated with DCM (5 mL) providing a dark brown powder (0.164 g, 85-90% pure). The powder
40 was chromatographed on silica gel eluting with 30% EtOAc in petroleum spirit and recrystallized
41 from isopropanol and petroleum spirit providing **14** as an off-white solid (0.058 g, 10% yield). Mp
42 238–241 °C. ¹H NMR (400 MHz, DMSO) δ 10.75 (s, 1H), 9.28 (s, 1H), 7.97 (d, *J* = 8.7 Hz, 2H),
43 7.61 (d, *J* = 8.7 Hz, 2H), 7.42 (d, *J* = 8.9 Hz, 2H), 6.79 (d, *J* = 8.9 Hz, 2H). ¹³C NMR (101 MHz,
44 DMSO) δ 168.6, 166.6, 153.5, 135.8, 129.5, 129.2, 128.6, 126.1, 120.1, 115.6. LCMS *R*_f (min) =
45
46
47
48
49
50
51
52
53
54
55
56
57
58
59
60

1
2
3 5.80. MS m/z 288.0 (M + H). HR-ESI calcd for $C_{14}H_{11}ClN_3O_2^+$ (M + H) 288.0534, found
4 288.0531.
5
6
7
8

9
10 **4-((5-(4-chlorophenyl)-1,2,4-thiadiazol-3-yl)amino)phenol 15**

11 Pd(PPh₃)₄ (0.102 g, 0.0882 mmol) and CuTC (0.034 g, 0.176 mmol) were added to a solution of
12 (4-chlorophenyl)trimethylstannane (0.730 g, 1.76 mmol) and 3-bromo-5-chloro-1,2,4-thiadiazole
13 (0.17 mL, 1.76 mmol) in dry 1,4-dioxane (5.5 mL) and N₂ (g) bubbled through the mixture for 10
14 min to remove any oxygen. The mixture was then heated under N₂ (g) to 60 °C and left to stir
15 overnight. Upon completion of the reaction (TLC), the mixture was partitioned in EtOAc (50 mL)
16 and washed with H₂O (2 x 30 mL). The aqueous layers were then collected and back extracted
17 with EtOAc (2 x 30 mL). The organic layers were then combined dried over MgSO₄ and
18 concentrated to a brown solid (0.994 g). The crude material was then chromatographed on silica
19 gel eluting with 5% EtOAc in petroleum spirit to give -bromo-5-(4-chlorophenyl)-1,2,4-thiadiazole
20 **56** as a white solid (0.336 g, 69% yield). ¹H NMR (400 MHz, CDCl₃) δ 7.89 (d, *J* = 8.8 Hz, 2H),
21 7.50 (d, *J* = 8.8 Hz, 2H). ¹³C NMR (101 MHz, CDCl₃) δ 189.1, 146.2, 139.3, 129.9, 128.7, 127.9.
22 LCMS *R*_f (min) = 4.14. MS m/z 275.0 (M + 2H).
23
24
25
26
27
28
29
30
31
32
33
34
35
36
37
38

39 A solution of **56** (0.129 g, 0.468 mmol), *p*-anisidine (0.231 g, 1.873 mmol) and DIPEA (0.38 mL,
40 2.107 mmol) in dry NMP (2 mL) was heated to 160 °C in a microwave reactor for 3.5 h. The
41 resultant mixture was diluted with EtOAc (50 mL) and washed with 0.5 M HCl (aq) (20 mL), H₂O
42 (2 x 20 mL) and brine (20 mL). The aqueous layers were then collected and back extracted with
43 EtOAc (3 x 30 mL). The organic layers were then combined dried over MgSO₄ and concentrated to
44 a dark brown solid (0.09 g). Trituration with DCM lead to a crystalline gold solid being produced
45 (0.022 g). The filtrate was then chromatographed on silica gel eluting with 10% EtOAc in
46 petroleum spirit. The appropriate fractions were collected and concentrated giving 5-(4-
47 chlorophenyl)-N-(4-methoxyphenyl)-1,2,4-thiadiazol-3-amine as a gold crystalline solid (0.077 g,
48
49
50
51
52
53
54
55
56
57
58
59
60

1
2
3 51% yield). ^1H NMR (400 MHz, DMSO) δ 10.20 (s, 1H), 7.98 (d, J = 8.7 Hz, 2H), 7.67 (dd, J =
4 8.9, 2.3 Hz, 4H), 6.90 (d, J = 9.1 Hz, 2H), 3.72 (s, 3H). ^{13}C NMR (101 MHz, DMSO) δ 183.8,
5 166.7, 154.0, 136.8, 133.9, 129.7, 128.7, 128.7, 118.5, 114.0, 55.2. LCMS R_f (min) = 7.03. MS m/z
6 318.0 (M + H).
7
8
9

10
11
12 BBr_3 (0.057 mL, 0.604 mmol) was added dropwise to a solution of 5-(4-chlorophenyl)-N-(4-
13 methoxyphenyl)-1,2,4-thiadiazol-3-amine (0.048 g, 0.151 mmol) in dry DCM (2.5 mL) at 0 °C and
14 the mixture left to stir at room temperature for 2 h. The mixture was then quenched with NaHCO_3
15 (aq) (sat., 5 mL), H_2O (20 mL) added and the mixture left to stir for 0.5 h. The solution was then
16 extracted with EtOAc (3 x 20 mL). The organic layers were combined and washed with NaHCO_3
17 (2x 20 mL) and brine (10 mL), dried over MgSO_4 and concentrated to dark brown solid (0.037 g).
18 The crude material was chromatographed on silica gel eluting with 15% EtOAc in petroleum spirit
19 giving **15** as a tan crystalline solid (0.019 g, 41% yield). ^1H NMR (400 MHz, DMSO) δ 10.06 (s,
20 1H), 9.04 (s, 1H), 7.97 (d, J = 8.6 Hz, 2H), 7.66 (d, J = 8.6 Hz, 2H), 7.54 (d, J = 8.9 Hz, 2H), 6.71
21 (d, J = 8.9 Hz, 2H). ^{13}C NMR (101 MHz, DMSO) δ 183.7, 166.9, 152.0, 136.7, 132.5, 129.7,
22 128.8, 128.7, 118.8, 115.2. LCMS R_f (min) = 6.36. MS m/z 304.0 (M + H). HR-ESI calcd for
23 $\text{C}_{14}\text{H}_{10}\text{ClN}_3\text{OS}^+$ (M + H) 304.0306, found 304.0316.
24
25
26
27
28
29
30
31
32
33
34
35
36
37
38
39
40
41

42 **4-((3-(4-Chlorophenyl)-1,2,4-thiadiazol-5-yl)amino)phenol 16.**

43
44 A solution of 3-bromo-N-(4-methoxyphenyl)-1,2,4-thiadiazol-5-amine **58**²⁶ (50 mg, 0.175 mmol),
45 DMAP (2 mg, 0.00875 mmol) and Boc_2O (115 mg, 0.525 mmol) in dry 1,4-dioxane (0.5 mL) was
46 heated to 60 °C for 20 min, at which point the evolution of gas ceased. The solution was cooled to
47 rt, diluted with EtOAc (30 mL) and filtered through a short silica plug. The filtrate was
48 concentrated under reduced pressure to produce *tert*-butyl(3-bromo-1,2,4-thiadiazol-5-yl)(4-
49 methoxyphenyl)carbamate as a pale yellow solid (68 mg, 100% yield). ^1H NMR (400 MHz,
50 DMSO) δ 7.37 (d, J = 9.0 Hz, 2H), 7.03 (d, J = 9.0 Hz, 2H), 3.82 (s, 3H), 1.40 (s, 9H). ^{13}C NMR
51
52
53
54
55
56
57
58
59
60

(101 MHz, CDCl₃) δ 180.3, 159.6, 153.4, 146.8, 140.8, 130.1, 128.8, 114.6, 55.5, 27.9, 27.4.
LCMS *R_f* (min) = 4.11. EIMS *m/z* 387.2 (M + H).

Pd(*t*Bu₃P)₂ (0.010 g, 0.0181 mmol) was added to a solution of *tert*-butyl(3-bromo-1,2,4-thiadiazol-5-yl)(4-methoxyphenyl)carbamate (0.140 g, 0.363 mmol) and (4-chlorophenyl)trimethyltin **55** (0.200 g, 0.725 mmol) in dry 1,4-dioxane (5 mL) and N₂ (g) was then bubbled through the mixture for 10 min then heated under N₂ (g) at reflux for 16 h. The mixture was diluted with EtOAc (50 mL), washed with H₂O (2 x 20 mL) and aqueous layers back extracted with EtOAc (2 x 20 mL). The combined organic layers were then dried over MgSO₄ and concentrated to a brown solid (0.254 g). This material was chromatographed on silica gel eluting with 5% EtOAc in petroleum spirit to give *tert*-butyl(3-(4-chlorophenyl)-1,2,4-thiadiazol-5-yl)(4-methoxyphenyl)carbamate as a light tan crystalline solid (0.069 g, 44% yield). ¹H NMR (400 MHz, CDCl₃) δ 7.98 (d, *J* = 8.7 Hz, 2H), 7.31 (d, *J* = 8.7 Hz, 2H), 7.20 (d, *J* = 9.0 Hz, 2H), 6.99 (d, *J* = 9.0 Hz, 2H), 3.90 (s, 3H), 1.48 (s, 9H). ¹³C NMR (101 MHz, CDCl₃) δ 179.6, 166.6, 159.4, 153.6, 135.9, 131.8, 131.2, 129.4, 129.2, 128.7, 114.4, 85.0, 55.6, 31.1, 28.1. LCMS *R_f* (min) = 4.761. EIMS *m/z* 418.1 (M + H).

To *tert*-butyl(3-(4-chlorophenyl)-1,2,4-thiadiazol-5-yl)(4-methoxyphenyl)carbamate (0.0224 g, 0.0536 mmol) in dry DCM (1 mL) was added TFA (0.1 mL) dropwise at 0 °C. The mixture was then left to stir at room temperature for 2.5 h. The mixture was then concentrated to produce 3-(4-chlorophenyl)-N-(4-methoxyphenyl)-1,2,4-thiadiazol-5-amine as a light brown crystalline solid (0.017 g, 100% yield). ¹H NMR (400 MHz, CDCl₃) δ 8.05 (d, *J* = 8.6 Hz, 2H), 7.52 (d, *J* = 8.6 Hz, 2H), 7.29 – 7.24 (m, 2H), 7.00 (d, *J* = 8.9 Hz, 2H), 3.85 (s, 3H). ¹³C NMR (101 MHz, CDCl₃) δ 179.9, 160.5, 158.9, 138.7, 130.7, 129.7, 129.2, 126.7, 122.6, 115.6, 55.8. LCMS *R_f* (min) = 6.97. EIMS *m/z* 318.0 (M + H).

BBr₃ (0.025 mL, 0.268 mmol) was added dropwise to 3-(4-chlorophenyl)-N-(4-methoxyphenyl)-1,2,4-thiadiazol-5-amine (0.0284 g, 0.0894 mmol) in dry DCM (1 mL) at 0 °C and left to stir at rt

1
2
3 for 2 h. The reaction was quenched with NaHCO₃ (aq) (sat., 3 mL) diluted with H₂O (15 mL) and
4
5 extracted with EtOAc (3 x 20 mL). The organic layers were combined and washed with NaHCO₃
6
7 (aq) (sat., 2 x 20 mL), brine (10 mL) before, dried over MgSO₄ and concentrated to brown solid
8
9 (0.024 g). The crude material was then chromatographed on silica gel eluting with 30% EtOAc in
10
11 petroleum spirit. The appropriate fractions were collected and concentrated to give **16** light brown
12
13 crystalline solid (0.017 g, 62% yield). ¹H NMR (400 MHz, CDCl₃) δ 8.12 (d, *J* = 8.7 Hz, 2H), 7.42
14
15 (d, *J* = 8.7 Hz, 2H), 7.21 (d, *J* = 8.8 Hz, 2H), 6.91 (d, *J* = 8.8 Hz, 2H). ¹³C NMR (101 MHz,
16
17 DMSO) δ 167.5, 153.8, 134.8, 131.7, 129.3, 128.9, 120.3, 115.9. LCMS *R*_f (min) = 6.31. EIMS
18
19 *m/z* 304.0 (M + H). HR-ESI calcd for C₁₄H₁₀ClN₃OS⁺ (M + H) 304.0306, found 304.0317.
20
21
22
23

24 **4-((5-(4-Chlorophenyl)oxazol-2-yl)amino)phenol 17.**

25
26 2-Bromo-1-(4-chlorophenyl)ethan-1-one (**59**) (1.07 g, 4.57 mmol) was dissolved in acetone (75
27
28 mL) and sodium azide (0.59 g, 9.08 mmol) was added to the stirred mixture in one portion and
29
30 allowed to stir at rt overnight. The mixture was concentrated to a residue and then partitioned
31
32 between DCM (50 mL) and H₂O (30 mL) and the aqueous layer extracted with DCM (2 × 30 mL).
33
34 The combined organic layers were dried over MgSO₄ and concentrated to the intermediate azide as
35
36 an orange solid (0.796 g, 89%). The azide (0.796 g, 4.069 mmol) was dissolved in anhydrous 1,4-
37
38 dioxane in an N₂ atmosphere and 1-isothiocyanato-4-methoxybenzene (468 μL, 3.391 mmol) was
39
40 added, followed by PPh₃ (1.07 g, 4.069 mmol). The mixture was stirred with heating on an oil bath
41
42 (100 °C) for 15 min. The cooled solution was concentrated and the resulting solid recrystallized
43
44 from DCM, providing 5-(4-chlorophenyl)-*N*-(4-methoxyphenyl)oxazol-2-amine (**60**) as an off-
45
46 white solid (0.77 g, 76% yield). Mp 165–167 °C. ¹H NMR (400 MHz, CDCl₃) δ 7.44 (d, *J* = 8.7
47
48 Hz, 2H), 7.40 (d, *J* = 9.1 Hz, 2H), 7.34 (d, *J* = 8.8 Hz, 2H), 7.11 (s, 1H), 6.92 (d, *J* = 9.1 Hz, 2H),
49
50 6.74 (s, 1H), 3.81 (s, 3H).
51
52
53
54

55
56 BBr₃ (79 μL, 0.831 mmol) was added to a solution of **60** (0.05 g, 0.166 mmol) in DCM (5 mL) at 0
57
58 °C and the mixture then warmed to rt for 3 h. The reaction was then quenched with NaHCO₃ (aq)
59
60

(sat., 10 mL) and diluted with EtOAc (20 mL). The organic layer was washed with NaHCO₃ (aq) (sat., 10 mL), H₂O (10 mL) and brine (10 mL), dried over MgSO₄ and concentrated to a pink solid (0.05 g). The solid was chromatographed on silica gel eluting with 5% MeOH in DCM providing **17** as a light pink solid (0.031 g, 65%). Mp 191–193 °C. ¹H NMR (400 MHz, DMSO) δ 9.97 (s, 1H), 9.05 (s, 1H), 7.56 (d, *J* = 8.7 Hz, 2H), 7.47 (d, *J* = 8.8 Hz, 2H), 7.45 (s, 1H), 7.41 (d, *J* = 8.9 Hz, 2H), 6.72 (d, *J* = 8.9 Hz, 2H). ¹³C NMR (101 MHz, DMSO) δ 157.3, 152.1, 142.2, 131.1, 130.9, 129.0, 127.1, 123.9, 123.6, 118.5, 115.4. LCMS *R*_f (min) = 5.85. MS *m/z* 287.0 (M + H). HR-ESI calcd for C₁₅H₁₂ClN₂O₂⁺ (M + H) 287.0582, found 287.0579.

(2S,3S)-2-((4-(5-(4-Chlorophenyl)-1,2,4-oxadiazol-3-yl)benzyl)carbamoyl)-3-hydroxypyrrolidin-1-ium chloride 18.

4-Chlorobenzoyl chloride (**46**) (332 μL, 2.615 mmol) was added to a solution of (*Z*)-4-(azidomethyl)-*N'*-hydroxybenzimidamide **63**²⁷ (0.5 g, 2.615 mmol) in xylene (10 mL) and pyridine (1.5 mL) and refluxed for 2 h. The cooled (rt) mixture was diluted with EtOAc (100 mL) and washed with HCl (aq) (1 M, 30 mL), water (50 mL), NaHCO₃ (aq) (sat., 50 mL) and finally brine (30 mL). The organic layer was dried over MgSO₄ and concentrated to give **63** as a white solid (0.8 g, 98%). ¹H NMR (400 MHz, CDCl₃) δ 8.25 – 8.12 (m, 4H), 7.55 (d, *J* = 8.8 Hz, 2H), 7.48 (d, *J* = 8.5 Hz, 2H), 4.44 (s, 2H).

Ammonium formate (0.303 g, 4.812 mmol) and freshly activated zinc dust (0.315 g, 4.812 mmol) were added to a solution oxadiazole **63** (0.2 g, 0.642 mmol) in MeOH (17 mL) and stirred at rt for 3 h. The mixture was diluted with water (50 mL) and DCM (50 mL) and vigorously stirred. Then three pellets of NaOH (~ 0.6 g) were added and vigorous stirring continued for a further 30 min. The mixture was then filtered through celite, the organic layer was separated, dried over MgSO₄ and concentrated to provide (4-(5-(4-chlorophenyl)-1,2,4-oxadiazol-3-yl)phenyl)methanamine as a solid (0.181 g, 98%). ¹H NMR (400 MHz, CDCl₃) δ 8.17 (d, *J* = 8.8 Hz, 2H), 8.13 (d, *J* = 8.3 Hz, 2H), 7.54 (d, *J* = 8.8 Hz, 2H), 7.47 (d, *J* = 8.5 Hz, 2H), 3.97 (s, 2H), 1.55 (bs, 2H).

HATU (0.359 g, 0.945 mmol) and DIPEA (429 μ L, 2.52 mmol) were added to a solution of (4-(5-(4-chlorophenyl)-1,2,4-oxadiazol-3-yl)phenyl)methanamine (above) (0.18 g, 0.629 mmol) and (2*S*,3*S*)-1-(*tert*-butoxycarbonyl)-3-hydroxypyrrolidine-2-carboxylic acid (**64**) (0.146 g, 0.629 mmol) in DMF (5 mL) and the mixture stirred at rt for 16 h, diluted with water (100 mL) and extracted with (2 \times 50 mL). The combined organics were washed with water (20 mL), HCl (aq) (0.5 M, 50 mL), NaHCO₃ (aq) (sat., 30 mL) and finally brine (30 mL). The organic layer was dried over MgSO₄ and concentrated to provide Boc protected product as a solid (0.36 g). The solid was recrystallised from MeOH providing an off-white solid (0.16 g, 51%). ¹H NMR (400 MHz, CDCl₃) δ 8.16 (d, *J* = 8.8 Hz, 2H), 8.11 (d, *J* = 8.1 Hz, 2H), 7.54 (d, *J* = 8.7 Hz, 2H), 7.40 (d, *J* = 8.3 Hz, 2H), 4.83 – 4.19 (m, 4H), 3.77 – 3.43 (m, 2H), 2.23 – 1.27 (m, 13H).

HCl in 1,4-dioxane (4 M, 1.0 mL) was added to a solution of the Boc derivative (above) (0.11 g, 0.221 mmol) in EtOAc (1 mL) and the mixture stirred at rt for 18 h. The resulting precipitate was filtered and washed with EtOAc (2 mL) providing **18** as an off-white solid (0.85 g, 89% yield. Mp 278 °C dec. ¹H NMR (400 MHz, DMSO) δ 9.98 (bs, 1H), 9.41 (t, *J* = 5.9 Hz, 1H), 8.68 (bs, 1H), 8.19 (d, *J* = 8.8 Hz, 2H), 8.06 (d, *J* = 8.4 Hz, 2H), 7.75 (d, *J* = 8.8 Hz, 2H), 7.52 (d, *J* = 8.4 Hz, 2H), 5.92 (bs, 1H), 4.55 – 4.34 (m, 3H), 4.14 (s, 1H), 3.40 (s, 2H), 2.03 – 1.85 (m, 2H). ¹³C NMR (101 MHz, DMSO) δ 174.6, 168.1, 166.6, 142.4, 138.2, 129.8, 129.7, 128.1, 127.2, 124.7, 122.2, 73.9, 66.3, 44.1, 42.4, 32.3. LCMS *R*_f (min) = 4.97. LCMS *R*_f (min) = 4.97. MS *m/z* 399.1 (M + H). HR-ESI calcd for C₂₀H₂₀ClN₄O₃⁺ (M + H) 399.1218, found 399.1217.

(2*S*,3*S*)-2-((4-(3-(4-Chlorophenyl)-1,2,4-oxadiazol-5-yl)benzyl)carbamoyl)-3-hydroxypyrrolidin-1-ium chloride **19.**

Isobutylchloroformate (0.34 mL, 2.6 mmol) was added dropwise to a solution of *N*-methylmorpholine (275 μ L, 2.5 mmol) and 4-(((*tert*-butoxycarbonyl) amino)methyl)benzoic acid (**65**) (0.628 g, 2.5 mmol) in 1,4-dioxane (25 mL) at 0 °C. After 5 min (*Z*)-4-chloro-*N*-hydroxybenzimidamide (**52**) (0.427 g, 2.5 mmol) was added and stirred at rt for 2 h then reflux for

1
2
3 2 h. The cooled (rt) solution was concentrated to a solid and then taken up in EtOAc (150 mL) and
4
5 washed consecutively with H₂O (50 mL), NaHCO₃ (sat., 50 mL), H₂O (50 mL), HCl (aq) (0.5 M,
6
7 50 mL) and brine (30 mL). The organic layer was dried over MgSO₄ and concentrated to a solid
8
9 (0.94 g) and chromatographed on silica gel eluting with 20% EtOAc in petroleum spirit providing
10
11 the Boc protected product as a white solid (0.48 g, 50%). ¹H NMR (400 MHz, CDCl₃) δ 8.18 (d, *J*
12
13 = 8.4 Hz, 2H), 8.12 (d, *J* = 8.7 Hz, 2H), 7.51 – 7.44 (m, 4H), 5.06 – 4.88 (m, 1H), 4.42 (d, *J* = 5.7
14
15 Hz, 2H), 1.48 (s, 9H).

16
17
18
19 A solution of HCl in 1,4-dioxane (4 M, 2 mL) was added to a solution of the oxadiazole above (0.2
20
21 g, 0.518 mmol) in EtOAc (2 mL) and the mixture stirred at rt for 20 h. The resultant precipitate
22
23 was filtered and washed with EtOAc (1.0 mL) and diethyl ether (2.0 mL) giving **66** as a white
24
25 (0.12 g, 72%). ¹H NMR (400 MHz, DMSO) δ 8.36 (bs, 3H), 8.26 (d, *J* = 8.4 Hz, 2H), 8.11 (d, *J* =
26
27 8.7 Hz, 2H), 7.76 (d, *J* = 8.4 Hz, 2H), 7.70 (d, *J* = 8.7 Hz, 2H), 4.18 (s, 2H).

28
29
30
31 A portion of the oxadiazole **66** (0.1 g, 0.3104 mmol) was suspended in DMF (2.5 mL) and to this
32
33 mixture was added HATU (0.177 g, 0.466 mmol), (2*S*,3*S*)-1-(*tert*-butoxycarbonyl)-3-
34
35 hydroxypyrrolidine-2-carboxylic acid (0.072 g, 0.3104 mmol) and finally DIPEA (264 μL, 1.552
36
37 mmol) and stirred at rt overnight. The mixture was diluted with EtOAc (50 mL), washed with H₂O
38
39 (30 mL), dried over MgSO₄, concentrated (0.191 g) and crystallised from a small amount of
40
41 EtOAc to give the Boc-**19** (0.15 g, 97%). ¹H NMR (400 MHz, CDCl₃) δ 8.16 (d, *J* = 8.1 Hz, 2H),
42
43 8.11 (d, *J* = 8.8 Hz, 2H), 7.49 (d, *J* = 8.7 Hz, 2H), 7.45 (d, *J* = 8.3 Hz, 2H), 4.92 – 4.17 (m, 4H),
44
45 3.79 – 3.42 (m, 2H), 2.27 – 1.86 (m, 4H), 1.57 – 1.32 (m, 9H).

46
47
48
49 HCl in 1,4-dioxane (4 M, 3 mL) was added to a solution of the Boc protected derivative (above)
50
51 (0.15 g, 0.3 mmol) in EtOAc (2 mL) and the solution at rt for 15 h. The resultant precipitate was
52
53 filtered and washed sequentially with small portions of EtOAc (2.0 mL), isopropanol (1.0 mL) and
54
55 diethyl ether (2.0 mL) providing **19** as an off-white solid (0.117 g, 90%). Mp 284 °C dec. ¹H NMR
56
57
58
59
60

(400 MHz, DMSO) δ 10.10 (bs, 1H), 9.51 (t, J = 6.0 Hz, 1H), 8.67 (bs, 1H), 8.15 (d, J = 8.4 Hz, 2H), 8.09 (d, J = 8.7 Hz, 2H), 7.68 (d, J = 8.7 Hz, 2H), 7.59 (d, J = 8.4 Hz, 2H), 5.97 (bs, 1H), 4.49 (d, J = 5.9 Hz, 2H), 4.43 (bs, 1H), 4.16 (d, J = 1.8 Hz, 1H), 3.43 – 3.24 (m, 4H), 2.03 – 1.85 (m, 2H). ^{13}C NMR (101 MHz, DMSO) δ 175.5, 167.5, 166.8, 144.4, 136.4, 129.5, 128.9, 128.3, 128.1, 125.0, 121.9, 73.9, 66.3, 44.1, 42.3, 32.4. LCMS R_f (min) = 4.98. MS m/z 399.1 (M + H). HR-ESI calcd for $\text{C}_{20}\text{H}_{20}\text{ClN}_4\text{O}_3^+$ (M + H) 399.1218, found 399.1217.

4-(5-(4-Chlorophenyl)-1,3,4-oxadiazol-2-yl)phenol **20**.

A solution of 5-(4-chlorophenyl)-2H-tetrazole (**67**) (0.5 g, 2.769 mmol), 4-methoxybenzoyl chloride **46** (750 μL , 5.537 mmol) and pyridine (269 μL , 3.322 mmol) in toluene (10 mL) was refluxed for 3 h. The cooled (rt) solution was diluted with EtOAc (50 mL) and then washed with water (30 mL), saturated NaHCO_3 aq (30 mL) and brine (20 mL), dried over MgSO_4 and concentrated to a solid (1.1 g) that was recrystallized from EtOH, providing **70** as a white solid (0.692 g, 87% yield). ^1H NMR (400 MHz, CDCl_3) δ 8.13 – 8.02 (m, 4H), 7.51 (d, J = 8.8 Hz, 2H), 7.04 (d, J = 9.0 Hz, 2H), 3.90 (s, 3H).

BBr_3 (296 μL , 3.14 mmol) was added dropwise to a solution of the oxadiazole **70** (0.3 g, 1.046 mmol) in DCM (10 mL) at 0 °C and stirred for 1 h. The mixture was quenched with NaHCO_3 (aq) (sat., 10 mL) then extracted with EtOAc (250 mL). The aqueous layer was separated and the organic layer was dried over MgSO_4 and concentrated to a solid that was triturated with DCM (7 mL) providing **20** as a white solid (0.26 g, 91% yield). Mp 262–266 °C. ^1H NMR (400 MHz, DMSO) δ 10.34 (s, 1H), 8.06 (d, J = 8.5 Hz, 2H), 7.93 (d, J = 8.7 Hz, 2H), 7.64 (d, J = 8.5 Hz, 2H), 6.96 (d, J = 8.7 Hz, 2H). ^{13}C NMR (101 MHz, DMSO) δ 164.4, 162.5, 161.0, 136.5, 129.5, 128.7, 128.2, 122.4, 116.2, 114.0. LCMS R_f (min) = 5.84. MS m/z 273.1 (M + H). HR-ESI calcd for $\text{C}_{14}\text{H}_{10}\text{ClN}_2\text{O}_2^+$ (M + H) 273.0425, found 273.0422.

4-((5-(4-Chlorophenyl)-1,3,4-oxadiazol-2-yl)thio)phenol **21**.

1
2
3 A solution of 5-(4-chlorophenyl)-1,3,4-oxadiazole-2(3*H*)-thione **78** (0.213 g, 1 mmol) in DMF (3
4 mL) was added to a solution of CuI (0.0096 g, 0.05 mmol), 1,10-phenanthroline (0.018 g, 0.1
5 mmol), K₂CO₃ (0.18 g, 1.3 mmol) and 4-iodoanisole (0.281 g, 1.2 mmol) in DMF (3 mL) and the
6 mixture stirred at 120 °C for 10 h. The cooled (rt) solution was diluted with water (100 mL) and
7 extracted with EtOAc (3 × 30 mL). The combined organics were washed with water (3 × 20 mL)
8 and brine (30 mL) dried over MgSO₄ and concentrated to a residue that was chromatographed on
9 silica gel eluting with 10% EtOAc in petroleum spirit providing an oil that slowly solidified to a
10 clear solid (0.225 g, 71% yield). ¹H NMR (400 MHz, CDCl₃) δ 7.88 (d, *J* = 8.8 Hz, 2H), 7.63 (d, *J*
11 = 9.0 Hz, 2H), 7.45 (d, *J* = 8.8 Hz, 2H), 6.97 (d, *J* = 8.9 Hz, 2H), 3.85 (s, 3H).
12
13
14
15
16
17
18
19
20
21
22

23
24 BBr₃ (200 μL, 2.12 mmol) was added dropwise to a solution of the above methyl ether (0.225 g,
25 0.706 mmol) in DCM (8 mL) at 0 °C then stirred for 4 h at rt. The mixture was quenched with
26 NaHCO₃ (sat., 10 mL) then diluted DCM (30 mL) and the aqueous layer extracted with DCM (10
27 mL). The combined organic phases were dried over MgSO₄ and concentrated to a foam and
28 chromatographed on silica gel eluting with 20% EtOAc in petroleum spirit providing **21** as a white
29 solid (0.183 g, 85% yield). Mp 154–156 °C. ¹H NMR (400 MHz, CDCl₃) δ 8.36 (s, 1H), 7.92 (d, *J*
30 = 8.7 Hz, 2H), 7.47 (d, *J* = 8.8 Hz, 2H), 7.45 (d, *J* = 8.8 Hz, 2H), 6.73 (d, *J* = 8.7 Hz, 2H). ¹³C
31 NMR (101 MHz, CDCl₃) δ 166.8, 165.3, 159.6, 138.5, 137.1, 129.7, 128.1, 121.8, 117.9, 113.4.
32 LCMS *R*_f (min) = 5.89. MS *m/z* 305.1 (M + H). HR-ESI calcd for C₁₄H₁₀ClN₂O₂S⁺ (M + H)
33 305.0146, found 305.0141.
34
35
36
37
38
39
40
41
42
43
44
45
46
47
48
49

50 **5-(4-Chlorophenyl)-N-(4-hydroxyphenyl)-1,3,4-oxadiazole-2-carboxamide 22.**

51
52 LiOH (aq) (10% w/v, 10 mL) was added to a solution of ethyl 5-(4-chlorophenyl)-1,3,4-
53 oxadiazole-2-carboxylate **77** (1 g, 3.958 mmol) in THF (20 mL) and MeOH (39 mL) at 0 °C. The
54 mixture was concentrated to a solid and triturated with 20% EtOAc in petroleum spirit. The solid
55
56
57
58
59
60

1
2
3 was collected and washed with ether providing lithium 5-(4-chlorophenyl)-1,3,4-oxadiazole-2-
4
5 carboxylate as an off-white solid (0.852 g, 93% yield). ^1H NMR (400 MHz, D_2O) δ 7.93 (dd, J =
6
7 8.4, 1.2 Hz, 1H), 7.55 (dd, J = 8.5, 1.1 Hz, 1H).
8
9

10 A solution of the lithium salt (above) (0.15 g, 6.507 mmol), 4-aminophenol (0.092 g < 0.846
11 mmol), HATU (0.371 g, 0.976 mmol) and Et_3N (272 μL , 1.952 mmol) in DMF (5 mL) was stirred
12
13 at rt for 15 h, then diluted with H_2O (10 mL) giving a precipitate. The solid was recrystallised from
14
15 EtOH providing **22** as an off-white solid (0.048 g, 23% yield). Mp 259 $^\circ\text{C}$ dec. ^1H NMR (400
16
17 MHz, DMSO) δ 11.02 (s, 1H), 9.46 (s, 1H), 8.13 (d, J = 8.8 Hz, 2H), 7.74 (d, J = 8.8 Hz, 2H), 7.59
18
19 (d, J = 9.0 Hz, 2H), 6.78 (d, J = 9.0 Hz, 2H). ^{13}C NMR (101 MHz, DMSO) δ 164.4, 158.8, 154.7,
20
21 150.9, 137.5, 129.8, 129.0, 129.0, 122.6, 121.8, 115.2. LCMS R_f (min) = 6.03. MS m/z 316.0 (M +
22
23 H). HR-ESI calcd for $\text{C}_{15}\text{H}_{11}\text{ClN}_3\text{O}_3^+$ (M + H) 316.0483, found 316.0482.
24
25
26
27
28

29 **N-((5-(4-Chlorophenyl)-1,3,4-oxadiazol-2-yl)methyl)-4-hydroxybenzenaminium chloride 23.**
30
31

32 2-(Chloromethyl)-5-(4-chlorophenyl)-1,3,4-oxadiazole **76** (0.1 g, 0.437 mmol) was dissolved in
33
34 DMSO (440 μL) and to the mixture was added 4-methoxyaniline (0.062 g, 0.5 mmol) followed by
35
36 K_2CO_3 (0.175 g, 1.264 mmol) and stirred at rt overnight. The mixture was diluted with EtOAc (20
37
38 mL) and washed with water (4 \times 30 mL) and then brine (10 mL). The organic layer was dried over
39
40 MgSO_4 and concentrated to a brown/amber resin (0.139 g). The resin was chromatographed on
41
42 silica gel eluting with 5% EtOAc in DCM providing the product as an off-white solid (0.057 g,
43
44 41% yield). ^1H NMR (400 MHz, CDCl_3) δ 7.98 (d, J = 8.8 Hz, 2H), 7.50 (d, J = 8.8 Hz, 2H), 6.83
45
46 (d, J = 9.1 Hz, 2H), 6.76 (d, J = 9.1 Hz, 2H), 4.63 (s, 2H), 4.09 (s, 1H), 3.77 (s, 3H).
47
48
49

50 The methyl ether above (0.057 g, 0.181 mmol) was dissolved in DCM (5 mL) and cooled in an ice-
51
52 bath in an N_2 atmosphere and neat BBr_3 (85 μL , 0.903 mmol) was added dropwise and stirred ice-
53
54 cold for 3h. The mixture was diluted with between EtOAc (20 mL) and NaHCO_3 (aq) (sat., 10 mL)
55
56 and the organic layer washed water (10 mL) and brine (10 mL). The organic phase was dried over
57
58
59
60

MgSO₄ and concentrated to a solid residue. This material was dissolved in EtOAc (10 mL) and a solution of HCl in 1,4-dioxane (4 M, 300 μL) added to give a precipitate that was filtered and washed with EtOAc (1 mL) providing **23** as a white solid (0.037 g, 61% yield). Mp 206°C dec. ¹H NMR (400 MHz, DMSO) δ 7.97 (d, *J* = 8.7 Hz, 2H), 7.69 (d, *J* = 8.7 Hz, 2H), 6.77 (d, *J* = 8.7 Hz, 2H), 6.63 (d, *J* = 8.8 Hz, 2H), 4.63 (s, 2H). ¹³C NMR (101 MHz, DMSO) δ 163.8, 162.8, 153.7, 137.0, 129.76, 128.4, 124.4, 124.1, 121.9, 119.4, 115.9, 41.4. LCMS *R*_f (min) = 5.84. MS *m/z* 302.1 (M + H). HR-ESI calcd for C₁₅H₁₃ClN₃O₂⁺ (M + H) 302.0691, found 302.0697.

4-(5-(4-chlorophenyl)-1,3,4-oxadiazol-2-yl)aniline 24.

Pd(PPh₃)₄ (0.089 g, 0.0771 mmol) was added to a solution of 2-bromo-5-(4-chlorophenyl)-1,3,4-oxadiazole **47** (0.2 g, 0.771 mmol), Na₂CO₃ (aq) (1 M, 3.9 mL) and 4-(4,4,5,5-tetramethyl-1,3,2-dioxaborolan-2-yl)aniline **72** (0.186 g, 0.848 mmol) in DMF (15 mL) and the mixture degassed by bubbling N₂ (g) then heated to 80 °C for 4 h. The resultant mixture was cooled to rt and slowly diluted with water (40 mL) providing **24** as a yellow precipitate that was filtered and washed with water and then recrystallized from DCM (0.2 g, 96% yield). Mp 197–200 °C. ¹H NMR (400 MHz, DMSO) δ 8.09 (d, *J* = 8.8 Hz, 2H), 7.78 (d, *J* = 8.7 Hz, 2H), 7.68 (d, *J* = 8.8 Hz, 2H), 6.70 (d, *J* = 8.8 Hz, 2H), 5.98 (bs, 2H). ¹³C NMR (101 MHz, DMSO) δ 165.0, 161.9, 152.5, 136.2, 129.5, 128.3, 128.1, 122.6, 113.6, 109.4. LCMS *R*_f (min) = 6.37. MS *m/z* 272.1 (M + H). HR-ESI calcd for C₁₄H₁₁ClN₃O⁺ (M + H) 272.0585, found 272.0582.

(4-(5-(4-Chlorophenyl)-1,3,4-oxadiazol-2-yl)phenyl)methanamine hydrochloride 25.

4-(Aminomethyl)benzoic acid (5 g, 33.075 mmol) and Boc₂O (7.2 g, 33 mmol) were taken up in a mixture of acetone (100 mL) and water (100 mL). Sodium hydroxide (1.32 g, 33 mmol) was added and the mixture and stirred overnight. The acetone was removed by rotary evaporation and the aqueous layer was washed with ether (2 × 50 mL) and then EtOAc (100 mL) was added to the aqueous layer and vigorously stirred while 10% citric acid was added slowly to the stirring mixture

1
2
3 until pH \approx 3–4. The organic layer was removed and the aqueous layer was extracted with EtOAc
4 (50 mL). The combined EtOAc layers were dried (MgSO₄), filtered and concentrated to provide 4-
5
6
7
8
9
10
11
12
13
14
15
16
17
18
19
20
21
22
23
24
25
26
27
28
29
30
31
32
33
34
35
36
37
38
39
40
41
42
43
44
45
46
47
48
49
50
51
52
53
54
55
56
57
58
59
60

until pH \approx 3–4. The organic layer was removed and the aqueous layer was extracted with EtOAc (50 mL). The combined EtOAc layers were dried (MgSO₄), filtered and concentrated to provide 4-(((*tert*-butoxycarbonyl)-amino)methyl)benzoic acid as a white solid (7.98 g, 96% yield). ¹H NMR (400 MHz, CDCl₃) δ 8.07 (d, *J* = 8.3 Hz, 2H), 7.38 (d, *J* = 8.4 Hz, 2H), 5.11 – 4.76 (m, 1H), 4.40 (d, *J* = 5.7 Hz, 2H), 1.47 (s, 9H).

Isobutylchloroformate (337 μ L, 2.588 mmol) was added dropwise was to a stirred solution of the above carbamate (0.65 g, 2.59 mmol) and *N*-methyilmorpholine (285 μ L, 2.59 mmol) in dry THF (25 mL) at 0 °C. After stirring for a further 20 min powdered 5-(4-chlorophenyl)-1*H*-tetrazole (0.467 g, 2.588 mmol) and the reaction allowed to warm to rt over 10 min and then refluxed for 2 h. The reaction mixture was then concentrated to a solid that was partitioned between EtOAc (150 mL) and NHCO₃ (aq) (sat., 50 mL) and vigorously stirred for 10 min. The aqueous layer was removed and the organic layer was washed with water (50 mL) and finally with brine (20 mL). The EtOAc layer was dried over MgSO₄ and concentrated to provide **71** as a white solid (0.997 g) that was recrystallized from EtOH (0.278 g, 28% yield). Mp 177–179 °C. ¹H NMR (400 MHz, CDCl₃) δ 8.15 – 8.04 (m, 4H), 7.52 (d, *J* = 8.6 Hz, 2H), 7.46 (d, *J* = 8.3 Hz, 2H), 4.96 (s, 1H), 4.41 (d, *J* = 5.8 Hz, 2H), 1.48 (s, 9H). ¹³C NMR (101 MHz, CDCl₃) δ 164.7, 163.8, 156.1, 143.5, 138.1, 129.6, 128.3, 128.0, 127.3, 122.7, 122.5, 79.9, 44.4, 28.5. LCMS *R*_f (min) = 6.91. MS *m/z* 386.1 (M + H). HR-ESI calcd for C₂₀H₂₁ClN₃O₃⁺ (M + H) 386.1266, found 386.1265.

A solution of HCl 1,4-dioxane (4 M, 5 mL) was added to a solution of *tert*-butyl (4-(5-(4-chlorophenyl)-1,3,4-oxadiazol-2-yl)benzyl)carbamate **71** (0.2 g, 0.518 mmol) in 1,4-dioxane (2 mL) and the mixture stirred at rt overnight. The mixture was then diluted with EtOAc (20 mL) and stirred for 0.5 h. The resulting precipitate was filtered and washed with cold EtOAc and finally ether giving the product **25** as a white solid (0.161 g, 96% yield). Mp 295–299 °C. ¹H NMR (400 MHz, DMSO) δ 8.35 (s, 3H), 8.21 (d, *J* = 8.4 Hz, 2H), 8.17 (d, *J* = 8.8 Hz, 2H), 7.77 – 7.68 (m, 4H), 4.16 (s, 2H). HR-ESI calcd for C₁₅H₁₃ClN₃O⁺ (M + H) 286.0742, found 286.0740.

4-(5-(4-Chlorophenyl)-1,3,4-oxadiazol-2-yl)benzoic acid 26.

Oxalyl chloride (4.84 mL, 55.51 mmol) was added dropwise to the stirred solution 4-(methoxycarbonyl)benzoic acid **79** (2 g, 11.101 mmol) and DMF (5 drops) in dry DCM (20 mL) and the resultant solution stirred at rt for 3 h. The mixture was concentrated to a solid and then taken up in THF (30 mL), cooled to 0 °C and 4-chlorobenzohydrazide **75** (1.89 g, 11.101 mmol) and pyridine (987 μL, 12.211 mmol) added and after 15 min the solution warmed to rt and stirred for 16 h. The mixture was diluted with water (100 mL) and the resulting precipitate filtered, washed with water (30 mL) providing the intermediate hydrazide as a white solid (3.47 g). The solid was taken up in POCl₃ (20 mL) and refluxed for 3 h. The mixture was cooled to rt and concentrated to remove most of the POCl₃ and then crushed ice/water mixture was added to the residue providing a solid. The solid was filtered and washed with water (30 mL) to give the oxadiazole ester as an off-white solid (3.47 g). The solid was taken in THF (50 mL), MeOH (100 mL) and DMSO (55 mL). To this mixture was added dropwise LiOH (aq) (10% w/v, 20 mL and stirred at rt overnight. The mixture was then concentrated to remove volatiles and then diluted with water (150 mL). The mixture was acidified to pH = 2 with 6 M HCl (aq) and the resultant precipitate washed with water and dried giving **26** as a cream solid (2.75 g, 83% yield). ¹H NMR (400 MHz, DMSO) δ 8.27 (d, *J* = 8.7 Hz, 2H), 8.18 (d, *J* = 6.0 Hz, 2H), 8.16 (d, *J* = 5.9 Hz, 2H), 7.73 (d, *J* = 8.8 Hz, 2H). The spectral data for this compound are consistent with that previously reported.³³

4-(5-(4-Chlorophenyl)-1,3,4-oxadiazol-2-yl)benzamide 27.

Oxalyl chloride (75 μL, 0.865 mmol) was added dropwise to a solution 4-(5-(4-chlorophenyl)-1,3,4-oxadiazol-2-yl)benzoic acid (**26**) (0.2 g, 0.665 mmol) in THF (10 mL) and DMF (one drop). The mixture was stirred at rt for 4h then cooled to 0 °C and concentrated NH₄.OH (3 mL) added dropwise with vigorous stirring, then the mixture brought to rt and stirred for a further 10 min. After this time it was diluted with water (50 mL) and the resultant precipitate filtered and washed

1
2
3 with NaHCO₃ (aq) (sat., 10 mL) and H₂O (20 mL) and dried under vacuum providing a white solid
4
5 (0.163 g). The crude solid was recrystallized from EtOH and again from DMSO giving **27** as a
6
7 white solid (0.085g, 43% yield). Mp 297–299 °C. ¹H NMR (400 MHz, DMSO) δ 8.23 (d, *J* = 8.6
8
9 Hz, 2H), 8.21 – 8.14 (m, 3H), 8.10 (d, *J* = 8.6 Hz, 2H), 7.73 (d, *J* = 8.7 Hz, 2H), 7.59 (s, 1H). ¹³C
10
11 NMR (101 MHz, DMSO) δ 166.9, 163.7, 163.6, 137.2, 136.9, 129.6, 128.6, 128.46, 126.7, 125.5,
12
13 122.1. LCMS *R*_f (min) = 5.53. MS *m/z* 300.1 (M + H). HR–ESI calcd for C₁₅H₁₁ClN₃O₂⁺ (M + H)
14
15 300.0534, found 300.0533.
16
17

18
19 **Amino(4-(5-(4-chlorophenyl)-1,3,4-oxadiazol-2-yl)phenyl)methaniminium chloride 28.**

20
21 LiHMDS (1M in THF, 900 μL, 0.9 mmol) was added dropwise to a solution of 4-(5-(4-
22
23 chlorophenyl)-1,3,4-oxadiazol-2-yl)benzotrile **83** (0.12 g, 0.426 mmol) in dry THF (5 mL) at 0
24
25 °C and left to stir at this temperature for 4 h then at rt for 12 h. The mixture was cooled to 0 °C and
26
27 a solution of HCl in 1,4-dioxane (4 M, 852 μL, 3.41 mmol) added and the solution allowed to
28
29 warm to rt for 20 min. The resultant precipitate was filtered and washed with EtOAc (10 mL) then
30
31 diethyl ether (10 mL) providing a white solid (0.182 g). The solid was dissolved in MeOH (5 mL)
32
33 and remaining precipitate removed by filtration. The filtrate was diluted with H₂O (10 mL) and 1
34
35 M NaOH (aq) added dropwise until a precipitate formed. The precipitate was collected, washed
36
37 with H₂O (5 mL) and diethyl ether (5 mL). The solid was then dsuspended in EtOAc (4 mL) and a
38
39 solution of HCl in 1,4-dioxane (4 M, 1 mL) added and stirred for 16 h. The precipitate was filtered
40
41 and washed with EtOAc (10 mL) and diethyl ether (10 mL) providing **28** as an off-white solid
42
43 (0.094 g, yield 66%). Mp > 300 °C. ¹H NMR (400 MHz, DMSO) δ 9.63 (s, 2H), 9.40 (s, 2H), 8.36
44
45 (d, *J* = 8.7 Hz, 2H), 8.20 (d, *J* = 8.8 Hz, 2H), 8.08 (d, *J* = 8.7 Hz, 2H), 7.73 (d, *J* = 8.8 Hz, 2H). ¹³C
46
47 NMR (101 MHz, DMSO) δ 164.9, 163.9, 163.2, 137.1, 131.0, 129.6, 129.3, 128.7, 127.6, 127.0,
48
49 122.0. LCMS *R*_f (min) = 4.23. MS *m/z* 299.1 (M + H). HR–ESI calcd for C₁₅H₁₂ClN₄O⁺ (M + H)
50
51 299.0694, found 299.0695.
52
53
54
55
56

57 **(Z)-4-(5-(4-Chlorophenyl)-1,3,4-oxadiazol-2-yl)-N'-hydroxybenzimidamide 29.**

1
2
3 A solution of 4-(5-(4-chlorophenyl)-1,3,4-oxadiazol-2-yl)benzotrile **83** (0.37 g, 1.314 mmol),
4
5 hydroxylamine hydrochloride (0.274 g, 3.941 mmol) and Et₃N (546 μL, 3.941 mmol) in EtOH (13
6
7 mL) was refluxed for 16 h. After cooling to rt the precipitate was filtered washed with H₂O (10
8
9 mL), EtOH (10 mL) and diethyl ether (10 mL) giving a tan solid (0.38 g). The solid was
10
11 recrystallized from EtOH providing **31** as a white solid (0.215 g, 52% yield). Mp 239–241 °C. ¹H
12
13 NMR (400 MHz, DMSO) δ 9.93 (s, 1H), 8.17 (d, *J* = 8.7 Hz, 2H), 8.14 (d, *J* = 8.7 Hz, 2H), 7.93
14
15 (d, *J* = 8.7 Hz, 2H), 7.73 (d, *J* = 8.7 Hz, 2H), 5.99 (s, 2H). ¹³C NMR (101 MHz, DMSO) δ 164.0,
16
17 163.3, 150.0, 136.8, 136.6, 129.6, 128.5, 126.6, 126.1, 123.3, 122.2. LCMS *R*_f (min) = 4.41. MS
18
19 *m/z* 315.1 (M + H). HR–ESI calcd for C₁₅H₁₂ClN₄O₂⁺ (M + H) 315.0643, found 315.0640.
20
21
22
23
24
25
26

27 **(S)-Amino(1-(4-(5-(4-chlorophenyl)-1,3,4-oxadiazol-2-yl)benzoyl)pyrrolidin-2-**
28
29 **yl)methaniminium chloride 30.**
30

31 4-(5-(4-Chlorophenyl)-1,3,4-oxadiazol-2-yl)benzoic acid **26** (1.92 g, 6.385 mmol) was added to a
32
33 solution of DMF (30 mL) containing the trifluoroacetate salt of (*S*)-pyrrolidine-2-carbonitrile **84**
34
35 [from 1.25 g of the corresponding Boc derivative that was deprotected at ice-cold mixture of
36
37 DCM:TFA (10 mL, 1:1) for 0.5h] and cooled to 0 °C. To the cold mixture was added Et₃N (4.57
38
39 mL, 32.97 mmol) and HATU (3.65 g, 9.578 mmol) and the solution stirred for 10 min at 0 °C then
40
41 at rt for 20 h. The mixture was diluted with EtOAc (150 mL) and washed sequentially with HCl
42
43 (aq) (1 M, 100 mL), H₂O (50 mL), NaHCO₃ (aq) (sat., 50 mL), H₂O (3 × 50 mL) and brine (30
44
45 mL). The organic layer was dried over MgSO₄, concentrated to a brown solid (2.78 g) and
46
47 chromatographed on a silica gel eluting with EtOAc to give a solid that was recrystallized from
48
49 MeOH providing the intermediate nitrile (0.691 g, 29% yield). Mp 204–206 °C. ¹H NMR (400
50
51 MHz, CDCl₃) δ 8.23 (d, *J* = 7.9 Hz, 2H), 8.10 (d, *J* = 8.7 Hz, 2H), 7.77 (d, *J* = 8.4 Hz, 2H), 7.54 (d,
52
53 *J* = 8.7 Hz, 2H), 5.04 – 4.84 (m, 1H), 3.75 – 3.49 (m, 2H), 2.44 – 2.04 (m, 4H).
54
55
56
57
58
59
60

1
2
3 NaOMe (0.5 M in MeOH, 264 μ L, 0.132 mmol) was added to a solution of the above nitrile
4
5 (above) (0.1 g, 0.264 mmol) in anhydrous MeOH (2.64 mL) then heated to 50 $^{\circ}$ C for 24 h. Then
6
7 NH_4Cl (0.028 g, 0.528 mmol) was added and left to stir at 50 $^{\circ}$ C for 72 h. The mixture was
8
9 concentrated and then taken up in EtOAc (30 mL) and stirred for 0.5 h then filtered and washed
10
11 with EtOAc (10 mL) to afford a cream solid (0.127 g). The solid was dissolved in 1:1 $\text{CH}_3\text{CN}:\text{H}_2\text{O}$
12
13 (20 mL) and the mixture was slowly concentrated under vacuum to remove CH_3CN providing a
14
15 solid that is filtered and washed with water. The aqueous filtrate was treated with NaHCO_3 (aq)
16
17 (sat., 4 mL) and slowly evaporated until a solid precipitates. The solid was collected and washed
18
19 with H_2O (10 mL) and diethyl ether (10 mL) to give a cream solid (0.059 g). The solid was
20
21 dissolved in a minimum of MeOH and diluted with an equal volume of 1,4-dioxane then a solution
22
23 of HCl in diethyl ether (2 M, 3 mL) was added dropwise with stirring. The mixture was
24
25 concentrated to a residue and then dissolved in isopropanol (3 mL) (required sonication) and then
26
27 diluted with EtOAc (10 mL) providing a precipitate that was filtered washed with EtOAc (5 mL)
28
29 and diethyl ether (10 mL) to give **30** as a white solid (0.039 g, 34% yield). Mp 183 $^{\circ}$ C dec. ^1H
30
31 NMR (400 MHz, DMSO) δ 9.22 – 9.07 (m, 2H), 8.87 – 8.72 (m, 2H), 8.25 (d, J = 8.2 Hz, 2H),
32
33 8.18 (d, J = 8.5 Hz, 2H), 7.95 (d, J = 8.2 Hz, 2H), 7.74 (d, J = 8.5 Hz, 2H), 4.70 – 4.61 (m, 1H),
34
35 3.87 – 3.75 (m, 1H), 3.50 – 3.41 (m, 1H), 2.44 – 2.35 (m, 1H), 1.99 – 1.84 (m, 3H). ^{13}C NMR (101
36
37 MHz, DMSO) δ 170.8, 168.6, 163.7, 163.6, 138.6, 136.9, 129.6, 128.7, 128.6, 126.6, 124.8, 122.2,
38
39 58.1, 50.1, 31.0, 25.1. LCMS R_f (min) = 4.71. MS m/z 396.2 (M + H). HR-ESI calcd for
40
41 $\text{C}_{20}\text{H}_{19}\text{ClN}_5\text{O}_2^+$ (M + H) 396.1222, found 396.1220.
42
43
44
45
46
47
48
49
50

51 **2-(4-(2H-tetrazol-5-yl)phenyl)-5-(4-chlorophenyl)-1,3,4-oxadiazole 31.**

52
53 A solution of 4-(5-(4-chlorophenyl)-1,3,4-oxadiazol-2-yl)benzotrile **83** (0.3 g, 1.065 mmol)
54
55 NaN_3 (0.083 g, 1.278 mmol) and NH_4Cl (0.068 g, 1.278 mmol) in DMF (1.5 mL) was heated to
56
57 100 $^{\circ}$ C for 18 h. The cooled solution was diluted with H_2O (10 mL) and acidified with HCl (aq)
58
59
60

(6M, 1 mL) providing a precipitate that was collected and washed with H₂O (10 mL). The solid was then suspended in NaOH (aq) (2.5 M, 10 mL) and stirred for 0.5 h at rt. The solution was filtered and the filter cake was washed with NaOH (aq) (2.5 M, 10 mL). The combined filtrate was acidified with 6 M HCl (aq) (pH ~ 1) and the precipitate was collected and washed with H₂O (10 mL). The solids were combined and triturated with boiling EtOH (10 mL) filtered and washed with EtOH and diethyl ether, providing **31** as a white solid (0.273 g, 79% yield). Mp 270 °C (decmp). ¹H NMR (400 MHz, DMSO) δ 8.38 (d, *J* = 8.5 Hz, 1H), 8.29 (d, *J* = 8.6 Hz, 1H), 8.19 (d, *J* = 8.6 Hz, 1H), 7.74 (d, *J* = 8.6 Hz, 1H). ¹³C NMR (101 MHz, DMSO) δ 163.6, 163.5, 155.3, 136.9, 129.6, 128.5, 127.8, 127.6, 127.4, 125.3, 122.1. LCMS *R*_f (min) = 5.80. MS *m/z* 325.0 (M + H). HR-ESI calcd for C₁₅H₁₀ClN₆O⁺ (M + H) 325.0599, found 325.0598.

4-((5-(4-chlorophenyl)-1,3,4-oxadiazol-2-yl)amino)benzamide 32.

4-((5-(4-Chlorophenyl)-1,3,4-oxadiazol-2-yl)amino)benzamide **81** (0.05 g, 0.169 mmol) was dissolved in conc. H₂SO₄ (2 mL) at rt and stirred for 18 h. The mixture was cooled to 0 °C and crushed ice (50 g) was added to the stirred solution providing a solid. The mixture was neutralized with saturated NaHCO₃ (aq) and the solid filtered and washed with H₂O (10 mL) providing **32** as a white solid (0.05 g, 94% yield). Mp > 300 °C. ¹H NMR (400 MHz, DMSO) δ 11.03 (s, 1H), 7.94 – 7.88 (m, 4H), 7.86 (s, 1H), 7.70 – 7.62 (m, 4H), 7.23 (s, 1H). ¹³C NMR (101 MHz, DMSO) δ 167.4, 159.7, 157.3, 141.1, 135.7, 129.5, 128.8, 127.6, 127.4, 122.6, 116.3. HR-ESI calcd for C₁₅H₁₂ClN₄O₂⁺ (M + H) 315.0643, found 315.0643.

Amino(4-((5-(4-chlorophenyl)-1,3,4-oxadiazol-2-yl)amino)phenyl)methaniminium chloride 33.

4-((5-(4-Chlorophenyl)-1,3,4-oxadiazol-2-yl)amino)benzamide **81**: A solution of 4-chlorobenzohydrazide (0.532 g, 3.121 mmol) and 4-isothiocyanatobenzonitrile (0.5 g, 3.121 mmol) in THF (15 mL) was stirred at rt for 15 h. To this mixture 4-toluoylsulfonyl chloride (0.714 g, 3.748 mmol) and pyridine (530 μL, 6.554 mmol) were added and the stirred mixture refluxed for 6

1
2
3 h. The solution was cooled to rt and diluted with H₂O (50 mL) and the resulting solid filtered and
4
5 washed sequentially with H₂O (20 mL), EtOH (5 mL) and DCM (20 mL) providing **81** as a pale
6
7 yellow solid (0.45 g, 49% yield). Mp 274–276 °C. ¹H NMR (400 MHz, DMSO) δ 11.34 (s, 1H),
8
9 7.92 (d, *J* = 8.8 Hz, 2H), 7.84 (d, *J* = 9.0 Hz, 2H), 7.77 (d, *J* = 9.0 Hz, 2H), 7.67 (d, *J* = 8.8 Hz,
10
11 2H).

12
13
14 Boc₂O (1.1 g, 5.055 mmol) was added was added to a solution of benzonitrile **81** (above) (0.5 g,
15
16 1.69 mmol) and DMAP (10.3 mg, 0.084 mmol) in 1,4-dioxane (0.5 mL) and the mixture stirred in
17
18 at 60 °C for 20 min (the evolution of gas ceases). The cooled solution was diluted with EtOAc (30
19
20 mL) and filtered through a short silica pad and concentrated to an oily residue (1.17 g). The oil was
21
22 triturated with 20% EtOAc in petroleum spirit providing a white solid that was filtered and washed
23
24 with 20% EtOAc in petroleum spirit giving Boc-**81** (0.495 g, 74%). ¹H NMR (400 MHz, CDCl₃) δ
25
26 7.96 (d, *J* = 8.8 Hz, 2H), 7.71 (d, *J* = 8.8 Hz, 2H), 7.52 (d, *J* = 6.3 Hz, 2H), 7.50 (d, *J* = 6.3 Hz,
27
28 2H), 1.51 (s, 9H).

29
30
31
32
33 LiHMDS (1 M in THF, 799 μL, 0.799 mmol) was added dropwise to the stirred solution of the
34
35 Boc-**81** (above) (0.15 g, 0.378 mmol) in anhydrous THF (4.5 mL) at 0 °C then stirred at rt
36
37 overnight. The a solution was cooled to 0 °C and HCl in 1,4-dioxane (4 M, 0.5 mL) added
38
39 dropwise and stirred for 2 h at 0 °C. The mixture was partitioned between HCl (aq) (1 M, 40 mL)
40
41 and EtOAc (30 mL) and the aqueous layer neutralised with saturated NaHCO₃ (aq) and left to
42
43 stand for 50 h. The precipitate was filtered and washed with H₂O (5 mL) providing a yellow solid
44
45 (0.038 g). The solid was suspended in EtOAc (10 mL) and HCl in 1,4-dioxane (4 M, 1 mL) added
46
47 and the solution stirred at rt for 2 h. The hydrochloride salt was filtered and washed with EtOAc
48
49 (15 mL) and diethyl ether (10 mL) providing **33** as a tan solid (0.036 g, 27% yield). Mp > 300 °C.
50
51 ¹H NMR (400 MHz, DMSO) δ 11.46 (s, 1H), 9.25 (bs, 2H), 8.97 (bs, 2H), 7.92 (d, *J* = 8.7 Hz,
52
53 2H), 7.90 (d, *J* = 8.8 Hz, 2H), 7.82 (d, *J* = 8.9 Hz, 2H), 7.68 (d, *J* = 8.7 Hz, 2H). ¹³C NMR (101
54
55 MHz, DMSO) δ 164.7, 159.4, 157.6, 143.5, 135.8, 129.5, 129.5, 127.4, 122.4, 120.3, 116.7. LCMS
56
57
58
59
60

1
2
3 R_f (min) = 4.72. MS m/z 314.1 (M + H). HR-ESI calcd for $C_{15}H_{13}ClN_5O^+$ (M + H) 314.0803,
4
5 found 314.0799.
6
7
8
9
10

11 **(Z)-4-((5-(4-Chlorophenyl)-1,3,4-oxadiazol-2-yl)amino)-N'-hydroxybenzimidamide 34.**

12
13 A solution of benzonitrile **81** (above) (0.15 g, 0.506 mmol), hydroxylamine hydrochloride (0.039
14 g, 0.556 mmol) and $NaHCO_3$ (0.047g, 0.556 mmol) in EtOH (5 mL) and H_2O (1 mL) was refluxed
15
16 for 18h, then cooled to rt giving a lemon colored precipitate that was filtered washed with EtOH (2
17 mL) and H_2O (4 mL) (0.132 g). The solid was recrystallized from EtOH providing **34** as a white
18
19 solid (0.12 g, 66% yield). Mp > 300 °C. 1H NMR (400 MHz, DMSO) δ 10.85 (s, 1H), 9.51 (s, 1H),
20
21 7.91 (d, J = 8.8 Hz, 2H), 7.68 (d, J = 6.5 Hz, 2H), 7.66 (d, J = 6.3 Hz, 2H), 7.60 (d, J = 8.9 Hz,
22
23 2H), 5.75 (s, 2H). ^{13}C NMR (101 MHz, DMSO) δ 159.9, 157.1, 150.5, 139.0, 135.6, 129.5, 127.4,
24
25 127.0, 126.3, 122.7, 116.6. LCMS R_f (min) = 4.71. MS m/z 330.1 (M + H). HR-ESI calcd for
26
27 $C_{15}H_{13}ClN_5O_2^+$ (M + H) 330.0752, found 330.0754.
28
29
30
31
32
33
34
35
36

37 **5-(4-Chlorophenyl)-N-[4-(1H-tetrazol-5-yl)phenyl]-1,3,4-oxadiazol-2-amine 35.**

38
39 Triethylamine (0.20 mL) was added to a solution of 2-bromo-5-(4-chlorophenyl)-1,3,4-oxadiazole
40
41 **47**²⁴ (80.5 mg, 0.310 mmol) and 4-(2H-tetrazol-5-yl) aniline **73** (60 mg, 0.3721 mmol) in DMF
42
43 (1.6 mL) and heated the mixture heated to 90 °C for 4 h. The reaction mixture was cooled to rt and
44
45 acidified (pH ~1) by addition of HCl (aq) (10% w/v). The precipitate was filtered and washed with
46
47 water to give a brown solid which was retained. The filtrate was diluted with water (75 mL)
48
49 extracted with EtOAc (3 x 50 mL). The organic layer was dried with $MgSO_4$ and concentrated to
50
51 give leave a yellow solid. The precipitate and the solid extract of the filtrate were combined and
52
53 chromatographed on silica gel eluting with EtOAc and recrystallised from EtOH to give **35** as
54
55 yellow crystals (30.6 mg, 29%). Mp 210 °C (decomp.). 1H NMR (400MHz, DMSO): 8.12 (d, 2H,
56
57
58
59
60

Ar), 7.79 (d, 2H, Ar), 7.75 (d, 2H, Ar), 6.72 (d, 2H, Ar), 5.72 (b, 2H). ¹³C NMR (101MHz, DMSO): 164.78, 160.01, 150.93, 142.02, 138.11, 129.74, 128.82, 126.44, 122.05, 113.70, 112.16. LCMS *R_f* (min) = 5.97. MS *m/z* 312.1 (M – N₂ + H). HR-ESI could not be obtained (too low intensity).

(E)-4-((5-(4-Chlorophenyl)-1,3,4-oxadiazol-2-yl)amino)benzaldehyde oxime 36.

DIBAL (1.5 M in toluene, 1.67 mL, 2.5 mmol) was added dropwise to a solution of benzonitrile **83** (0.297 g, 1.0 mmol) in anhydrous toluene (5 mL) at 0 °C then stirred at rt overnight. The this HCl (aq) (10% w/v, 10 mL) was added slowly and cautiously, causing a precipitate to form. The precipitate was filtered and washed with EtOAc (10 mL) and H₂O (15 mL) providing the crude aldehyde, 4-((5-(4-chlorophenyl)-1,3,4-oxadiazol-2-yl)amino)benzaldehyde, as a yellow solid (0.185 g, 62% yield). ¹H NMR (400 MHz, DMSO) δ 11.35 (s, 1H), 9.89 (s, 1H), 7.96 – 7.89 (m, 4H), 7.81 (d, *J* = 8.7 Hz, 2H), 7.67 (d, *J* = 8.7 Hz, 2H).

A solution of the aldehyde (above) (0.1 g, 0.334 mmol), hydroxylamine hydrochloride (0.035 g, 0.51 mmol) and Et₃N (1 mL) in MeOH (5 mL) was stirred at rt overnight and the resultant precipitate filtered and washed with MeOH (10 mL) then dethyl ether (10 mL). The solid was recrystallised from MeOH providing an off-white solid (0.035 g). The solid material was dissolved in a mixture of EtOAc and MeOH and evaporated down on silica gel (10 g). The silica gel was filtered on a buchner funnel and washed with EtOAc (40 mL) and concentrated to a solid that was triturated in EtOAc giving **36** as a white solid (0.033 g, 31% yield). Mp 226–229 °C. ¹H NMR (400 MHz, DMSO) δ 11.04 (s, 1H), 10.92 (bs, 1H), 8.08 (s, 1H), 7.91 (d, *J* = 8.8 Hz, 2H), 7.69 – 7.57 (m, 6H). ¹³C NMR (101 MHz, DMSO) δ 159.8, 157.2, 147.6, 139.4, 135.6, 129.5, 127.4, 127.3, 126.8, 122.7, 117.2. LCMS *R_f* (min) = 5.23. MS *m/z* 315.1 (M + H). HR-ESI calcd for C₁₅H₁₂ClN₄O₂⁺ (M + H) 315.0643, found 315.0639.

4-((5-Phenyl-1,3,4-oxadiazol-2-yl)amino)phenol 37.

1
2
3 5-(4-Iodophenyl)-N-(4-methoxyphenyl)-1,3,4-oxadiazol-2-amine **87**: A solution of 4-
4 iodobenzahydride (3.79 g, 14.48 mmol) and 1-isothiocyanato-4-methoxy benzene (2 mL, 14.48
5 mmol) in THF (100 mL) was stirred at rt for 16 h during which time a white precipitate formed. To
6 this suspension tosyl chloride (3.312 g, 17.37 mmol) and pyridine (2.44 mL, 30.41 mmol) were
7 added and the mixture refluxed for 20 h. H₂O (120 mL) was added to the mixture and allowed to
8 stir for 10 min. The gold precipitate formed was then filtered and recrystallised in hot EtOH (450
9 mL) to produce **87** as gold crystalline solid (4.94 g, 89% yield). Mp 269 °C. ¹H NMR (400 MHz,
10 DMSO) δ 10.49 (s, 1H, NH), 7.95 (d, J = 8.6 Hz, 2H, CH), 7.64 (d, J = 8.6 Hz, 2H, CH), 7.52 (d, J
11 = 9.1 Hz, 2H, CH), 6.95 (d, J = 9.1 Hz, 2H, CH), 3.73 (s, 3H, CH₃). ¹³C NMR (101 MHz, DMSO)
12 δ 160.68 (C), 157.37 (C), 154.95 (C), 138.62 (CH), 132.19 (C), 127.57 (CH), 123.71 (C), 119.09
13 (CH), 114.78 (CH), 98.28 (C), 55.67 (CH₃). LCMS R_f(min) = 3.510 MS m/z 394.0 (M + H).

14
15
16
17
18
19
20
21
22
23
24
25
26
27
28 **87** (0.150 g, 0.382 mmol) was added to a suspension of Pd/C 10% (0.080 g) in EtOAc/MeOH
29 (13.5 mL/4.5 mL) under N₂ (g). The atmosphere was exchanged for H₂ (g) through exposure to a
30 vacuum source and backfilling with H₂ (g) (4 x). The mixture was then left to stir at rt overnight
31 then filtered to remove Pd/C 10% catalyst before being concentrated to form a grey solid. The solid
32 was triturated with DCM and filtered to produce a white crystalline solid (0.053 g), which was
33 retained. The filtrate was then diluted with DCM (50 mL) and washed with NaHCO₃ (aq) (sat., 30
34 mL), dried over MgSO₄ and concentrated to give a white solid (0.021 g). Both solid samples of **89**
35 were combined (74.2 mg, 73% yield). Mp 210 °C. ¹H NMR (400 MHz, DMSO) δ 10.46 (s, 1H,
36 NH), 7.89 (m, 2H, CH), 7.58 (m, J = 5.1, 1.9 Hz, 3H, CH), 7.54 (d, J = 9.1 Hz, 2H, CH), 6.97 (d, J
37 = 9.1 Hz, 2H, CH), 3.75 (s, 3H, CH₃). ¹³C NMR (101 MHz, DMSO) δ 160.21 (C), 157.56 (C),
38 154.51 (C), 131.92 (C), 130.91 (C), 129.38 (CH), 125.49 (CH), 123.92 (CH), 118.64 (CH), 114.39
39 (CH), 55.28 (CH₃). LCMS R_f(min) = 3.647 MS m/z 268.2 (M + H).

40
41
42
43
44
45
46
47
48
49
50
51
52
53
54
55
56 BBr₃ (0.0710 mL, 0.748 mmol) was added dropwise to a solution **87** (above) (0.050 g, 0.187
57 mmol) in DCM (3 mL) at 0 °C and stirred at rt for 2 h. The reaction was quenched with NaHCO₃
58
59
60

1
2
3 (aq) (sat., 1 mL) and diluted with H₂O (20 mL) then extracted with EtOAc (3 x 50 mL) and the
4
5 combined extracts washed with NaHCO₃ (aq) (sat., 3 x 30 mL). The organic layer dried over
6
7 MgSO₄ and concentrated giving 4-((5-phenyl-1,3,4-oxadiazol-2-yl)amino)phenol **37** as a cream
8
9 solid (45.1 mg, 95% yield). Mp 231 °C. ¹H NMR (400 MHz, DMSO) δ 10.29 (s, 1H, NH), 9.15 (s,
10
11 1H, OH), 7.87 (m, 2H, CH), 7.56 (m, 3H, CH), 7.40 (d, 2H, CH), 6.75 (d, 2H, CH). ¹³C NMR (101
12
13 MHz, DMSO) δ 160.37 (C), 157.46 (C), 152.61 (C), 130.83 (C), 130.43 (C), 129.38 (CH), 125.41
14
15 (CH), 123.96 (CH), 118.95 (CH), 115.59 (CH). LCMS R_f (min) = 3.065 MS m/z 254.2 (M + H).
16
17 HR-ESI calcd for C₁₄H₁₁N₃O₂⁺ (M + H) 254.0924, found 254.0928.
18
19
20
21
22
23

24 25 **4-((5-(4-(Trifluoromethyl)phenyl)-1,3,4-oxadiazol-2-yl)amino)phenol 38.**

26
27 A solution of 4-(trifluoromethyl)benzohydrazine **86**³⁴ (0.5 g, 2.45 mmol) and 1-isothiocyanato-4-
28
29 methoxybenzene (0.338 mL, 2.45 mmol) in THF (20 mL) was stirred at rt overnight. To this, tosyl
30
31 chloride (0.560 g, 2.94 mmol) and pyridine (0.414 mL, 5.14 mmol) were added and the mixture
32
33 refluxed for 20 h. H₂O (50 mL) was added to the mixture and the resultant cream precipitate
34
35 filtered and chromatographed on silica gel eluting with 10% EtOAc in petroleum spirits yielding
36
37 an off-white solid which was recrystallized from EtOH to produce **88** as a white crystalline solid
38
39 (0.155 g, 19% yield). Mp 258 °C. ¹H NMR (400 MHz, DMSO) δ 10.58 (s, 1H, NH), 8.09 (d, J =
40
41 8.2 Hz, 2H, CH), 7.96 (d, J = 8.2 Hz, 2H, CH), 7.54 (d, 2H, CH), 6.98 (d, 2H, CH), 3.75 (s, 3H,
42
43 CH₃). ¹³C NMR (101 MHz, DMSO) δ 160.84 (C), 156.77 (C), 154.86 (C), 131.88 (C), 130.48 (C),
44
45 127.88 (C), 126.57 (CF₃), 126.37 (CH), 126.37 (CH), 125.45 (CH), 119.02 (CH), 119.02 (CH),
46
47 114.60 (CH), 114.60 (CH), 55.47 (CH₃) (CH ortho to CF₃ group does not appear in ¹³C NMR due
48
49 to effects fluorine coupling). LCMS R_f (min) = 3.480 MS m/z 336.1 (M + H).
50
51
52
53

54
55 BBr₃ (0.0566 mL, 0.597 mmol) was added dropwise to a solution of **88** (0.050 g, 0.141 mmol) in
56
57 DCM (3 mL) at 0 °C then left to stir at rt for 2 h. The reaction was quenched by dropwise addition
58
59
60

1
2
3 of NaHCO₃ (aq) (sat., 2 mL) at 0 °C then diluted with H₂O (20 mL) and left to stir for 15 min. The
4
5 mixture was extracted with EtOAc (3 x 50 mL) and the combined extracts washed with H₂O (2 x
6
7 50 mL), NaHCO₃ (aq) (sat., 2 x 50 mL) and brine (1 x 30 mL), dried over MgSO₄ and concentrated
8
9 to give a cream solid. Crude material was recrystallised using hot EtOH and petroleum spirit to
10
11 afford **38** as a white solid (0.014 g, 31% yield). Mp 265 °C. ¹H NMR (400 MHz, DMSO) δ 10.42
12
13 (s, 1H, NH), 9.20 (s, 1H, OH), 8.07 (d, J = 8.2 Hz, 2H, CH), 7.94 (d, J = 8.2 Hz, 2H, CH), 7.41 (d,
14
15 J = 8.8 Hz, 2H, CH), 6.78 (d, J = 8.8 Hz, 2H, CH). ¹³C NMR (101 MHz, DMSO) δ 160.81 (C),
16
17 156.50 (C), 152.81 (C), 130.58 (C), 130.19 (C), 127.74 (C), 126.39 (CF₃), 126.15 (CH), 119.17
18
19 (CH), 115.62 (CH) (CH ortho to CF₃ group does not appear in ¹³C NMR due to effects fluorine
20
21 coupling). LCMS R_f (min) = 3.267 MS m/z 322.1 (M + H). HR-ESI calcd for C₁₅H₁₀F₃N₃O₂⁺ (M +
22
23 H) 322.0798, found 322.0802.

24 25 26 27 28 29 **4-((5-(4-Iodophenyl)-1,3,4-oxadiazol-2-yl)amino)phenol 49.**

30
31 BBr₃ (2.20 mL, 7.63 mmol) was added dropwise to a solution of **87** (above) (1.0 g, 2.54 mmol) in
32
33 DCM (25 mL) at 0 °C then stirred at rt for 2 h. The reaction was quenched by dropwise addition of
34
35 NaHCO₃ (aq) (sat., 4 mL) at 0 °C then diluted with H₂O (100 mL) and left to stir for 15 min. The
36
37 solution was then extracted with EtOAc (3 x 70 mL), washed with NaHCO₃ (aq) (sat., 3 = 50 mL),
38
39 dried over MgSO₄ and concentrated to give **39** as a yellow crystalline solid (0.713 g, 74% yield).
40
41 Mp 279 °C. ¹H NMR (400 MHz, DMSO) δ 10.34 (s, 1H, NH), 9.18 (s, 1H, OH), 7.95 (d, J = 8.6
42
43 Hz, 2H, CH), 7.63 (d, J = 8.6 Hz, 2H, CH), 7.39 (d, J = 8.9 Hz, 2H, CH), 6.76 (d, J = 8.9 Hz, 2H,
44
45 CH). ¹³CNMR (101 MHz, DMSO) δ 160.41 (C), 156.95 (C), 152.64 (C), 138.18 (CH), 130.26 (C),
46
47 127.11 (CH), 123.43 (C), 118.98 (CH), 115.54 (CH), 97.75 (C). LCMS R_f (min) = 3.271 MS m/z
48
49 258.3 (M + H). HR-ESI calcd for C₁₄H₁₀IN₃O₂⁺ (M + H) 379.9890, found 379.9900.

50 51 52 53 54 55 56 57 **4-((5-(4-(2-Cyclohexylethyl)phenyl)-1,3,4-oxadiazol-2-yl)amino)phenol 40.**

1
2
3 Pd(PPh₃)₂Cl₂ (17.9 mg, 0.025 mmol) and CuI (2.42 mg, 0.013 mmol) were added to a
4
5 deoxygenated solution (N₂ (g) was bubbled through the mixture for 10 min) of 5-(4-iodophenyl)-
6
7 N-(4-methoxyphenyl)-1,3,4-oxadiazol-2-amine **87** (above) (0.2 g, 0.51 mmol) and 1-
8
9 ethynylcyclohexene (0.09 mL, 0.76 mmol) in DMF (3 mL) and Et₃N (3 mL) and left to stir at rt for
10
11 18 h. The solution was diluted in EtOAc (20 mL) and washed with H₂O (2 x 30 mL) and HCl (aq)
12
13 (1.0 M, 2 x 30 mL). The organic layers were then collected and washed with H₂O (1 x 30 mL) and
14
15 brine (1 x 30 mL) before being dried over MgSO₄ and concentrated to a brown-cream solid (0.284
16
17 g). The crude material was chromatographed on silica gel eluting with 20% EtOAc in DCM
18
19 affording 5-(4-(cyclohex-1-en-1-ylethynyl)phenyl)-N-(4-methoxyphenyl)-1,3,4-oxadiazol-2-amine
20
21 as a gold crystalline solid (0.181 g, 96% yield). Mp 219 °C. ¹H NMR (400 MHz, CDCl₃) δ 7.87
22
23 (d, J = 8.6 Hz, 2H, CH), 7.50 (d, J = 8.6 Hz, 2H, CH), 7.44 (d, J = 9.0 Hz, 2H, CH), 7.02 (s, 1H),
24
25 6.94 (d, J = 9.0 Hz, 2H, CH), 6.26 (m, 1H), 3.82 (s, 3H), 2.24 (m, J = 2.2 Hz, 2H), 1.66 (m, J =
26
27 23.9, 5.9, 2.1 Hz, 5H). LCMS R_f (min) = 3.867 MS m/z 372.2 (M + H).

28
29
30
31
32
33 Pd/C 10% (0.160 g) was added to a solution of the alkyne above (0.160 g, 0.4308 mmol) in EtOAc
34
35 (7 mL) and MeOH (3 mL) under N₂ (g). The N₂ (g) atmosphere was replaced with H₂ (g) by
36
37 evacuation and backfilling with H₂ (g) (4 cycles). The mixture was then left to stir at rt overnight
38
39 then filtered to remove the catalyst and concentrated to afford 5-(4-(2-cyclohexylethyl)phenyl)-N-
40
41 (4-methoxyphenyl)-1,3,4-oxadiazol-2-amine (**90**) as a white solid (0.105 g, 64%). ¹H NMR (400
42
43 MHz, CDCl₃) δ 7.84 (d, J = 8.3 Hz, 2H, CH), 7.43 (d, J = 9.0 Hz, 2H, CH), 7.28 (d, 2H, CH), 6.93
44
45 (d, J = 9.0 Hz, 2H, CH), 3.81 (s, 3H, CH₃), 2.66 (dd, J = 9.2, 7.0 Hz, 2H, CH₂), 1.71 (m, 9H, CH₂),
46
47 1.52 (dd, J = 16.3, 6.6 Hz, 4H, CH₂). ¹³C NMR (101 MHz, DMSO) δ 197.41 (C), 195.03 (C),
48
49 191.83 (C), 183.33 (C), 169.38 (C), 166.53 (CH), 162.88 (CH), 158.82 (C), 155.97 (CH), 151.77
50
51 (CH), 92.68 (CH₃), 75.89 (CH₂), 74.05 (CH), 70.12 (CH₂), 69.78 (CH₂), 63.59 (CH₂), 63.18 (CH₂).
52
53 63.18 (CH₂). LCMS R_f (min) = 4.127 MS m/z 394.3 (M + H).

1
2
3 BBr₃ (0.1 mL, 1.019 mmol) was added dropwise to a solution of **90** (0.096 g, 0.255 mmol) in
4 DCM (4 mL) at 0 °C then left to stir at rt for 2 h. The reaction was quenched by dropwise addition
5 NaHCO₃ (aq) (sat., 2 mL) at 0 °C diluted H₂O (20 mL) and left to stir for 15 min. The solution was
6 then extracted with EtOAc (3 x 50 mL) and the combined organic layers washed with NaHCO₃
7 (aq) (sat., 3 x 50 mL), dried over MgSO₄ and concentrated to a brown solid (0.221 g). The crude
8 material was chromatographed on silica gel eluting with 25% EtOAc in DCM giving **40** as a light
9 brown solid (0.109 g, 100% yield). Mp 260 °C. ¹H NMR (400 MHz, DMSO) δ 10.24 (s, 1H, NH),
10 9.14 (s, 1H, OH), 7.77 (d, *J* = 8.2 Hz, 2H, CH), 7.38 (dd, *J* = 8.5, 4.8 Hz, 4H, CH), 6.75 (d, *J* = 8.9
11 Hz, 2H, CH), 2.66 (m, 3H, CH₂), 1.69 (dd, *J* = 42.6, 11.9 Hz, 6H, CH₂), 1.49 (dd, *J* = 15.4, 7.0 Hz,
12 2H), 1.17 (t, *J* = 7.1 Hz, 2H, CH₂), 0.93 (t, *J* = 12.0 Hz, 2H, CH₂). ¹³C NMR (101 MHz, DMSO) δ
13 160.12 (C), 157.48 (C), 152.48 (C), 145.79 (C), 130.38 (C), 129.16 (CH), 125.45 (CH), 121.45
14 (C), 118.82 (CH), 115.52 (CH), 38.44 (CH₂), 36.63 (CH), 32.70 (CH₂), 32.37 (CH₂), 26.17 (CH₂),
15 25.79 (CH₂). LCMS R_f (min) = 3.788 MS m/z 364.2 (M + H). HR-ESI calcd for C₂₂H₂₅N₃O₂⁺ (M
16 + H) 364.202, found 364.2029.

17
18
19
20
21
22
23
24
25
26
27
28
29
30
31
32
33
34
35 **4-((5-(4-Chlorophenyl)-1,3,4-oxadiazole-2-carboxamido)methyl)pyridin-1-ium chloride 41.**

36 Ethyl 5-(4-chlorophenyl)-1,3,4-oxadiazole-2-carboxylate (**77**) (0.2 g, 0.79 mmol) and pyridin-4-
37 ylmethanamine (241 μL, 2.38 mmol) were refluxed in EtOH (2 mL) for 18 h. The cooled (rt)
38 solution was filtered and the filter-cake washed with EtOH and dried to give pink solid (0.184 g).
39 The solid was dissolved in a mixture EtOAc (1 mL) and 1,4-dioxane (3 mL) (required heating) and
40 a solution of HCl in 1,4-dioxane (4 M, 1 mL) added. After stirring for 15 min the solution was then
41 concentrated and resuspended in EtOAc (2.0 mL), sonicated then filtered (0.2 g). The solid was
42 triturated in hot EtOH, filtered and then recrystallised from DMSO (54 mg, 19%). Mp 264 °C dec.
43
44
45
46
47
48
49
50
51
52
53
54
55
56
57
58
59
60
¹H NMR (400 MHz, DMSO) δ 10.12 (t, *J* = 6.0 Hz, 1H), 8.82 (d, *J* = 6.4 Hz, 2H), 8.11 (d, *J* = 8.8
Hz, 2H), 7.90 (d, *J* = 6.3 Hz, 2H), 7.74 (d, *J* = 8.8 Hz, 2H), 4.75 (d, *J* = 6.0 Hz, 2H). ¹³C NMR
(101 MHz, DMSO) δ 164.3, 158.4, 156.9, 153.6, 143.6, 137.5, 129.8, 128.86, 124.3, 121.7, 42.0.

1
2
3 LCMS R_f (min) = 4.69. MS m/z 315.1 (M + H). HR-ESI calcd for $C_{15}H_{12}ClN_4O_2^+$ (M + H)
4
5 315.0643, found 315.0639.
6
7

8 **5-(4-Chlorophenyl)-N-(pyridin-4-ylmethyl)-1,3,4-oxadiazol-2-amine 42.**
9

10 2-Bromo-5-(4-chlorophenyl)-1,3,4-oxadiazole (47)²² (0.150 g, 0.578 mmol), 4-
11 (aminomethyl)piperidine (0.176 mL, 1.734 mmol) and DIPEA (0.3 mL, 1.734 mmol) in DMF (3
12 mL) were heated to 70 °C for 3 h in which time the solution changed from yellow to orange. The
13 mixture was diluted in EtOAc (50 mL) and washed with H₂O (3 x 30 mL) and brine (1 x 30 mL)
14 dried over MgSO₄ and concentrated to a yellow semi-solid (0.177 g). The crude solid was then
15 triturated in Et₂O and filtered to produce an orange solid (0.143 g). This solid dissolved in EtOAc
16 (4 mL), and a solution of HCl in diethyl ether (2.0 M, 1 mL) was added at 0 °C. The mixture was
17 left to stir at rt overnight before being filtered and washed with EtOAc (2.0 mL), forming a light
18 brown solid (54 mg, 43% yield). Mp 191 °C. ¹H NMR (400 MHz, DMSO) δ 9.01 (s, 1H, NH),
19 8.90 (d, J = 6.7 Hz, 2H, CH), 8.08 (d, J = 6.6 Hz, 2H, CH), 7.82 (d, J = 8.7 Hz, 2H, CH), 7.62 (d, J
20 = 8.7 Hz, 2H, CH), 4.81 (s, 2H, CH₂). ¹³C NMR (101 MHz, DMSO) δ 163.35 (C), 159.92 (C),
21 157.82 (C), 141.45 (CH), 135.75 (C), 129.78 (CH), 127.42 (CH), 125.45 (CH), 123.03 (C), 45.61
22 (CH₂). LCMS R_f (min) = 3.185 MS m/z 287.1 (M + H). HR-ESI calcd for $C_{14}H_{16}ClN_3O_2^+$ (M + H)
23 287.0694, found 287.0706.
24
25
26
27
28
29
30
31
32
33
34
35
36
37
38
39
40
41

42 **Acknowledgments:**

43
44 BLF supported by the National Breast Cancer Foundation (NC-11-13). SMP supported by the Fay
45 Fuller Foundation and a Senior Research Fellowship (1042589) and Project Grant (1004695) from
46 the National Health and Medical Research Council (NHMRC) of Australia. MRP supported by a
47 Royal Adelaide Hospital Research Fund Early Career Fellowship. LF supported by a Movember
48 Young Investigator Award from the Prostate Cancer Foundation of Australia (YI-0310). DJC
49 supported by a Career Development Fellowship from the NHMRC of Australia (1088855). The
50 authors thank Dr Michael J. Christopher for assistance with some experiments.
51
52
53
54
55
56
57
58
59
60

Supporting Information

Copies of HPLC, ¹H NMR and ¹³C NMR spectra for all test compounds.

Ancillary Information

Address for correspondence: Bernard L. Flynn: Monash Institute of Pharmaceutical Science, Monash University, 381 Royal Pde, Parkville, VIC, 3052, Australia. Phone: +61 3 99039650.

Email: bernard.flynn@monash.edu. Stuart M. Pitson: Centre for Cancer Biology, University of

South Australia and SA Pathology, Frome Road, Adelaide SA, 5000, Australia. Email:

stuart.pitson@unisa.edu.au

Abbreviations Used

APCI, acylpyrrolidine-2-carboximidamide; CBR5, NADH-cytochrome b5 reductase; Cer, ceramide; CyEt, (cyclohexyl)ethyl; Des1, dihydroceramide desaturase-1; dhCer, dihydroceramide; LELP, lipophilicity-corrected ligand efficiency; GI₅₀, concentration required to inhibit 50% of cell growth; HEK293, human embryonic kidney-293; NBD, *N*-(7-Nitrobenz-2-Oxa-1,3-Diazol-4-yl)amino; PC3, prostate cancer-3; S1P, sphingosine-1-phosphate; SD, standard deviation; SEM, standard error of the mean; SK, sphingosine kinase; Sph, sphingosine.

References

-
- ¹ (a) Xia, P.; Gamble, J. R.; Wang, L.; Pitson, S. M.; Moretti, P. A.; Wattenberg, B. W.; D'Andrea, R. J.; Vadas, M. A. An oncogenic role of sphingosine kinase. *Curr. Biol.* **2000**, *10*, 1527–1530. (b) Rosen, H.; Sanna, M. G.; Cahalan, S. M.; Gonzalez-Cabrera, P. J. Tipping the gatekeeper: S1P regulation of endothelial barrier function. *Trends Immunol.* **2007**, *28*, 102–107. (c) Cuvillier, O. Sphingosine kinase-1, a potential therapeutic target in cancer. *Anti-Cancer Drugs* **2007**, *18*, 105–110. (d) Oskeritzian, C. A.; Milstien, S.; Spiegel, S. Sphingosine-1-phosphate in allergic responses, asthma and anaphylaxis. *Pharmacol. Ther.* **2007**, *115*, 390–399. (e) Rivera, J.; Proia, R.

1
2
3
4 L.; Olivera, A. The alliance of sphingosine-1-phosphate and its receptors in immunity. *Nat. Rev.*
5 *Immunol.* **2008**, *8*, 753–763. (f) Huwiler, A.; Pfeilschifter, J. New players on the center stage:
6 sphingosine 1-phosphate and its receptors as drug targets. *Biochem. Pharmacol.* **2008**, *75*,
7 1893–1900. (g) Pitman, M. R.; Pitson S., M. Inhibitors of the sphingosine kinase pathway as
8 potential therapeutics *Curr. Cancer Drug Targets* **2010**, *10*, 354-67. (h) Okamoto, Y.; Wang, F.;
9 Yoshioka, K.; Takuwa, N.; Takuwa, Y. Sphingosine-1-phosphate-specific G protein-coupled
10 receptors as novel therapeutic targets for atherosclerosis. *Pharmaceuticals* **2011**, *4*, 117–137. (i)
11 Maceyka, M.; Harikumar, K. B.; Milstien, S.; Spiegel, S. Sphingosine-1-phosphate signaling and
12 its role in disease. *Trends Cell Biol.* **2012**, *22*, 50–60. (j) Neubauer, H. A.; Pitson, S. M. Roles and
13 regulation of sphingosine kinase 2. *FEBS J.*, **2013**, *280*, 5317-5336. (k) Plano, D.; Amin, S.;
14 Sharma, A. K. Importance of sphingosine kinase (SphK) as a target in developing cancer
15 therapeutics and recent developments in the synthesis of novel SphK inhibitors *J. Med. Chem.*
16 **2014**, *57*, 78–97. (l) Maceyka, M.; Spiegel, S. Sphingolipid metabolites in inflammatory disease.
17 *Nature* **2014**, *510*, 58–67. (m) Schwal, S.; Pfeilschifter, J.; Huwiler, A. Targeting the Sphingosine
18 Kinase/Sphingosine 1-Phosphate Pathway to Treat Chronic Inflammatory Kidney Diseases. *Bas.*
19 *Clin. Pharmacol. Toxicol.* **2014**, *114*, 44–49.

20
21
22
23
24
25
26
27
28
29
30
31
32
33
34
35
36
37
38
39
40
41
42
43
44
45
46
47
48
49
50
51
52
53
54
55
56
57
58
59
60

² (a) Cuvillier, O.; Pirianov, G.; Kleuser, B.; Vanek, P. G.; Coso, O. A.; Gutkind, S.; Spiegel, S. Suppression of ceramide-mediated programmed cell death by sphingosine-1-phosphate. *Nature* **1996**, *381*, 800–803. (b) Ponnusamy, S.; Meyers-Needham, M.; Senkal, C. E.; Saddoughi, S. A.; Sentelle, D.; Selvam, S. P.; Salas, A.; Ogretmen, B. Sphingolipids and cancer: ceramide and sphingosine-1-phosphate in the regulation of cell death and drug resistance. *Future Oncol.* **2010**, *6*, 1603–1624.

³ For a review see: Santos, W. L.; Lynch, K, R. Drugging Sphingosine Kinases, *ACS Chem. Biol.*, **2015**, *10*, 225–233

⁴ For selected references see: (a) French, K. J.; Schrecengost, R. S.; Lee, B. D.; Zhuang, Y.; Smith, S. N.; Eberly, J. L.; Yun, J. K.; Smith, C. D. Discovery and evaluation of inhibitors of human sphingosine kinase. *Cancer Res.* **2003**, *63*, 5962–5969. (b) Xiang, Y.; Hirth, B.; Kane, Jr J. L.; Liao, J.; Noson, K. D.; Yee, C. Discovery of novel sphingosine kinase-1 inhibitors. Part 2. *Bioorg. Med. Chem. Lett.* **2010**, *20*, 4550–54. (c) Kennedy, A. J.; Mathews, T. P.; Kharel, Y.; Field, S. D.; Moyer, M. L.; East, J. E.; Houck, J. D.; Lynch, K. R.; Macdonald, T. L. Development of amidine-based sphingosine kinase 1 nanomolar inhibitors and reduction of sphingosine 1-phosphate in human leukemia cells. *J. Med. Chem.* **2011**, *54*, 3524–3548. (d) Kharel, Y.; Mathews, T. P.; Gellett, A. M.; Tomsig, J. L.; Kennedy, P. C.; Moyer, M. L.; Macdonald, T. L.; Lynch, K. R. Sphingosine kinase type 1 inhibition reveals rapid turnover of circulating sphingosine 1-phosphate. *Biochem. J.* **2011**, *440*, 345–353. (e) Schnute, M. E.; McReynolds, M. D.; Kasten, T.; Yates, M.; Jerome, G.; Rains, J. W.; Hall, T.; Chrencik, J.; Kraus, M.; Cronin, C. N.; Saabye, M.; Highkin, M. K.; Broadus, R.; Ogawa, S.; Cukyne, K.; Zawadzke, L. E.; Peterkin, V.; Iyanar, K.; Scholten, J. A.; Wendling, J.; Fujiwara, H.; Nemirovskiy, O.; Wittwer, A. J.; Nagiec, M. M. Modulation of cellular S1P levels with a novel, potent and specific inhibitor of sphingosine kinase-1. *Biochem. J.* **2012**, *444*, 79–88. (f) Kharel, Y.; Raje, M.; Gao, M.; Gellett, A. M.; Tomsig, J. L.; Lynch, K. R.; Santos, W. L. Sphingosine kinase type 2 inhibition elevates circulating sphingosine 1-phosphate. *Biochem. J.* **2012**, *447*, 149–157. (g) Byun H. S.; Pyne S.; Macritchie N.; Pyne N. J.; Bittman, R.; Novel sphingosine-containing analogues selectively inhibit sphingosine kinase (SK) isozymes, induce SK1 proteasomal degradation and reduce DNA synthesis in human pulmonary arterial smooth muscle cells. *Med. Chem. Comm.* **2013**, *4*, 1394–1399. (h) Gustin, D. J.; Li, Y.; Brown, M. L.; Min, X.; Schmitt, M. J.; Wanska, M.; Wang, X.; Connors, R.; Johnstone, S.; Cardozo, M.; Cheng, A. C.; Jeffries, S.; Franks, B.; Li, S.; Shen, S.; Wong, M.; Wesche, H.; Xu, G.; Carlson, T. J.; Plant, M.; Morgenstern, K.; Rex, K.; Schmitt, J.; Coxon, A.; Walker, N.; Kayser, F.; Wang, Z. Structure guided design of a series of sphingosine kinase (SphK) inhibitors. *Bioorg. Med. Chem.*

1
2
3
4 *Lett.* **2013**, *23*, 4608–4616. (i) Rex, K.; Jeffries, S.; Brown, M. L.; Carlson, T.; Coxon, A.; Fajardo,
5 F.; Frank, B.; Gustin, D.; Kamb, A.; Kassner, P. D.; Li, S.; Li, Y.; Morgenstern, K.; Plant, M.;
6 Quon, K.; Ruefli-Brasse, A.; Schmidt, J.; Swearingen, E.; Walker, N.; Wang, Z.; Watson, J. E.;
7 Wickramasinghe, D.; Wong, M.; Xu, G.; Wesche, H. Sphingosine kinase activity is not required
8 for tumor cell viability. *PLoS One* **2013**, *8*, e68328. (j) Liu, K.; Guo, T. L.; Hait, N. C.; Allegood,
9 J.; Parikh, H. I.; Xu, W.; Kellogg, G. E.; Grant, S.; Spiegel, S.; Zhang, S. Biological
10 characterization of 3-(2-amino-ethyl)-5-[3-(4-butoxyl-phenyl)-propylidene]-thiazolidine-2,4-dione
11 (K145) as a selective sphingosine kinase-2 inhibitor and anticancer agent. *PLoS One* **2013**, *8*,
12 e56471. (k) Pitman M. R.; Powell J. A.; Coolen, C.; Moretti P. A. B.; Zebol J. R.; Pham D. H.;
13 Ebert L. M.; Bonder C. S.; Gliddon B. L.; Pitson S. M. A selective ATP-competitive sphingosine
14 kinase inhibitor demonstrates anti-cancer properties. *Oncotarget* **2015**, *6*, 7065-83. (l) Patwardhan,
15 N. N.; Morris, E. A.; Kharel, Y.; Raje, M. R.; Gao, M.; Tomsig, J. L.; Lynch, K. R.; Santos, W. L.
16 Structure–Activity Relationship Studies and in Vivo Activity of Guanidine-Based Sphingosine
17 Kinase Inhibitors: Discovery of SphK1- and SphK2-Selective Inhibitors *J. Med. Chem.* **2015**, *58*,
18 1879–1899.
19
20 ⁵ (a) Loveridge, C.; Tonelli, F.; Leclercq, T.; Lim, K. G.; Long, J. S.; Berdyshev, E.; Tate, R. J.;
21 Natarajan, V.; Pitson, S. M.; Pyne, N. J.; Pyne, S. The sphingosine kinase 1 inhibitor 2-(p-
22 hydroxyanilino)-4-(pchlorophenyl) thiazole induces proteasomal degradation of sphingosine kinase
23 1 in mammalian cells. *J. Biol. Chem.* **2010**, *285*, 38841–38852. (b) Tonelli, F.; Lim, K. G.;
24 Loveridge, C.; Long, J.; Pitson, S. M.; Tigyi, G.; Bittman, R.; Pyne, S.; Pyne, N. J. FTY720 and
25 (S)-FTY720 vinylphosphonate inhibit sphingosine kinase 1 and promote its proteasomal
26 degradation in human pulmonary artery smooth muscle, breast cancer and androgen-independent
27 prostate cancer cells. *Cell Signal.* **2010**, *22*, 1536–1542. (c) Lim, K. G.; Tonelli, F.; Li, Z.; Lu, X.;
28 Bittman, R.; Pyne, S.; Pyne, N. J. FTY720 analogues as sphingosine kinase 1 inhibitors: enzyme
29
30
31
32
33
34
35
36
37
38
39
40
41
42
43
44
45
46
47
48
49
50
51
52
53
54
55
56
57
58
59
60

1
2
3
4 inhibition kinetics, allosterism, proteasomal degradation and actin rearrangement in MCF-7 breast
5 cancer cells. *J. Biol. Chem.* **2011**, *286*, 18633–18640.

6
7
8 ⁶ Cingolani, F.; Casasampere, Mi.; Sanllehi, P.; Casas, J.; Bujons, J.; Fabrias, G. Inhibition of
9 dihydroceramide desaturase activity by the sphingosine kinase inhibitor SKI-II. *J. Lipid Res.* **2014**,
10 *55*, 1711–1720. (b) Noack, J.; Choi, J.; Richter, K.; Kopp-Schneider, A.; Regnier-Vigouroux, A. A
11 sphingosine kinase inhibitor combined with temozolomide induces glioblastoma cell death through
12 accumulation of dihydrosphingosine and dihydroceramide, endoplasmic reticulum stress and
13 autophagy. *Cell Death and Disease*, **2014**, *5*, e1425.

14
15
16
17
18
19
20
21 ⁷ (a) French, K. J.; Zhuang, Y.; Maines, L. W.; Gao, P.; Wang, W.; Beljanski, V.; Upson, J. J.;
22 Green, C. L.; Keller, S. N.; Smith, C. D. Pharmacology and antitumor activity of ABC294640, a
23 selective inhibitor of sphingosine kinase-2. *J. Pharmacol. Exp. Ther.* **2010**, *333*, 129–139. (b)
24 Beljanski, V.; Knaak, C.; Smith, C. D. A novel sphingosine kinase inhibitor induces autophagy in
25 tumor cells. *J. Pharmacol. Exp. Ther.* **2010**, *333*, 454–464. (c) Antoon, J. W.; White, M. D.;
26 Meacham, W. D.; Slaughter, E. M.; Muir, S. E.; Elliott, S.; Rhodes, L. V.; Ashe, H. B.; Wiese, T.
27 E.; Smith, C. D.; Burow, M. E.; Beckman, B. S. Antiestrogenic effects of the novel sphingosine
28 kinase-2 inhibitor ABC294640. *Endocrinology* **2010**, *151*, 5124–5135. (d) Beljanski, V.; Lewis, C.
29 S.; Smith, C. D. Antitumor activity of sphingosine kinase 2 inhibitor ABC294640 and sorafenib in
30 hepatocellular carcinoma xenografts. *Cancer Biol. Ther.* **2011**, *11*, 524–534. (e) Gao, Peng;
31 Peterson, Yuri K.; Smith, Ryan A.; Smith, Charles D. Characterization of isoenzyme-selective
32 inhibitors of human sphingosine kinases. *PLoS One* **2012**, *7*, e44543.

33
34
35
36
37
38
39
40
41
42
43
44
45
46
47
48 ⁸ (a) French, K. J.; Upson, J. J.; Keller, S. N.; Zhuang, Y.; Yun, J. K.; Smith, C. D. Antitumor
49 activity of sphingosine kinase inhibitors. *J. Pharmacol. Exp. Ther.* **2006**, *318*, 596–603. (b)
50 Leroux, M. E.; Auzenne, E.; Evans, R.; Hail, N., Jr.; Spohn, W.; Ghosh, S. C.; Farquhar, D.;
51 McDonnell, T.; Klostergaard, J. Sphingolipids and the sphingosine kinase inhibitor, SKI-II, induce
52 BCL-2-independent apoptosis in human prostatic adenocarcinoma cells. *Prostate*, **2007**, *67*, 1699-

1
2
3
4 1717. (c) Leroux, M. E.; Auzenne, E.; Evans, R.; Hail, N., Jr.; Spohn, W.; Ghosh, S. C.; Farquhar,
5
6 D.; McDonnell, T.; Klostergaard, J. Sphingolipids and the sphingosine kinase inhibitor, SKI-II,
7
8 induce BCL-2-independent apoptosis in human prostatic adenocarcinoma cells. *Prostate*, **2007**, *67*,
9
10 1699-1717. (d) Yan, G.; Chen, S.; You, B.; Sun, J. Activation of sphingosine kinase-1 mediates
11
12 induction of endothelial cell proliferation and angiogenesis by epoxyeicosatrienoic acids.
13
14 *Cardiovasc. Res.* **2008**, *78*, 308-314. (e) Ader, I.; Brizuela, L.; Bouquerel, P.; Malavaud, B.;
15
16 Cuvillier, O. Sphingosine Kinase 1: A New Modulator of Hypoxia Inducible Factor 1 α during
17
18 Hypoxia in Human Cancer Cells. *Cancer Res.* **2008**, *68*, 8635-8642. (f) Ader, I.; Malavaud, B.;
19
20 Cuvillier, O. When the Sphingosine Kinase 1/Sphingosine 1-Phosphate Pathway Meets Hypoxia
21
22 Signaling: New Targets for Cancer Therapy *Cancer Res.* **2009**, *69*, 3723-3726. (g) Antoon, J. W. ;
23
24 Meacham, W. D.; Bratton, M.R.; Slaughter, E. M.; Rhodes, L.V.; Ashe, H. B.; Wiese, T.; E.;
25
26 Burow, M. E.; Beckman, B. S. Pharmacological inhibition of sphingosine kinase isoforms alters
27
28 estrogen receptor signaling in human breast cancer. *J. Mol. Endocrinol.* **2011**, *46*, 205-16. (h)
29
30 Yang, Y. L.; Ji, C.; Cheng, L.; He, L.; Lu, C. C.; Wang, R.; Bi, Z. G. (i) Sphingosine kinase-1
31
32 inhibition sensitizes curcumin-induced growth inhibition and apoptosis in ovarian cancer cells.
33
34 *Cancer Sci.*, **2012**, *103*, 1538-45. (j) Zhu, Z. A.; Zhu, Z. Q.; Cai, H. X.; Liu, Y. Reversion of
35
36 multidrug resistance by SKI-II in SGC7901/DDP cells and exploration of underlying mechanisms.
37
38 *Asian Pac. J. Cancer Prev.* **2012**, *13*, 625-31. (k) Zhang, C.; He, H.; Zhang, H.; Yu, D.; Zhao, W.;
39
40 Chen, Y.; Shao, R. The blockage of Ras/ERK pathway augments the sensitivity of SphK1 inhibitor
41
42 SKI II in human hepatoma HepG2 cells. *Biochem. Biophys. Res. Commun.* **2013**, *434*, 35-41. (l)
43
44 Casson, L.; Howell, L.; Mathews, L. A.; Ferrer, M.; Southall, N.; Guha, R.; Keller, J. M.; Thomas,
45
46 C.; Siskind, L. J.; Beverly, L. J.; Inhibition of ceramide metabolism sensitizes human leukemia
47
48 cells to inhibition of BCL2-like proteins. *PLoS One.* **2013**, *8*, e54525.
49
50
51
52
53
54

55 ⁹ Akao, Y.; Banno, Y.; Nakagawa, Y.; Hasegawa, N.; Kim, T. J.; Murate, T.; Igarashi, Y.; Nozawa,
56
57 Y. High expression of sphingosine kinase 1 and S1P receptors in chemotherapy-resistant prostate
58
59
60

1
2
3
4 cancer PC3 cells and their camptothecin-induced up-regulation. *Biochem. Biophys. Res. Commun.*
5
6 **2006**, 342, 1284-90.

7
8 ¹⁰ (a) Baell, J. B., Holloway, G. A. New Substructure Filters for Removal of Pan Assay
9
10 Interference Compounds (PAINS) from Screening Libraries and for Their Exclusion in Bioassays,
11
12 *J. Med. Chem.* **2010**, 53, 2719-2740. (a) Edwards, P. J.; Sturino, C. Managing the Liabilities
13
14 Arising from Structural Alerts: A Safe Philosophy for Medicinal Chemists, *Curr. Med. Chem.*
15
16 **2011**, 18, 3116-3135.

17
18 ¹¹ Pitman, M. R.; Pham, D. H.; Pitson, S. M. Isoform-selective assays for sphingosine kinase
19
20 activity. *Methods Mol. Biol.* **2012**, 874, 21-31.

21
22 ¹² Sources of recombinant SK1 and SK2 (a) Pitson S. M.; Moretti P. A. B.; Zebol J. R.; Zareie R.;
23
24 Derian C. K.; Darrow A. L.; Qi J.; D'Andrea R. J.; Bagley C. J.; Vadas M. A.; Wattenberg B. W.
25
26 The nucleotide-binding site of human sphingosine kinase 1. *J. Biol. Chem.* **2002**, 277, 49545-
27
28 49553. (b) Roberts J. L.; Moretti P. A. B.; Darrow A. L.; Derian C. K.; Vadas M. A.; Pitson S. M.
29
30 An assay for sphingosine kinase activity using biotinylated sphingosine and streptavidin-coated
31
32 membranes. *Anal. Biochem.* **2004**, 331, 122-129.

33
34 ¹³ Hopkins, A. L. Ksererü, G. M. P. D. Leeson, P. D.; Rees, D. C.; Reynolds, C. H. The role of ligand
35
36 efficiency metrics in drug discovery. *Nat. Rev. Drug Discov.* **2014**, 13, 105-121

37
38 ¹⁴ Munoz-Olaya J. M.; Matabosch X.; Bedia C.; Egido-Gabas M.; Casas J.; Llebaria A.; Delgado
39
40 A.; Fabrias G. Synthesis and biological activity of a novel inhibitor of dihydroceramide desaturase.
41
42 *ChemMedChem* **2008**, 3, 946-953

43
44 ¹⁵ Rahmaniyan, M.; Curley, R. W. Jr.; Obeid, L. M.; Hannun, Y. A.; Kraveka, J. M. Identification
45
46 of Dihydroceramide Desaturase as a Direct in Vitro Target for Fenretinide. *J. Biol. Chem.* **2011**,
47
48 286, 24754-24764.
49
50
51
52
53
54
55
56
57
58
59
60

- 1
2
3
4 ¹⁶ Roberson K. M.; Penland, S. N.; Padilia, G. M.; Rathinam, S. S.; Kim, C.-S.; Fine, R. L.;
5
6 Roberston, C. N. Fenretinide: induction of apoptosis and endogenous transforming growth factor
7
8 beta in PC-3 prostate cancer cells. *Cell Growth Differ.* **1997**, *8*, 101–111.
9
- 10 ¹⁷ Mahy, J. P.; Mansuy, D. Formation of prostaglandin synthase-iron-nitrosoalkane inhibitory
11
12 complexes upon in situ oxidation of N-substituted hydroxylamines. *Biochem.*, **1991**, *30*, 4165-72
13
14
- 15 ¹⁸ Fabrias, G.; Munoz-Olaya, J.; Cingolani, F.; Signorelli, P.; Casas, J.; Gagliostro, V.; Ghidoni, R.
16
17 Dihydroceramide desaturase and dihydrosphingolipids: debutant players in the sphingolipid arena.
18
19 *Prog. Lipid Res.* **2012**, *51*, 82–94.
20
- 21 ¹⁹ Antoon, J. W.; White, M. D.; Meacham, W. D.; Slaughter, E. M.; Muir, S. E.; Elliott, S.;
22
23 Rhodes, L. V., Ashe, H. B.; Wiese, T. E.; Smith, C. D.; Burow, M. E.; Beckman, B. S.
24
25 Antiestrogenic effects of the novel sphingosine kinase-2 inhibitor ABC294640. *Endocrinology*,
26
27 **2010**, *151*, 5124–5135
28
29
- 30 ²⁰ During the review of this manuscript the SK2 inhibitor **2** was reported to inhibit Des1 (40%
31
32 Des1 activity at 30 μM of **2**): Venant, H.; Rahmaniyan, M.; Jones, E. E.; Lu, P.; Lilly, M. B.;
33
34 Garrett-Maye, E.; Drake, R. R.; Kraveka, J. M.; Smith, C. D.; Voelkel-Johnson, C. The
35
36 sphingosine kinase 2 inhibitor ABC294640 reduces the growth of prostate cancer cells and results
37
38 in accumulation of dihydroceramides in vitro and in vivo. *Mol. Cancer Ther.* OnlineFirst, Oct. 22,
39
40 2015; DOI: 10.1158/1535-7163.MCT-15-0279.
41
42
- 43 ²¹ Furic, L.; Rong, L.; Larsson, O.; Koumakpayi, I. H.; Yoshida K.; Brueschke, A.; Petroulakis, E.;
44
45 Robichaud, N.; Pollak, M.; Gaboury, L. A.; Pandolfi, P. P.; Saad, F.; Sonenberg, N. eIF4E
46
47 phosphorylation promotes tumorigenesis and is associated with prostate cancer progression. *Proc.*
48
49 *Natl. Acad. Sci. USA* **2010**, *107*, 14134–14139.
50
51
- 52 ²² Vachal, P.; Toth, L. M. General facile synthesis of 2,5-diarylheteropentalenes. *Tetrahedron Lett.*
53
54
55 **2004**, *45*, 7157–7161.
56
57
58
59
60

- 1
2
3
4
5
6
7
8
9
10
11
12
13
14
15
16
17
18
19
20
21
22
23
24
25
26
27
28
29
30
31
32
33
34
35
36
37
38
39
40
41
42
43
44
45
46
47
48
49
50
51
52
53
54
55
56
57
58
59
60
-
- ²³ Rasmussen, C. R.; Villani, Jr., F. J.; Weaner, L. E.; Reynolds, B. E.; Hood, A. R.; Hecker, L. R.; Nortey, S. O.; Hanslin, A.; Costanzo, M. J.; Powell, E. T.; Molinari, A. J. *Synthesis* **1988**, 456–459.
- ²⁴ Layton, M. E.; Kelly, M. J.; Rodzinak, K. J.; Sanderson, P. E.; Young, S. D.; Bednar, R. a; Dilella, A. G.; McDonald, T. P.; Wang, H.; Mosser, S. D.; Fay, J. F.; Cunningham, M. E.; Reiss, D. R.; Fandozzi, C.; Trainor, N.; Liang, A.; Lis, E. V.; Seabrook, G. R.; Urban, M. O.; Yergey, J.; Koblan, K. S. Discovery of 3-Substituted Aminocyclopentanes as Potent and Orally Bioavailable NR2B Subtype-Selective NMDA Antagonists *ACS Chem. Neurosci.* **2011**, *2*, 352–62.
- ²⁵ Wehn, P. M.; Harrington, P. E.; Eksterowicz, J. E. Facile Synthesis of Substituted 5-Amino- and 3-Amino-1,2,4-Thiadiazoles from a Common Precursor. *Org. Lett.* **2009**, *11*, 5666-5669.
- ²⁶ Schaefer, H.; Gewald, K. 5-Arylamino-3-brom-1, 2,4-thiadiazole und 5-Arylamino-3-bromisothiazole *J. Prakt. Chem.* **1987**, *329*, 355-8
- ²⁷ Weber, L.; Fuchs, T.; Illgen, K.; Doemling, A.; Cappi, M.; Nerdinger, S. PCT Int. Appl. (2001), WO 2001014320 A1 20010301.
- ²⁸ Padmavathi, V.; Reddy, D. G.; Reddy, N. S.; Mahesh, K. Synthesis and biological activity of 2-bis((1,3,4-oxadiazolyl/1,3,4-thiadiazolyl)methylthio)methylene)malononitriles. *Eur. J. Med. Chem.* **2011**, *46*, 1367–73.
- ²⁹ Bartroli, J.; Turmo, E.; Algueró, M.; Boncompte, E.; Vericat, M. L.; Conte, L.; Ramis, J.; Merlos, M.; García-Rafanell, J.; Forn, J. García-Rafanell, J.; Forn, J. New azole antifungals. 2. Synthesis and antifungal activity of heterocyclecarboxamide derivatives of 3-amino-2-aryl-1-azolyl-2-butanol. *J. Med. Chem.* **1998**, *41*, 1855–68.
- ³⁰ Kawano, T.; Yoshizumi, T.; Hirano, K.; Satoh, T.; Miura, M. Copper-Mediated Direct Arylation of 1,3,4-Oxadiazoles and 1,2,4-Triazoles with Aryl Iodides. *Org. Lett.* **2009**, *11*, 3072–5.

- 1
2
3
4 ³¹ Singh, A. K.; Prakash, S.; Kulshrestha, V.; Shahi, V. K. Cross-linked hybrid nanofiltration
5
6 membrane with antibiofouling properties and self-assembled layered morphology. *ACS Appl. Mat.*
7
8 *Interfaces* **2012**, *4*, 1683–92
9
10 ³² Creek, D. J.; Jankevics, A.; Burgess, K. E.; Breitling, R.; Barrett, M. P. IDEOM: an Excel
11
12 interface for analysis of LC-MS-based metabolomics data. *Bioinformatics*, **2012**, *128*, 1048-9.
13
14 ³³ Bi, Y.; Xu, P.-X.; Zhu, H.-H.; Lei, Y.-J. Synthesis and fluorescent properties of compounds
15
16 containing bis-1,3,4-oxadiazoles. *Huaxue Yanjiu*, **2012**, *55*, 49-51.
17
18 ³⁴ Chen, Y.; Xu, X.; Liu, X.; Yu, M.; Liu, B-F.; Zhang, G. Synthesis and evaluation of a series of
19
20 2-substituted-5-thiopropylpiperazine (piperidine)-1,3,4-oxadiazoles derivatives as atypical
21
22 antipsychotics. *PloS One*. **2012**, *7*, e35186.
23
24
25
26
27
28
29
30
31
32
33
34
35
36
37
38
39
40
41
42
43
44
45
46
47
48
49
50
51
52
53
54
55
56
57
58
59
60

Table of Contents graphic

